Aus der Klinik für Hals-, Nasen- und Ohrenheilkunde
der Heinrich-Heine-Universität Düsseldorf
Direktor: Univ.-Prof. Dr. Jörg Schipper

Characterization of pro- and anti-inflammatory interactions in chronic rhinosinusitis with and without nasal polyps

Dissertation

zur Erlangung des Grades Doktor der Medizin
der Medizinischen Fakultät der Heinrich-Heine-Universität Düsseldorf

vorgelegt von
Dr. rer. nat. Svenja Daschkey
2026

Als Inauguraldissertation gedruckt mit der Genehmigung der
Medizinischen Fakultät der Heinrich-Heine-Universität Düsseldorf

gez.:
Dekan: Prof. Dr. med. Nikolaj Klöcker
Erstgutachterin: Prof. Dr. med. Kathrin Scheckenbach
Zweitgutachter: Prof. Dr. med. Johannes Stegbauer

„Diese Arbeit ist dir gewidmet, Mama – für jedes aufmunternde Gespräch, jedes „Du schaffst das schon“ und jede Mahlzeit, die du mir mitgegeben hast, damit ich nicht verhungere“.

Zusammenfassung

Die chronische Rhinosinusitis (CRS) ist durch folgende Symptome gekennzeichnet: eine Behinderung der Nasenatmung, vermehrte nasale Sekretion, Schmerzen und/oder Druck im Gesicht und/oder eine Geruchsminderung oder -verlust. Sie dauert länger als 12 Wochen an. CRS wird allgemein in zwei Hauptphänotypen unterteilt: CRS mit Nasenpolypen (CRSwNP; 10–25% der CRS-Fälle) und CRS ohne Nasenpolypen (CRSsNP; 75–90% der CRS-Fälle) sowie durch drei Endotypen T1, T2 und T3 gekennzeichnete Entzündungen, die verschiedene entzündliche Muster der Krankheit und die Grundlage für den Gewebeumbau bei CRS darstellen. Für jeden Endotyp wurden bereits mehrere potenzielle Biomarker, meist pro-inflammatorische Zytokine, identifiziert und als Grundlage für diese Arbeit verwendet.
Von mehr als 400 Patienten wurden Nasenabstriche und teilweise Gewebeproben entnommen, RNA isoliert und revers in cDNA transkribiert. qRT-PCRs wurden zur Verifizierung der potenziellen Biomarker *CXCL9, CXCL10, CCL26, CLC* und *CSF3* etabliert. Ebenso wurde *ACE2* (Angiotensin Converting Enzyme 2), einer der Hauptakteure des Renin-Angiotensin-Aldosteron-Systems (RAAS) und wichtige Zytokine wie *IFN-γ, IL-1β* und *IL-6* mittels hierarchischem Clustering und dem Student's t-Test analysiert. *ACE2* wird zudem von SARS-CoV-2 als zellulärer Rezeptor verwendet, um in Wirtszellen einzudringen und die virale Replikation im Epithel der Atemwege durchzuführen. Es hat sich gezeigt, dass T1- und T2-Entzündungen die *ACE2*-Expression im respiratorischen Epithel regulieren und das Risiko einer SARS-CoV-2-Infektion bei CRS-Patienten senken kann.

In dieser Arbeit konnte gezeigt werden, dass die T2-assoziierten Gene (*CCL26* und *CLC*), vor allem in den Abstrichproben ähnliche Expressionsprofile besitzen. Wohingegen die T1- und T3-assoziierten Gene inklusive *ACE2* ähnlichere Expressionsprofile zeigen und eine separate Gruppe bilden. Dies deutet darauf hin, dass chronische Entzündungsreaktionen häufig die T1- und T3-Signalwege in Kombination nutzen. Darüber hinaus konnte eine signifikant geringere Expression von *ACE2* in CRSwNP und CRSsNP im Vergleich zu den gesunden Kontrollen nachgewiesen werden, wodurch die Bindung von SARS-CoV-2 inhibiert werden und CRS eine schützende Wirkung haben kann. Aufgrund der Ergebnisse dieser Arbeit kann vermutet werden, dass *ACE2* einen inhibierenden Einfluss auf T2 und *IL-6* hat aufgrund der negativen Korrelation von *ACE2* zwischen den gesunden Kontrollen und den beiden CRS-Erkrankungen.

Zusammenfassend zeigt diese Doktorarbeit, dass die Endotypen T1, T2 und T3 sowohl bei CRSwNP als auch bei CRSsNP durch unterschiedliche Gensignaturen und Expressionsprofile geprägt sind, die jeweils verschiedene Mechanismen und Signalwege nutzen, einschließlich *ACE2* im Kontext des Renin-Angiotensin-Aldosteron-Systems und der SARS-CoV-2-Infektion. Die Identifizierung dieser endotyp-spezifischen Mechanismen bietet Hinweise auf mögliche neue therapeutische Ziele und könnte zur Entwicklung präziserer und personalisierter Behandlungsstrategien für Patienten mit CRS beitragen.

Summary

Chronic rhinosinusitis (CRS) is characterized by symptoms such as nasal blockage, increased nasal discharge, along with a reduction or loss of smell, as well as facial pain and/or pressure. These symptoms persist for more than 12 weeks. CRS is typically classified into two main phenotypes: CRS with nasal polyps (CRSwNP), which accounts for 10-25% of CRS cases, and CRS without nasal polyps (CRSsNP), which represents 75-90% of CRS cases. Furthermore, CRS can be categorized into three endotypes T1, T2, and T3 based on distinct inflammatory patterns, which influence tissue remodeling in CRS. Several potential biomarkers, primarily pro-inflammatory cytokines, have been identified for each endotype and serve as the foundation for this thesis.

Nasal swabs and partially tissue samples were collected from over 400 patients. RNA was isolated from these samples and reverse transcribed into complementary DNA (cDNA). Quantitative reverse transcription PCR (qRT-PCR) assays were developed to validate key biomarkers, including *CXCL9, CXCL10, CCL26, CLC*, and *CSF3*, as well as *ACE2*, a crucial component of the renin-angiotensin-aldosterone system (RAAS). Important cytokines such as IFN-γ, IL-1β, and IL-6 were also analyzed. Data were evaluated using hierarchical clustering and Student's t-test. *ACE2* acts as a cellular receptor for SARS-CoV-2, facilitating viral entry and replication in the airway epithelium. Evidence suggests that T1 and T2 inflammatory responses modulate *ACE2* expression in the respiratory epithelium, potentially reducing the risk of SARS-CoV-2 infection in CRS patients.

This thesis demonstrates that genes associated with endotype T2 (*CCL26* and *CLC*) cluster together with significantly lower expression levels, particularly in swab samples. In contrast, genes linked to endotypes T1 and T3, including *ACE2*, form a distinct cluster due to similar gene expression profiles. This suggests that chronic inflammatory responses often involve a combination of T1 and T3 pathways. Additionally, a significantly lower expression of *ACE2* was observed in both CRSwNP and CRSsNP compared to healthy controls. This reduction in *ACE2* expression may offer a protective effect against CRS by decreasing the likelihood of SARS-CoV-2 binding, as *ACE2* serves as the viral entry receptor. Furthermore, the results suggest that *ACE2* may negatively influence T2 and *IL-6*, as indicated by a negative correlation between *ACE2* levels and both CRS conditions in comparison to healthy controls.

In conclusion, this doctoral thesis demonstrates that the inflammatory endotypes T1, T2, and T3 in both CRSwNP and CRSsNP are governed by distinct gene signatures and expression profiles, each utilizing different mechanisms and signaling pathways, including *ACE2* in the context of the RAAS and SARS-CoV-2 infection. The identification of these endotype-specific mechanisms provides insight into potential new therapeutic targets and may contribute to the development of more precise and personalized treatment strategies for patients with CRS.

Abbreviations

ABI	Applied Biosystems
ACE	Angiotensin-Converting-Enzyme
ACT	Actin
CCL	Canine Ceroid Lipofuscinose
CLC	Charcot-Leyden Crystal Galectin
CRS	Chronic Rhinosinusitis
CRSsNP	Chronic Rhinosinusitis without Nasal Polyps
CRSwNP	Chronic Rhinosinusitis with Nasal Polyps
CSF	Colony Stimulation Factor
CT	Computed tomography
CXCL	Chemokine (C-X-C motif) Ligand
DNA	Desoxyribonucleic acid
DC	Dendritic cell
dNTP	desox Nucleotide-Tri-Peptide
ET	Ethmoid tissue
FRET	Fluorescence-Resonance-Energy-Transfer
GO	Gene Ontology
HC	Healthy control
IFN	Interferon
Ig	Immunglobulin
IL	Interleukin
NEB	New England Biolabs
NFL	Nasal Lavage Fluid
NP	Nasal Polyps
RNA	Ribonucleic acid
rRT-PCR	reverse transcriptase Real Time Polymerase Chain Reaction
RT	Reverse Transcriptase
Th	T-helper cell

Figure Directory

Table Directory

Table of Contents

1 Introduction

1.1 Background

Rhinitis is characterized by inflammation of the mucosa in the upper respiratory tract, particularly the nasal mucous membranes. When this inflammation extends from the nasal cavities into the paranasal sinuses, it is referred to as sinusitis, which often occurs concurrently with rhinitis, leading to the condition known as rhinosinusitis (RS). RS is further categorized into acute rhinosinusitis (ARS) and chronic rhinosinusitis (CRS). ARS can develop from a common cold with nasal discharge if the flow of secretion is obstructed due to swelling of the mucous membranes. The underlying cause can be either viral or bacterial pathogens. Symptoms of sinusitis may include fever, fatigue, visible swelling of the paranasal sinuses, headache, facial pain, and a purulent nasal discharge (Fokkens *et al.*, 2020; Stuck *et al.*, 2018). Chronic rhinosinusitis (CRS) is a prevalent and persistent inflammatory disease, with an incidence of 10-15% in Germany and other developed countries. The prevalence of CRS increases with age and is higher among individuals with asthma, chronic obstructive pulmonary disease (COPD), allergies, and women. CRS imposes significant direct and indirect costs on the healthcare system, with substantial expenses associated with surgeries due to a high rate of relapses (up to 75%). In Germany, the annual cost per CRS patient is approximately €2,500, with direct costs for patients with CRSwNP averaging €1,501 per year. In the USA, the annual direct costs for managing CRS range between $10 and $13 billion, translating to about $2,609 per patient per year (Fokkens *et al.*, 2020). Moreover, CRS is associated with a significant decline in quality of life, impaired sleep quality, and reduced ability to perform daily activities (Beule, 2015). Therefore, the indirect costs of CRS are substantial, as 85% of CRS cases occur in individuals of working age (18 to 65 years), leading to missed workdays and decreased productivity (Fokkens *et al.*, 2020).

Therefore, a better and deeper immunological understanding of this disease is needed to develop more precise and personalized treatments. Thus, this medical thesis focuses on the inflammatory mechanisms of CRS.

1.2 Chronic rhinosinusitis with nasal polyps (CRSwNP) and without nasal polyps (CRSsNP)

1.2.1 Clinical definition of CRS

„Chronic rhinosinusitis (with or without nasal polyps) in adults is defined as: presence of two or more symptoms, one of which should be either nasal blockage / obstruction / congestion or nasal discharge (anterior / posterior nasal drip): ± facial pain/pressure; ± reduction or loss of smell; for ≥ 12 weeks; with validation by telephone or interview. Questions on allergic symptoms (i.e. sneezing, watery rhinorrhoea, nasal itching, and itchy watery eyes) should be included“ (Fokkens *et al*., 2020).

CRS is commonly divided into two main phenotypes according to rhinoscopic and endoscopic visible polyps: CRS with nasal polyps (CRSwNP; 10-25%) and CRS without (lat. sine) nasal polyps (CRSsNP; 75-90%) (Klingler *et al.*, 2021).

1.2.2 Prevalence, distribution and ages

CRS is a global condition that affects individuals across all age groups. According to studies by Starry *et al.,* the prevalence of CRSwNP increased from approximately 2,100 per million in 2015 to about 3,500 per million in 2019, as shown in **Table 1.2.2**, using data from AOK Plus and SHI (German statutory health insurance). The AOK Plus database recorded 11,479 adult cases of CRSwNP between 2015 and 2019, reflecting a 5-year prevalence of 0.58%, or about 5,800 per million. The 5-year prevalence was higher in males, at approximately 7,200 per million, compared to females, who had a prevalence of about 4,700 per million. The highest age-specific prevalence among males was observed in the 75- to 80-year age group (about 11,500 per million), while for females, it was in the 60- to 65-year age group (about 5,900 per million) (Starry *et al.*, 2022).

Table 1.2.2: Prevalence and incidence of CRSwNP

	Prevalence of CRSwNP			Incidence of CRSwNP		
	Number of identified CRSwNP patients; and percentage from all adults in the database, who were alive at the beginning of the respective year					
Year	AOK PLUS *N* (%)	SHI *N* (%)	Germany *N* (%)	AOK PLUS *N* (%)	SHI *N* (%)	Germany *N* (%)
2015	4409 (0.21%)	113,817 (0.20%)	131,423 (0.20%)	-	-	-
2016	5260 (0.26%)	139,421 (0.24%)	160,348 (0.24%)	1726 (0.08%)	48,589 (0.08%)	60,457 (0.09%)
2017	6944 (0.34%)	190,183 (0.32%)	217,591 (0.32%)	2751 (0.14%)	79,419 (0.13%)	98,658 (0.15%)
2018	7245 (0.36%)	203,128 (0.34%)	231,346 (0.34%)	1769 (0.09%)	53,069 (0.09%)	65,960 (0.10%)
2019	6939 (0.35%)	195,157 (0.32%)	222,192 (0.33%)	1138 (0.06%)	34,283 (0.06%)	42,805 (0.06%)
5-year period (2015–2019)	11,479 (0.58%)	328,743 (0.55%)	374,115 (0.55%)	7384 (0.38%)	215,360 (0.36%)	267,880 (0.40%)

Abbreviation: AOK PLUS: Health insurance for Saxony & Thuringia, SHI: German statutory health insurance (Starry *et al.*, 2022)

85% of CRS cases are aged between 18 and 65 years. The estimated prevalence in Germany and developed countries is between 10-15%, 12.3% in the USA, 10.9% in Europe, and 13% in China (Albu, 2020; Fokkens *et al.*, 2020).

As mentioned in the background section, CRS incurs both direct and substantial indirect costs. Direct costs in the USA are estimated to be between $10 billion and $13 billion per year. While precise figures for the indirect costs of CRS are not available, it is estimated that these costs exceed $20 billion annually in the USA. This estimation accounts for missed workdays, absenteeism, and productivity loss (Albu, 2020; Fokkens *et al.*, 2020). Lourijsen *et al*. found yearly direct costs of 1,501 Euro per year and patient in a group of patients with CRSwNP (Fokkens *et al.*, 2020; Lourijsen *et al*., 2020).

1.2.3 Causes, risk factors, and complications

The exact causes of CRS and the development of nasal polyps are not yet fully understood, including why some individuals experience persistent inflammation, irritation, and chronic nasal congestion, which can lead to the formation of polyps. Previous studies have suggested that individuals who develop polyps have distinct immunological pathways activated and different biomarkers upregulated in their mucous membranes. Persistent irritation and inflammation in the nasal passages and/or sinuses, as well as conditions such as asthma and allergic rhinitis, increase the risk of developing nasal polyps (Stevens *et al*., 2016).

Comorbidities often associated with CRS and nasal polyps include asthma, aspirin sensitivity, allergic fungal sinusitis, allergies to airborne fungi, cystic fibrosis, Eosinophilic Granulomatosis with Polyangiitis (EGPA, formerly known as Churg-Strauss syndrome), gastroesophageal reflux disease (GERD), inflammatory and autoimmune diseases, tobacco exposure, chronic obstructive pulmonary disease (COPD), vitamin D deficiency, and female gender (Min & Tan,

2015). Moreover, there is evidence suggesting that certain genetic variations related to immune system function may contribute to the development of CRS. (Min & Tan, 2015).
Furthermore, nasal polyps can lead to complications by obstructing normal airflow and fluid drainage, potentially resulting in asthma exacerbations, obstructive sleep apnea, or recurrent sinus infections (Tint *et al.*, 2016). An association between CRS and asthma has been described in several studies, but it remains incompletely understood. Asthma is more commonly observed in individuals with CRS compared to the general population, and 80% of asthma patients exhibit radiologic signs of CRS. Conversely, patients with CRS are at a higher risk of developing severe asthma, with more frequent exacerbations (Carr, 2016). Both CRSwNP and CRSsNP can contribute to obstructive sleep apnea by increasing upper airway resistance through inflammatory mechanisms. Patients with sleep-disordered breathing may experience several consequences, including neurobehavioral disturbances, cardiovascular diseases, excessive daytime sleepiness, and decreased libido (Carr, 2016).
Moreover, allergic fungal rhinosinusitis (AFRS) is a subtype of CRS and is typically caused by fungal infections such as *Aspergillus fumigatus* in chronic invasive fungal rhinosinusitis or *Aspergillus flavus* in granulomatous invasive fungal rhinosinusitis. AFRS is characterized by an atopic inflammatory reaction to mold in the sinus cavities (Carr, 2016).
CRS, particularly in patients with AFRS, can also lead to bone changes and deformities as side effects. Generally, CRS is associated with osteitis, which can cause bone demineralization, focal sclerosis, loss of trabecular structure, cortical destruction, bone erosion, and thinning. These bone changes are often identified through imaging (Carr, 2016; Tint *et al.*, 2016).

1.2.4 Most frequent comorbidities

Associated comorbidities for CRS, particularly CRSwNP, are listed in section 1.2.3. Among airway diseases, allergic rhinitis (AR) has been found to have a significant association with both CRSwNP and CRSsNP. The symptoms of these two conditions overlap substantially, which can make them challenging to differentiate (Tan *et al.*, 2013). Similar to allergic rhinitis, asthma is strongly associated with CRS, particularly CRSwNP. Studies by Bresciani *et al.* and Lin *et al*. have demonstrated that the severity of asthma may correlate with the radiographic severity of CRS. Furthermore, the frequency and severity of CRS can influence the severity of coexisting asthma (Bresciani *et al.*, 2001; Lin *et al.*, 2011). In some patients, CRSwNP, asthma, and aspirin sensitivity are associated in a condition known as aspirin-exacerbated respiratory disease (AERD), or Samter's triad. Following exposure to aspirin, patients with AERD are believed to overproduce cysteinyl leukotrienes and prostaglandin D2, which are mediators of eosinophilic inflammation, while simultaneously downregulating the anti-inflammatory prostaglandin E2 (Bousquet *et al.*, 2009; Leung *et al.*, 2011).

Additionally, CRS patients are significantly more likely to develop conditions such as chronic bronchitis and pneumonia, suggesting that acute respiratory diseases may alter host sensitivity. This increased sensitivity can lead to higher rates of rhinovirus (RV) and respiratory syncytial virus (RSV) infections, which may subsequently contribute to the development of asthma (Carroll *et al.*, 2009; James *et al.*, 2012). Studies from Chung *et al*. support that "chronic pulmonary disease" was the second most strongly associated condition, after asthma, with Otolaryngologist diagnosed CRS (Chung *et al.*, 2014).

Moreover, there exists a strong association between CRS and cystic fibrosis (CF) (De Boeck *et al.,* 2006; Farrell *et al.*, 2008). CRS is particularly challenging to treat in patients with cystic fibrosis (CF) due to increased mucus viscosity, chronic sinus infections, and biofilm formation. The severity of CRS in CF patients is exacerbated by the presence of specific sinus pathogens, including *Staphylococcus aureus* and *Pseudomonas aeruginosa* (Cho *et al.*, 2020; Hamilos, 2016).

1.2.5 Pathophysiology of Chronic Rhinosinusitis

The etiology of CRS is highly complex and multifactorial. Contributing factors include environmental influences such as allergens, toxins, and pathogens, as well as individual factors like immunological dysfunctions, anatomical abnormalities, and comorbid conditions. Additionally, the microbiome appears to play a significant role in the pathogenesis of CRS (Cuevas & Zahnert, 2021). Colonization of the mucosa with *Staphylococcus aureus* appears to be a significant factor in the pathophysiology of nasal polyposis, as suggested by recent studies (**Figure 1.2.5**). In 60-80% of nasal polyps, IgE antibodies against staphylococcal enterotoxins can be detected in the tissue, and also in the serum, particularly in the presence of concurrent asthma. Enterotoxins function as superantigens, which enhance eosinophilic inflammation and induce polyclonal IgE synthesis (Stuck *et al.*, 2012).

In addition, approximately 80% of CRSwNP cases are associated with type 2 inflammation, leading to an imbalance among T helper cell subtypes. This type of inflammation often results in eosinophilic cell infiltration in nasal polyps and a functional loss of the nasal barrier, which facilitates the invasion of allergens and pathogens. Epithelial cells produce Thymic Stromal Lymphopoietin (TSLP), which activates dendritic cells. These dendritic cells, in turn, stimulate the production of interleukins such as IL-4, IL-13, and IL-5 by T helper 2 (Th2) cells, leading to the initiation of inflammatory processes. IL-4 and IL-13 facilitate communication between immune cells and are secreted by T cells to promote B cell activation and class switching, particularly to IgE. The induction of goblet cell hyperplasia by IL-4 leads to disruption of the epithelial barrier and increased mucus secretion (Cuevas & Zahnert, 2021). CD4+ T cells, particularly those differentiated into Th2 cells, are the primary source of IL-4. IL-5, a crucial cytokine in immune regulation, plays an important role in eosinophil and B cell function. It is

mainly produced by Th2 cells and mast cells, and is essential for the development, maturation, and activation of eosinophils (Fokkens *et al*., 2020; Kato, 2015). Eosinophil cationic protein (ECP) and eotaxins (eotaxin-1, -2, and -3) are also involved in the inflammatory process and are increasingly detectable in nasal polyps. IL-25, IL-33, and TSLP, produced by epithelial cells, are key regulators of Th2 cells, mast cells, basophils, and dendritic cells. These factors activate type 2 innate lymphoid cells (ILC2), which, in turn, secrete IL-5 and IL-13, further sustaining eosinophilic inflammation (Cuevas & Zahnert, 2021).

Nasal polyps are protrusions of inflamed mucosa that may present as stalked or broad-based growths extending into the lumen of a paranasal sinus or the main nasal cavity (**Figure 1.2.5**). These growths are typically soft, painless, and noncancerous. While small nasal polyps often cause no symptoms, larger polyps or clusters of polyps can lead to issues such as obstructed breathing and drainage, frequent infections, and loss of the sense of smell. Histologically, nasal polyps are characterized by edema and/or fibrosis, loss of vascularization, and the presence of damaged epithelium, often accompanied by a reduction in glands and nerve endings (Larsen *et al.*, 1998).

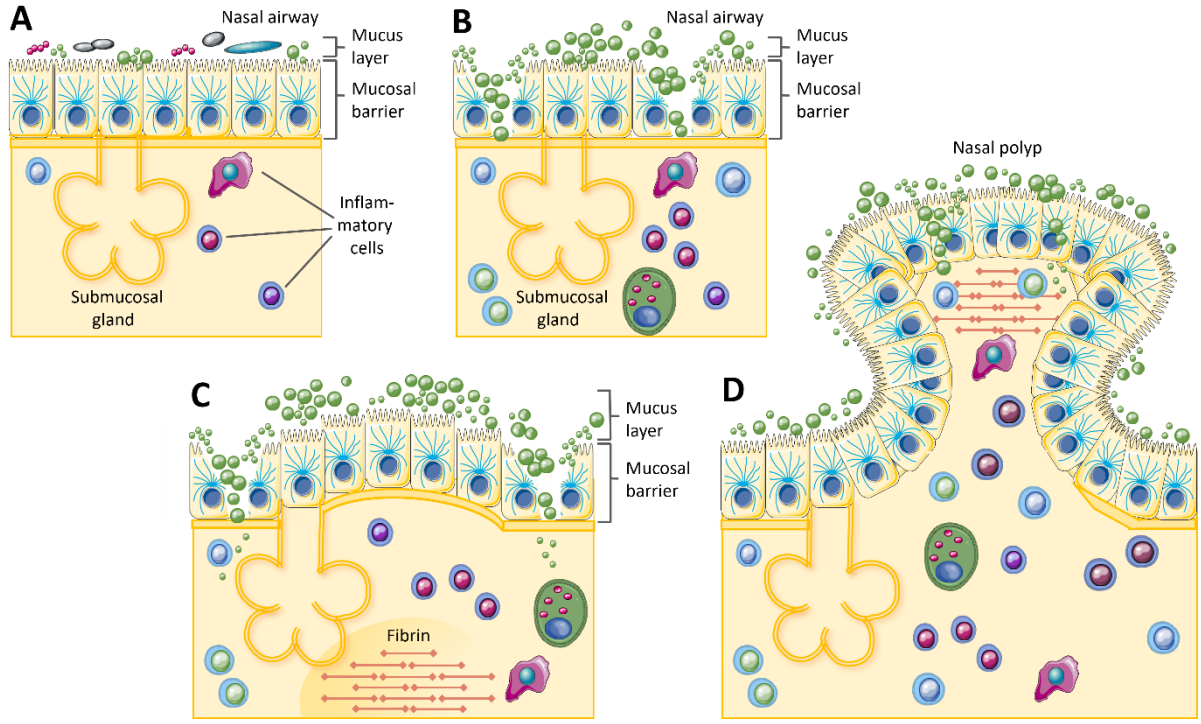

Figure 1.2.5: Development of nasal polyposis. A) Normal nasal mucosa and colonization with microbes (green dots) **B)** Loss of barrier and decreased diversity of microbes **C)** Recruitmet and expansion of inflammatory cells, tissue swelling, inflammation, and deposition of crosslinked fibrin **D)** Tissue remodeling with loss of submucosal glands in polyp and profound inflammatory cell expansion - modified accroding to (Stevens *et al*., 2016).

CRS without polyp formation is thought to cause gradual obstruction due to increased tissue growth in the ostiomeatal complex, leading to ventilation and drainage disorders (Stuck *et al.*, 2012). Disruption of mucociliary clearance is also considered a crucial pathophysiological factor in inflammatory diseases of the paranasal sinuses (Gwaltney, 2002).

1.2.6 Diagnosis

It is important to assess the general condition of the patient, including symptoms such as lethargy and neurological signs, as well as to inspect the face for redness and swelling. A clinical examination should include evaluating for pressure or percussion pain in the maxillary or frontal sinuses. During a rhinoscopic examination, findings such as redness or swelling of the nasal mucosa, purulent discharge in the main nasal cavity or middle nasal passage, nasal polyps, or other space-occupying lesions can be detected (**Figure 1.2.6.I**) (Weber & Hosemann, 2015).

Nasal endoscopy allows for a detailed examination of the anterior and posterior nasal and pharyngeal structures. It facilitates the identification of structural features and differential diagnoses, making it indispensable for the evaluation and diagnosis of CRS (Wuister *et al*., 2014).

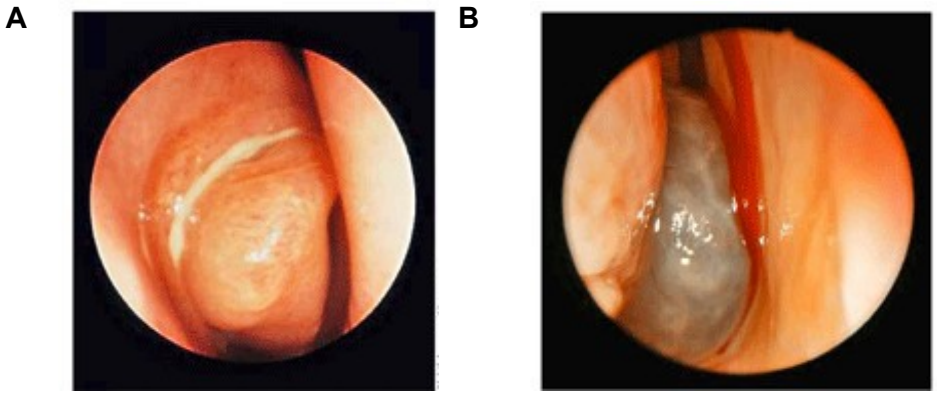

Figure 1.2.6.I: **Endoscopy of nasal passages. A)** Endoscopy of the right middle nasal passage with suppuration and extensive hyperplasia of the mucosa: **CRSsNP**. **B)** Endoscopy of the left middle and inferior nasal passage: **CRSwNP** (Weber & Hosemann, 2015)

Ultrasound examination of the paranasal sinuses was performed as a non-invasive procedure to reveal fluid retention in the maxillary and frontal sinuses. Compared to X-ray methods such as CT (computed tomography), DVT (digital volume tomography), and MRI (magnetic resonance imaging), the diagnostic capabilities of ultrasound are significantly limited (Mafee *et al*., 2006; Younis *et al.*, 2002). Currently, high-resolution computed tomography (CT) has been established as the best method for imaging the sinus system (**Figure 1.2.6.II**) (Batra *et al*., 2015; Zinreich *et al*., 1987). To assess the paranasal system, especially for surgical

planning, cross-sectional images should be available in all three layers (axial, coronal, sagittal). These can be calculated from a single data set (Dammann, 2007; Lang *et al.*, 2002).

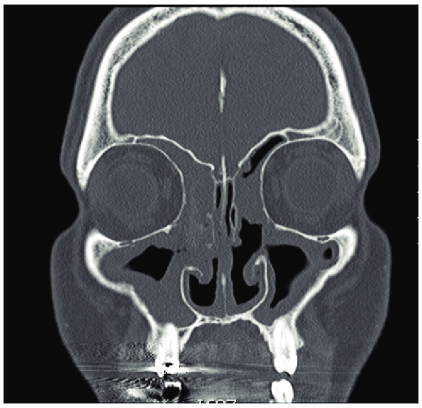

Figure 1.2.6.II: Computed tomography (CT) imaging the sinus system. Coronal CT scan of CRSwNP showing extensive polyposis lining in the bilateral maxillary, ethmoid, and frontal sinuses (Jaksha *et al.*, 2016)

The detection of allergen-specific IgE antibodies (sIgE), in conjunction with information from the medical history, clinical findings, and results from skin tests and organ-specific provocation tests, helps to indicate an allergy. In the context of a comprehensive evaluation, these tests contribute to understand the clinical relevance of allergic factors in rhinosinusitis (Settipane *et al.*, 2013; Stevens *et al.*, 2016). Immunodeficiencies can be identified through appropriate laboratory tests that assess both humoral and cellular immune functions. Key aspects include the measurement of immunoglobulins such as IgA and IgG, and the evaluation of cellular defects involving B cells, T cells, neutrophils/monocytes, and complement system components (Nayan *et al.*, 2015; Schwitzguébel *et al.*, 2015).

Further diseases to exclude:

- **Cystic Fibrosis**: Assessed using a sweat test and potentially a genetic test.
- **Immune Deficiency**: Evaluated through specific immunological tests.
- **NSAID-Exacerbated Respiratory Disease (NERD)**: Diagnosed based on clinical history and response to NSAIDs.
- **Metabolic Disorders**: Assessed through relevant metabolic tests.
- **Sarcoidosis**: Diagnosed by measuring angiotensin-converting enzyme (ACE) levels.
- **HIV**: Diagnosed through HIV serology.
- **Granulomatosis with Polyangiitis**: Identified using tests for antineutrophil cytoplasmic antibodies (ANCA).
- **Immotile Cilia Syndrome**: Diagnosed through methods evaluating mucociliary clearance and ciliary activity (Pfaar *et al.*, 2023).

1.2.7 Treatment options for CRS

1.2.7.1 Conservative therapy of CRS

The use of topical glucocorticosteroids is considered as first-line therapy for CRS (Fokkens *et al.*, 2020; Stuck *et al*., 2012). High-quality studies provide evidence that long-term use of nasal corticosteroids is both safe and effective for treating patients with CRS, leading to an improvement in the quality of life. The impact on CRSwNP is more pronounced than on CRSsNP, as glucocorticosteroids can reduce the size of nasal polyps and help to prevent their recurrence after endoscopic surgery. No significant differences have been observed between different types of nasal glucocorticosteroids in terms of efficacy (Fokkens *et al*., 2020).

Short-term use of oral antibiotics, typically defined as a treatment period of around two to four weeks, was often prescribed for CRS patients. Antibiotics such as amoxicillin/clavulanate, clarithromycin, levofloxacin, ciprofloxacin, and cefaclor have been used. However, due to low-quality evidence, it remains uncertain whether short-term antibiotics have a significant positive impact on patient outcomes in adults with CRS compared to a placebo. Additionally, gastrointestinal side effects, such as diarrhea and anorexia, are frequently reported (Fokkens *et al*., 2020).

Treatment with long-term antibiotics, including macrolides and topical antibiotics, shows no significant difference compared to placebo for patients with CRS. There is some indication that macrolides may be beneficial for CRS patients with low IgE levels; however, serious side effects, such as cardiac toxicity, should be considered. Consequently, more extensive and higher-quality studies conducted in Europe are needed to further evaluate the efficacy and safety of these treatments (Fokkens *et al*., 2020).

Similarly, the evidence supporting the use of antihistamines and anti-leukotrienes is very limited, with no positive effects reported in the few trials conducted. Leukotrienes, which are inflammatory mediators synthesized by eosinophils and mast cells, play a role in the pathophysiology of rhinitis, asthma, and potentially CRSwNP (Fokkens *et al*., 2020).

For rhinosinusitis, the use of analgesics and anti-inflammatory medications is only recommended for managing pain and not as a decongestant measure. Medications such as paracetamol, diclofenac, and ibuprofen can be used to alleviate symptoms such as facial pain or headache (Stuck *et al.*, 2012). Saline solutions, applied as nasal drops, sprays, or rinses, can help improve symptoms of CRS by enhancing mucociliary clearance, reducing inflammation, and decongesting the mucosa (Rudmik & Soler, 2015).

According to surveys, the recommendation of decongestants by ENT doctors is rather low and should not be used for more than two weeks (Sylvester *et al.*, 2013). The risks like rebound congestion, chronic sinusitis, damage of nasal mucosa or atrophic rhinitis associated with the long-term use of over-the-counter decongestants in CRS or for chronic nasal obstruction of various origins appears to be significantly elevated (Wahid *et al*., 2023).

In the treatment of allergic and eosinophilic-inflammatory diseases, such as bronchial asthma, urticaria, and atopic dermatitis, monoclonal antibodies have demonstrated good efficacy. This is also true in some cases for CRSwNP. However, there is no evidence to support the use of monoclonal antibodies for patients with CRSsNP (Klimek *et al*., 2019) All biologics are for long-term treatment, very expensive and therefore, not used in first-line.

Dupilumab is a human monoclonal antibody that targets and inhibits the IL-4/IL-13 signaling pathway by binding to the α-subunit of the IL-4 receptor. Approved since November 2019, Dupilumab is indicated for the treatment of severe CRSwNP, particularly in cases where the disease remains uncontrolled despite treatment with oral glucocorticosteroids and/or surgical interventions (Pfaar *et al.*, 2023).

The monoclonal anti-IL-4Rα antibody was initially investigated in CRSwNP in connection with severe eosinophilic asthma (Wenzel *et al.*, 2016), but also in a randomized phase II DBPC study in patients with nasal polyps (Bachert *et al*., 2020). Dupilumab, administered subcutaneously once a week for 16 weeks in addition to mometasone nasal spray, demonstrated significant improvement in the primary endpoint of endoscopic polyp score. Additionally, it showed notable benefits in secondary endpoints, including symptom score, olfactory function, and nasal airflow (Bachert *et al.*, 2020; Klimek *et al.*, 2022).

Omalizumab is a recombinant, humanized anti-IgE monoclonal antibody approved since August 2020 for the treatment of severe CRSwNP (Gevaert *et al.,* 2020). Omalizumab binds to immunoglobulin E (IgE), preventing its attachment to FcεRI, the IgE receptor on mast cells and basophils (Pfaar *et al*., 2023).

Mepolizumab is a humanized monoclonal antibody (IgG1, kappa) that targets human interleukin-5 (IL-5) (Han *et al.,* 2021). Approved since November 2021, Mepolizumab is indicated as an adjunctive treatment to nasal corticosteroids for severe CRSwNP that remains uncontrolled despite corticosteroid therapy and/or surgery (Pfaar *et al.*, 2023). The anti-IL-5 antibody resulted in a significant reduction in polyp size following administration (Gevaert *et al*., 2011).

Reslizumab is a monoclonal anti-IL-5 antibody as well but not approved for the indication of CRSwNP (November 2022) (Pfaar *et al*., 2023).

1.2.7.2 Surgical therapy of CRS

Surgery of the paranasal sinuses is primarily used in chronic and relapsed forms. Surgery is typically indicated when conservative treatments have failed. The decision for endonasal surgery of the paranasal sinuses is based on the medical history and current symptoms, in conjunction with findings from rhinoscopy, endoscopy, and appropriate imaging (CT, DVT, or possibly MRI) (Marple *et al.*, 2009). Based on this information, an individualized surgical strategy is developed, taking into account the specific characteristics of the disease and the patient's anatomy. Currently, the standard approach for surgical treatment of the paranasal sinuses is endoscopic endonasal surgery (Weber & Hosemann, 2015).

The following imminent or manifest complications may occur after surgery:

- **Bleeding**, including more severe injury to the internal carotid artery (A. carotis interna)
- **Orbital injury**, which can lead to diplopia (double vision) or blindness
- **Orbital edema** (“preseptal edema” or “periorbital inflammation”), which may not improve with antibiotic therapy
- **Endocranial complications**, including injury to the base of the skull or brain tissue, which can result in:
    - Meningitis
    - Liquorrhea (cerebrospinal fluid leakage)
    - Epidural abscess
    - Subdural empyema
    - Inflammation of the brain (“cerebritis”)
    - Brain abscess
    - Cavernous sinus thrombosis
- **Infections** of the cranial bone or mucocele (Pfaar *et al.*, 2023).

In a study by Dhamija *et al*., 116,669 patients from 55 healthcare organizations were analyzed for complications during and after surgery. The risk of hemorrhagic complications within 30 days post-surgery was 3.00%, orbital complications had a risk of 0.741%, and skull base complications accounted for 0.212% (Dhamija *et al.,* 2025). Overall, in patients without comorbidities, operation of the paranasal sinuses is successful in about 80% of the cases (Cuevas & Zahnert, 2021).

Over a period of 12 years, approximately 80% of patients with CRSwNP experience a recurrence, and approximately 37% undergo a revision (Bachert and Holtappels 2015). CRSsNP patients experienced six weeks post-surgery a decreased need to blow their nose from 37% to 23.5%, to sneeze from 33.3% to 23.3%, a post-nasal discharge from 40% to 10%, and a thick nasal discharge from 26.6% to 17% (Romano *et al.,* 2025).

1.3 Endotyping

Chronic rhinosinusitis (CRS) is primarily categorized into three main clinical phenotypes: CRS without nasal polyps (CRSsNP), CRS with nasal polyps (CRSwNP), and allergic fungal rhinosinusitis (AFRS). Within this framework, there are specific subphenotypes, such as “cystic fibrosis CRS” and “aspirin-exacerbated respiratory disease (AERD),” as well as less well-defined subtypes like “CRS vasculitis” and “CRS sarcoidosis” (Cho *et al.,* 2020). This medical thesis focuses on the first two phenotypes, including healthy controls.

Additionally, CRS can be characterized by three endotypes—T1, T2, and T3—based on gene expression profiles of the cells and cytokines involved in nasal tissue inflammation. Endotype T1 is associated with defense against intracellular bacteria and viruses, T2 is linked to responses against helminth infections and plays a role in allergic diseases, and T3 is involved in acute inflammatory and host defense responses (Klingler *et al.*, 2021).

1.3.1 Clinical classification of endotypes in CRS

Histologically, CRSwNP is characterized by subepithelial and perivascular infiltration of inflammatory cells, accompanied by an edematous stroma. Activated T lymphocytes drive the associated immune response (Fokkens *et al.*, 2020). In chronic sinusitis and nasal polyps, T-cell subpopulations are categorized into CD8-positive (CD8+) T-suppressor cells and CD4+ T-helper cells. The CD4+ T-helper cells are further divided into several subsets, including Th1, Th2, Th9, Th17, Th22, and follicular T-helper (Tfh) effector cells (Annunziato & Romagnani, 2009; Zygmunt & Veldhoen, 2011). In CRSwNP, the balance between T-helper cell subtypes is disrupted by persistent inflammatory processes. The most frequently observed endotype is characterized by a Th2-dominated and eosinophilic cell pattern, with elevated production of interleukins IL-4, IL-5, and IL-13 (Scheckenbach & Wagenmann, 2016). Polyclonal antibodies of the IgE type or antibodies directed against *Staphylococcus aureus* can also be detected. Less frequently, an endotype characterized by Th1-dominated cell formation and the production of IFN-γ and TNFα is observed (Koennecke *et al.,* 2018; Tomassen *et al.*, 2016).

There are also numerous inflammatory endotypes with intermediate and mixed forms (Koennecke *et al.*, 2018; Tomassen *et al.*, 2016). A barrier dysfunction resulting from persistent inflammation renders the mucosa permeable to various antigens, such as allergens, bacterial or fungal antigens, and nanoparticles (Fokkens *et al.*, 2020). Furthermore, both B cells and the antibodies of the IgA, IgG, and IgE types produced by B cells are found to be elevated in nasal polyps (Klimek *et al.*, 2019).

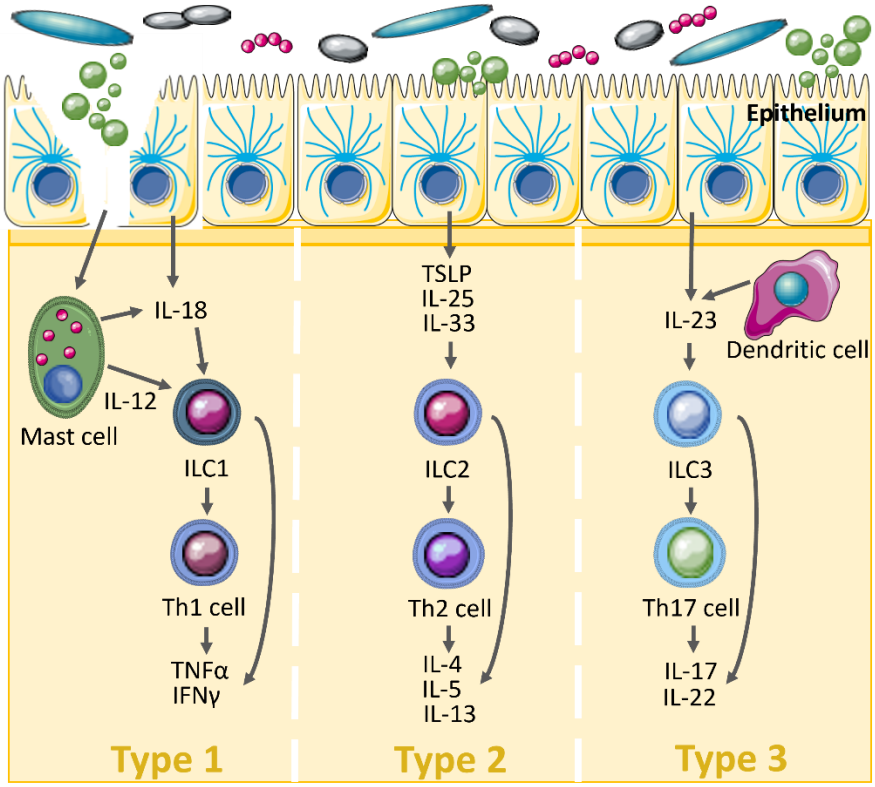

Figure 1.3.1: Physiologic immune responses within the nasal mucosa are perfectly synchronized to fight pathogens. On the left side the Type 1 responses are directed against intracellular pathogens, most commonly viruses. The key cytokines are TNFα and IFN-γ. In the center Type 2 responses are activated to fight large, extracellular parasites. The key cytokines are IL-4, IL-5 and IL-13. On the right side Type 3 responses are directed against extracellular bacteria and fungi. The key cytokines are IL-17 and IL-22. Each immune response is mediated by an innate lymphocyte subset (ILC1, 2 and 3 respectively) that is linked to a corresponding delayed T helper subset (Th1, Th2 and Th17, respectively) - modified according to (Fokkens *et al.*, 2020).

Studies indicate that CRS is characterized by a chronic inflammatory response that typically involves the Type 1 (T1), Type 2 (T2), or Type 3 (T3) endotypes, either alone or in combination. **Figure 1.3.1** illustrates that the primary cytokines activated during T2 inflammation are IL-4, IL-5, and IL-13. Additionally, eosinophils and mast cells are activated and recruited. Patients with a pure or mixed T2 endotype often exhibit higher resistance to current therapies and have a higher recurrence rate compared to those with T1 or T3 endotypes. Furthermore, the intensity of inflammation can vary among patients with T2 CRS, suggesting the presence of distinct subtypes within this category (Fokkens *et al.*, 2020).

These circumstances present a challenge in providing personalized therapy for each individual patient. Therefore, suitable biomarkers are required for each endotype, such as differently regulated genes, as demonstrated by (Klingler *et al.*, 2021).

1.3.2 Detection of endotype markers for CRS

To detect endotype markers, various methods and samples were utilized. For instance, Klingler *et al.* collected nasal lavage fluid from patients before surgery, as well as ethmoid

tissue samples during surgery, alongside swabs from both control patients and those with CRS. They assessed gene expression profiles using commercial ELISA (Enzyme-Linked Immunosorbent Assay), Luminex assays, real-time quantitative RT-PCR (qRT-PCR), and microarray analysis (Klingler *et al.*, 2021).

In contrast, Kato *et al.* employed advanced techniques such as genomics (transcriptomics), proteomics, and metabolomics to study biological systems. These approaches helped identify previously unrecognized mechanistic pathways in health and disease and to establish endotypes within CRS (Kato *et al.*, 2022). Proteomic analysis of nasal mucus in CRS reveals insights into immunological and metabolic tissue remodeling. Transcriptomic studies using microarrays and RNA sequencing have effectively characterized specific phenotypes, such as CRSwNP and CRSsNP, as well as distinct endotypes, including T2 and non-T2 (T1 and T3). These studies also aid in identifying potential endotypic biomarkers in CRS (Kato *et al.*, 2022).

Stevens *et al.* investigated the associations between inflammatory endotypes and clinical presentations in CRS. They measured mRNA and protein levels for endotypic markers in ethmoid and nasal polyp tissues. For endotype T1, they observed high gene expression and protein levels of IFN-γ. Endotype T2 was characterized by elevated CLC mRNA and ECP levels, while endotype T3 showed increased gene expression and protein levels of IL-17A (Klingler *et al*., 2021; Stevens *et al.*, 2019).

As outlined in section 1.2.5 regarding pathophysiology, patients with T2 endotype inflammation are more likely to present with nasal polyps, asthma, smell loss, and allergic mucin among all CRS patients. Stevens *et al*. also noted that T1 endotype inflammation is more prevalent in females, while the presence of pus was significantly associated with T3 endotype inflammation. However, no significant differences among the three inflammatory endotypes were found in terms of nasal congestion, purulent nasal drainage, sinus pressure, headache, fatigue, ear fullness, ocular symptoms, or history of Functional Endoscopic Sinus Surgery (FESS) (Stevens *et al*., 2019).

The study by Klingler *et al*. concentrated on CRSsNP, a more complex phenotype, by examining tissue from various sinonasal biopsy sites. This approach revealed tissue-specific molecular differences, such as variations in the expression of host defense molecules, highlighting the underlying heterogeneity of inflammation in CRSsNP (Klingler *et al*., 2021). Therefore, biopsy specimens from three anatomical structures—inferior turbinate tissue, uncinate tissue, and ethmoid tissue (ET)—as well as nasal lavage fluid, were used for further analyses. The study found that ET exhibited both the highest level of inflammation and the greatest heterogeneity, suggesting that ET is the most informative sinonasal tissue for studying the pathogenesis of CRSsNP (Klingler *et al.*, 2021). For the identification of potential biomarkers, Klingler *et al.* employed real-time qRT-PCR, microarray analysis, and protein

assays. In addition, to the known endotype-specific cytokines and immunoglobulins described in section 1.3.1, they discovered that IFN-γ, CXCL9, and CXCL10 were significantly elevated in T1 CRSsNP compared to controls, non-T1 CRSsNP, and CRSwNP. For the T2 endotype, gene levels of *CLC, IL-13*, and *CCL26* were elevated in ET and NP from CRSwNP patients. *CLC* and *CCL26* could serve as biomarkers in nasal lavage fluid (NLF) to predict the T2 endotype in CRS tissue. In tissue from patients with T3 CRSsNP, genes such as *IL-17F, CSF3*, *SAA1, IL-1β,* and *IL-6* were identified as potential biomarkers. „However, the concentrations of *SAA, IL-1β*, and *IL-6* did not show significant elevation in the samples of NLF from patients with T3 CRSsNP“, so that *CSF3* emphasized to be the best biomarker tested to predict the T3 endotype in CRS tissue (Klingler *et al.*, 2021).

This medical doctoral thesis builds on the results of Klingler *et al.* to investigate whether the identified biomarkers can be detected in our CRS patient cohort using atraumatic sampling methods, such as swabs, and cost-effective qRT-PCR analysis for rapid and straightforward risk stratification. This approach aims to identify potential biomarkers and facilitate the selection of appropriate therapies, particularly when considering the use of expensive biologics.

1.4 Influence of SARS-CoV-2 entry receptor, ACE2, on CRS endotypes

Although it is known that CRS patients can be infected by various viruses, there is no established evidence that CRS itself serves as a comorbidity or risk factor for COVID-19. On the contrary, some studies suggest that CRS may potentially have a protective role against COVID-19 infection (Akhlaghi *et al.,* 2021; Workman & Bhattacharyya, 2022). Data from Chinese studies show that CRS prevalence of 6.1% of COVID-19 patients is similar to the prevalence of 8% in the general population in China without any severe COVID-19 outcome (Wang *et al.*, 2020). For asthmatic patients similar results were reported. Asthma is a known comorbidity in CRS patients and associated with T2 inflammation as described in chapter 1.2.4 (Chhiba *et al.*, 2020).

SARS-CoV-2 uses the angiotensin converting enzyme 2 (ACE2) as cellular receptors to enter host cells and the expression of *ACE2* facilitates viral replication in airway epithelium possibly leading to infection (Hoffmann *et al.*, 2020; Liu *et al.*, 2020). *ACE2* is a 40 kb gene located on chromosome Xp22 (Donoghue *et al.*, 2000; Tipnis *et al.*, 2000). The human ACE2 is a type I transmembrane glycoprotein composed of 805 amino acids. As a carboxypeptidase, it cleaves a single residue from angiotensin II to produce angiotensin (1-7) and from angiotensin I to produce angiotensin (1-9). Angiotensin II plays a critical role in the renin-angiotensin-aldosterone system (RAAS) by mediating vasoconstriction and contributing to the overactivation of RAAS, which is implicated in conditions such as heart failure, hypertension, and renal disease (Chen & Hao, 2020; Patel *et al.*, 2017). RAAS is a hormone system that

regulates blood pressure and fluid-salt balance. In conclusion, ACE2 is a potential key player keeping the balance of RAAS by countering the activities of Ang II (Yao *et al.*, 2020).

„It is considered that factors leading to upregulation of *ACE2* expression in host cells are likely to be risk factors for COVID-19 infection“ (Walls *et al.,* 2020). Evidence indicates that endotypes T1 and T2 are associated with downregulation of *ACE2* gene expression in the airway epithelium leading to a potential lower risk for COVID-19 infection among CRS patients (Sajuthi *et al.*, 2020). Different working groups could show that in epithelial cells of the respiratory airways including nasal polyps, the *ACE2* expression on mRNA and protein levels was reduced compared to noneosinophilic CRS and control subjects (Marin *et al*., 2021; Ziegler *et al.*, 2020). Similar findings were reported in asthmatic patients (Bradding *et al.*, 2020; Wakabayashi *et al.*, 2021).

This down regulation of *ACE2* in CRSwNP patients may be a protective effect against binding of SARS-CoV-2 to the airway epithelium as well as the negative correlation between ACE2 and the levels of cytokines IL-4, IL-5, and IL-13 associated with T2 inflammation (Kimura *et al.,* 2020). For example, Jackson *et al.* could show that the stimulation of IL-13 suppresses *ACE2* expression in nasal and bronchial epithelial cells (Jackson *et al.*, 2020; Kimura *et al.*, 2020; Sajuthi *et al.*, 2020). Increased T2 inflammation in CRS patients may downregulate the expression of *ACE2* in airway epithelial cells, potentially providing a protective effect against COVID-19 infection (**Figure 1.4**). Conversely, IFN-γ, a T1 inflammatory cytokine, is associated with increased *ACE2* expression in the nasal respiratory tissue of CRSwNP patients, suggesting that IFN-γ may induce *ACE2* expression in upper airway cells (Ziegler *et al.,* 2020).

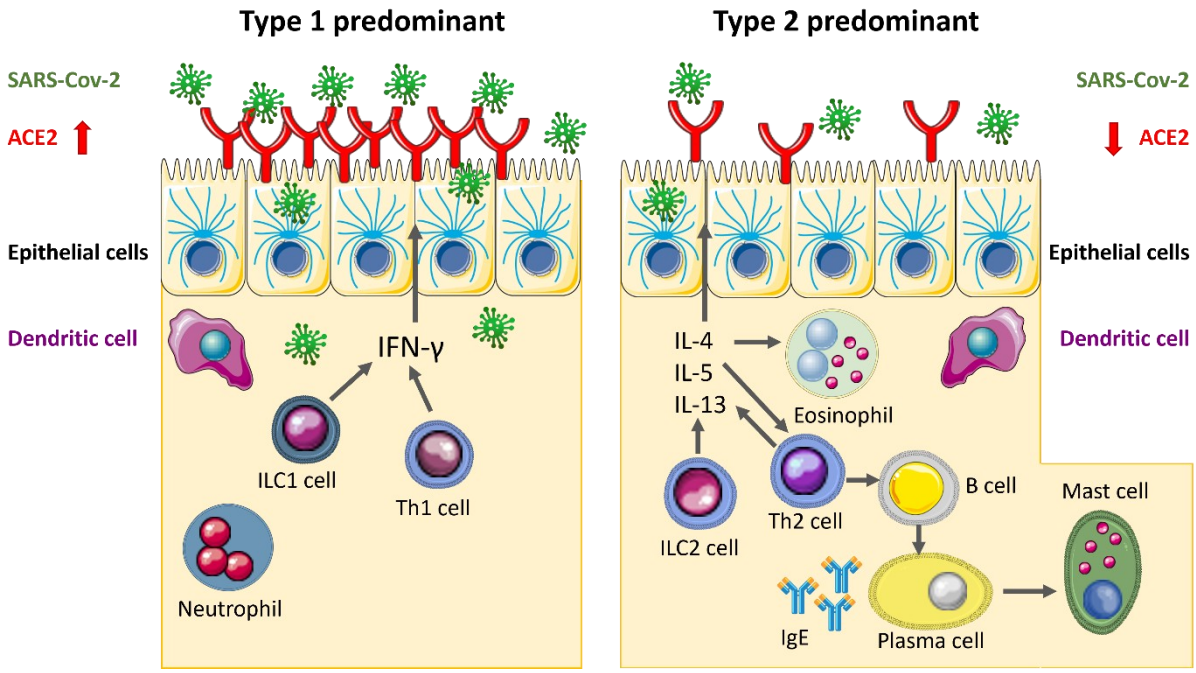

Figure 1.4: Influence of SARS-CoV-2 infection. On the left-side patients without CRSwNP (type 1 predominant) and on the right-side patients with CRSwNP (type 2 predominant) are shown. Type 2 eosinophilic inflammation may decrease *ACE2* expression in airway epithelial cells, which potentially protects these cells against COVID-19 infection. ILC, innate lymphoid cell - modified according to (Ziegler *et al.,* 2020)

Jackson *et al*. reported that in asthmatic children nasal corticosteroids were not associated with alterations in *ACE2* mRNA expression profiles of airway epithelial cells (Jackson *et al.*, 2020) and that dexamethasone treatment did not change *ACE2* mRNA expression in cultured human nasal epithelial cells *in vitro* as well (H. Wang, J. Song, Y. Yao, *et al*., 2021). In addition, dexamethasone and budesonide did not directly influence *ACE2* expression but inhibit IFN-γ-induced expression of *ACE2* (M. Wang *et al.,* 2021).

Current studies indicate that *ACE2* expression was reduced in eosinophilic nasal polyps and that biologics like omalizumab, mepolizumab and dupilumab which suppress T2 and eosinophilic inflammation possibly leading to higher *ACE2* expression and increased risk for COVID-19 infection (H. Wang, J. Song, L. Pan, *et al.,* 2021). However, up to now no official studies are available investigating a higher risk of COVID-19 infection by T2 biologics in CRSwNP patients. „Although the European Academy of Allergy and Clinical Immunology position paper recommends that biologics should be stopped until patients with COVID-19 symptoms are completely recovered“ (Xu *et al.,* 2021).

The rare scientific information available on CRS in the context of COVID-19 and *ACE2* expression underscores the importance of the investigations conducted in this medical doctoral thesis.

1.5 Aims of the medical doctoral thesis

The introductory sections of this thesis clearly highlight the urgent need for personalized medicine in managing chronic rhinosinusitis with nasal polyps (CRSwNP) and without nasal polyps (CRSsNP). While current treatment strategies are tailored to address the specific CRS phenotype, there is a growing need for endotype-specific therapies, such as biologics, to enhance treatment efficacy and patient outcomes.

Furthermore, there is a pressing need to develop personalized diagnostic approaches that are both atraumatic and cost-effective. For instance, non-invasive methods such as swab-based sampling combined with rapid, affordable techniques like RT-PCR could significantly improve the speed and accuracy of CRS diagnostics in clinical practice.

Additionally, the relationship between cytokine-triggered inflammation and the role of the SARS-CoV-2 entry receptor, ACE2, in CRS remains poorly understood. While the inflammatory mechanisms of RAAS are well-documented, the specific function of ACE2 in CRS has not been extensively studied. Given that ACE2 has garnered significant attention due to the COVID-19 pandemic, understanding its role and interactions within the context of CRS is crucial.

This medical doctoral thesis aims to advance the understanding of endotypes and their associated genetic markers in CRS. By identifying and characterizing molecular biomarkers corresponding to the specific endotype present in individual patients, this research aims to enhance personalized medicine to improve treatment efficacy and patient outcomes in CRS. (Fokkens *et al.*, 2020). Therefore, this thesis aims to answer the following questions:

1. Proof of principle: Do endotype- and RAAS-specific biomarkers exist that can be reliably detected and verified using real-time qRT-PCR?

2. Does the choice of tissue and swab sampling methods influence the identification and quantification of biomarkers?

3. Can the selected biomarkers effectively differentiate between CRS phenotypes (CRSwNP and CRSsNP) and healthy controls?

4. Can the selected biomarkers distinguish between the three identified endotypes in CRS (T1, T2, and T3)?

5. Is there a distinct role of *ACE2* in CRS, and can it serve as a biomarker to differentiate CRS patients from healthy controls?

2 Material

2.1 Patient cohort

To establish a comprehensive dataset for analysis, a total of 462 samples were collected, with 200 samples obtained retrospectively and 262 samples prospectively. These samples were collected as nasal swabs in the outpatient clinic and mucosal tissue samples in the operating room of the otorhinolaryngology department. The collected samples were surplus to the requirements for disease validation and histopathological examination and would have otherwise been discarded. With patient consent, these samples were stored in a biobank for research purposes.

All samples were sourced from fully competent adults, and patient data was pseudonymized by encrypting with numerical codes. This process ensures that the data sets extracted from the University Clinic Düsseldorf's patient database cannot be traced back to individual patients by others.

The research was approved by the ethics committee of the medical faculty of Heinrich Heine University Düsseldorf. The ethics vote was granted on July 26th, 2021, under study number 2021-1460, for the project titled "Investigation of the Modulations and Interactions of Inflammatory Reactions of the Mucous Membranes in the Upper Respiratory Tract."

2.2 Chemicals

2.2.1 General chemicals

Identifier	Company	Ordernumber
2-Propanol for cleaning	Merck, Darmstadt, Germany	67-63-0
DEPC-treated water	invitrogen, Carlsbad, CA, USA	750024
Ethanol	Merck, Darmstadt, Germany	1.00983.2511
β-Mercaptoethanol	Merck, Darmstadt, Germany	15433.0100

Abbreviations: DEPC - Diethyldicarbonat, CA - California

2.2.2 Specific chemicals

Identifier	Company	Ordernumber
TaqMan Fast Advanced Master Mix	ABI by Thermo Fisher Scientific	4444557
10x M -MuLV Reverse Transcriptase Buffer	NEB, Frankfurt a. M., Germany	B0253S
QIAzol Lysis Reagent	Qiagen, Hilden, Germany	79306

Abbreviations: NEB - New England Biolabs, a.M. - am Main, ABI - applied biosystems

2.3 Nucleic acids

2.3.1 TaqMan probes for real time qrtRT-PCR

Identifier	Company	Ordernumber	Assay ID	Description
β-ACT	ABI by Thermo Fisher Scientific	4331182	Hs01060665	TaqMan Gene Expr. Assay
CXCL10	ABI by Thermo Fisher Scientific	4331182	Hs00171042	TaqMan Gene Expr. Assay
CSF3	ABI by Thermo Fisher Scientific	4331182	Hs99999083	TaqMan Gene Expr. Assay
CCL26	ABI by Thermo Fisher Scientific	4331182	Hs00171146	TaqMan Gene Expr. Assay
CXCL9	ABI by Thermo Fisher Scientific	4331182	Hs00171065	TaqMan Gene Expr. Assay
CLC	ABI by Thermo Fisher Scientific	4331182	Hs00171342	TaqMan Gene Expr. Assay
ACE2	ABI by Thermo Fisher Scientific	4331182	Hs01085333	TaqMan Gene Expr. Assay
IFN-γ	ABI by Thermo Fisher Scientific	4331182	Hs00989291	TaqMan Gene Expr. Assay
IL-1β	ABI by Thermo Fisher Scientific	4331182	Hs01555410	TaqMan Gene Expr. Assay
IL-6	ABI by Thermo Fisher Scientific	4331182	Hs00174131	TaqMan Gene Expr. Assay
TNF-α	ABI by Thermo Fisher Scientific	4331182	Hs00174128	TaqMan Gene Expr. Assay
IL-4	ABI by Thermo Fisher Scientific	4331182	Hs00174122	TaqMan Gene Expr. Assay
IL-5	ABI by Thermo Fisher Scientific	4331182	Hs01548712	TaqMan Gene Expr. Assay
IL-13	ABI by Thermo Fisher Scientific	4331182	Hs00174379	TaqMan Gene Expr. Assay
ACE	ABI by Thermo Fisher Scientific	4331182	Hs00174179	TaqMan Gene Expr. Assay

Abbreviations: ABI – applied biosystems

2.3.2 Other nucleic acids and nucleotides

Identifier	Company	Ordernumber
dNTP Mix 10 mM	Thermo Scientific, Dreieich, DE	R0192
Random Hexamer Primer 0.2 µg/µl	Thermo Scientific, Dreieich, DE	SO142

2.3.3 Kits and other materials

Kit Identifier	Company	Ordernumber
NucleoSpin RNA Kit	Macherey-Nagel, Düren, Germany	740955.250

2.4 Enzymes

Identifier	Company	Ordernumber
M-MuLV Reverse Transcriptase (200 U/µl)	NEB, Frankfurt a. M., Germany	M0253L

Abbreviations: NEB - New England Biolabs, a.M. - am Main

2.5 Software and hardware

2.5.1 Software and databases

Software and Databases	Available at	Reference
R 4.0.3	http://www.r-project.org/	(Ihaka & Gentleman, 1996)
UniProt	https://www.uniprot.org/	The UniProt Consortium
The Gene Ontology Resource	http://geneontology.org/	Ashburner et al., 2000
Microsoft® Excel® 365 MSO	https://www.microsoft.com/de-de	Microsoft Cooperation

2.5.2 Hardware

Hardware	Company
7900 HT Fast Real-Time PCR System	ABI, Carlsbad, CA, USA
Centrifuge 5403	Eppendorf, Hamburg, Germany
Centrifuge 5417R	Eppendorf, Hamburg, Germany
NanoDrop Spectrophotometer ND-1000	PeqLab, Erlangen, Germany
TissueRuptor	Qiagen, Hilden, Germany

Abbreviations: ABI – applied biosystems

3 Methods

3.1 Methods of molecular biology

3.1.1 Isolation of RNA

Before RNA isolation, tissue samples were homogenized for 30 seconds at highest level using the TissueRuptor (Qiagen). RNA was extracted from swab and tissue patient samples according to the NucleoSpin® RNA kit protocol from Macherey-Nagel following the single steps:

1. Lyse cells with 350 µl RA1 and 3.5 µl β-mercaptoethanol and mix
2. Filtrate lysate by centrifugation with 11,000 x g for 1 minutes
3. Adjust RNA binding conditions with 350 µl 70% ethanol and mix
4. Bind RNA by loading on the filter and centrifugation with 11,000 x g for 30 seconds
5. Desalt silica membrane with 350 µl MDB and centrifugation with 11,000 x g for 1 minutes
6. Digest DNA with 95 µl DNase reaction mixture at room temperature for 15 minutes
7. Wash and dry silica membrane: 1st wash with 200 µl RAW2, 2nd wash with 600 µl RA3 and 3rd wash with 250 µl RA3; after 1st and 2nd wash centrifuge at 11,000 x g for 30 seconds and after the 3rd wash centrifuge at 11,000 x g for 2 minutes
8. Elute highly pure RNA with 30 µl RNase-free water followed by centrifugation with 11,000 x g for 1 minute

3.1.2 Concentration and purity determination of nucleic acids

The concentration of nucleic acids was determined using the NanoDrop™ spectrophotometer with absorption at 260 nm. 1 µl per RNA sample was placed between the two optical fibers. The ratio 260/280 served as estimation for the purity of the RNA patient samples. 2.0 and above was accepted as “pure” for the RNA samples used in this thesis.

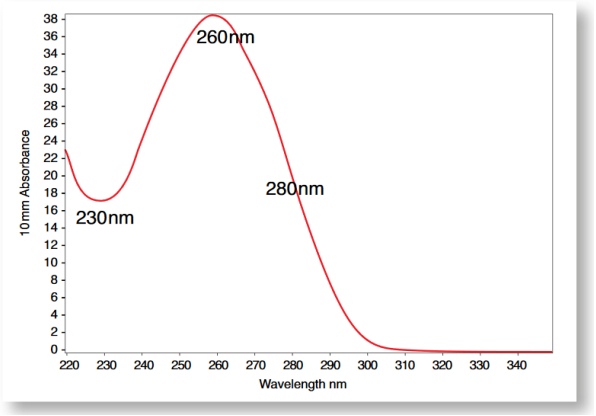

Figure 3.1.2: Typical nucleic acid spectrum.

Although purity ratios are important indicators of sample quality, the best indicator of RNA quality is functionality in the downstream application of interest (e.g., real-time PCR).

3.1.3 cDNA synthesis of total RNA

0.2, 0.5 or 1 µg total RNA according to the availability was used for cDNA synthesis and diluted into 15.5 µl overall. To each RNA sample the cDNA synthesis master mix (10 x M-MuLV reverse transcriptase buffer (NEB, Frankfurt a. M., Germany), dNTPs 10 mM each, random hexamer primer 0.2 µg, M-MuLV reverse transcriptase 200 U (NEB, Frankfurt a. M., Germany)) was added and reverse transcribed using the following parameters: 25°C for 5 minutes, 42°C for 60 minutes, 65°C for 20 minutes and chilled at 4°C.

3.1.4 Quantitative reverse transcription-real time-PCR (qrt-RT-PCR)

For quantitative reverse transcription-real time-PCR, the TaqMan™ Gene Expression Assays (Applied Biosystems by Thermo Fisher Scientific) were used. One reaction was performed in 20 µl overall containing ~ 5% of cDNA mix (1 µl), 10 µl TaqMan™ Fast Advanced Master Mix, 0.5 µl TaqMan™ probe and 8.5 µl H_2O. The qrtRT-PCR was performed using the following parameters: 1) 50 °C for 2 minutes, 2) 95 °C for 3 minutes, 3) 95 °C for 15 seconds, 4) 60 °C for 45 seconds, repeating steps 3 and 4 for 40 cycles. The successfully finished run was analyzed to generate the corresponding cycle-threshold values (Ct-values) within the

amplification curves. For the performance of the qrt-RT-PCR, the 7300 HT Real-Time PCR System (Applied Biosystems) was used.

3.1.5 RNA expression analysis using qrRT-PCR

Quantitative reverse transcription Real-Time Polymerase Chain Reaction (qrRT-PCR) was employed to detect and quantify the expression profiles of the genes of interest. For this analysis, hydrolysis TaqMan™ probes were utilized, specifically targeting the following genes: *β-ACT, CXCL10, CSF3, CCL26, CXCL9, CLC, ACE2, IFN-γ, IL-1β*, and *IL-6*. Each probe is composed of a 5' reporter fluorophore (FAM) and a 3' quencher, attached to a short oligonucleotide that is complementary to the target sequence. The principle of fluorescence resonance energy transfer (FRET) is employed in this assay. In the intact TaqMan probe, the fluorophore and quencher are in close proximity, which prevents the emission of fluorescence. During the PCR amplification process, the DNA polymerase enzyme hydrolyzes the TaqMan probe while the primers extend and amplify the target sequence. This hydrolysis separates the fluorophore from the quencher, resulting in an increase in fluorescence that can be measured after each cycle.

To calculate the relative quantification of gene expression, the following steps were taken:

Average Ct values for technical replicates: For each patient sample, triplicate measurements were obtained. The average Ct (cycle threshold) value was calculated from these triplicates to ensure accuracy and consistency.

Normalization: To account for variability and experimental errors, the expression levels of the target genes were normalized against a non-regulated housekeeping gene, *β-Actin*. This normalization helps to reduce variance and control for differences in sample quantity and quality.

Calculation of ΔCt values: The relative quantification, termed as ΔCt (Delta Ct), was calculated by subtracting the average Ct value of the housekeeping gene (*β-Actin*) from the average Ct value of the target gene. This step provides the difference in the threshold cycle between the target gene and the reference gene. The formula for calculating ΔCt is as follows:

$$\Delta Ct = Ct_{target} - Ct_{housekeeping}$$

Where:

- Ct_{target} is the average Ct value of the target gene.
- $Ct_{housekeeping}$ is the average Ct value of the housekeeping gene (*β-Actin*).

In the analysis, the symbol Δ (delta) represents the difference between two values. Since Ct-values are inversely proportional to gene expression levels (i.e., a higher Ct-value indicates lower gene expression, and a lower Ct-value indicates higher gene expression), it was necessary to adjust the Ct-values for accurate visualization.

Steps for visualization:

Reverse Ct-values: To properly illustrate the data in heatmaps and boxplots, the Ct-values were reversed to reflect expression levels correctly. This reversal was achieved by subtracting each Ct-value from a constant value of 20.

$$Adjusted\ Ct = 20 - Ct$$

This adjustment ensures that higher gene expression (originally indicated by lower Ct-values) is represented as a higher value, making it easier to interpret in visual formats.

Rationale for the constant value: The number 20 was chosen as a constant because, after normalization with the housekeeping gene, no Ct-values exceeded 20. This choice keeps all adjusted Ct-values positive and maintains consistency with the original Ct-values.

Example calculation: If a normalized Ct-value was 15, the adjusted Ct-value would be:

$$Adjusted\ Ct = 20 - 15 = 5$$

Purpose: By reversing the Ct-values, the data visualization (e.g., heatmaps and boxplots) will correctly represent higher gene expression with higher values, making the interpretation more intuitive.

3.1.6 Statistical testing and data analysis

Statistical testing:

ΔΔCt calculation:

$$\Delta\Delta Ct = \Delta Ct_{patient\ sample} - \Delta Ct_{healthy\ control}$$

This calculation assesses the relative difference in gene expression between patient samples and healthy controls.

Fold change in gene expression:

$$Fold\ Change = 2^{-\Delta\Delta Ct}$$

This transformation converts ΔΔCt values into fold changes, quantifying the change in gene expression relative to healthy controls.

Data transformation: Fold change values were transformed using the natural logarithm before performing t-tests to meet the normality assumption required for parametric testing.

Correlation coefficient (r): The correlation coefficient was calculated using Microsoft Excel to determine the strength and direction of linear relationships between gene expression levels or between gene expression and clinical parameters.

Hierarchical clustering and heatmap illustrations:

Hierarchical clustering: Genes and samples were clustered based on expression profiles to identify patterns and group similar data together.

Heatmap illustrations: Heatmaps were generated to visually represent gene expression levels across samples, with color gradients indicating the magnitude of expression.

Statistical analysis:

Software: Hierarchical clustering, heatmap generation, and statistical tests were performed by implementing R code (R version 4.0.3; Ihaka & Gentleman, 1996).

R Programming: The use of R provided flexibility for advanced statistical analysis and visualization (R version 4.0.3; Ihaka & Gentleman, 1996).

t-Test:

Purpose: The t-test, developed by William Sealy Gosset under the pseudonym Student, compares the means of one or two populations to determine if there are significant differences between them.

Application: The independent two-sample t-test (two-sided, assuming unequal variances) was used to compare gene expression levels between different groups, including endotypes and phenotypes.

Assumptions:

Continuity: Data should be continuous.
Random sampling: Samples must be randomly selected.
Homogeneity of variance: Variability within each group should be similar.
Normality: Data distribution should be approximately normal.
Independence: For two-sample t-tests, samples should be independent.

Significance: A p-value < 0.05 indicates a statistically significant difference between the groups. In null hypothesis significance testing, a smaller p-value suggests a greater likelihood of rejecting the null hypothesis, which posits no difference in gene expression between the compared groups.

3.2 Bioinformatics

3.2.1 Hierarchical clustering methodology (algorithm and source code)

Software and Tools:

- Agglomerative, unsupervised hierarchical clustering was performed using R version 4.0.3 (R Project for Statistical Computing, Ihaka & Gentleman, 1996).
- The `heatmap.2` function from the `gplots` package was employed to generate enhanced heatmaps.

Heatmap visualization:

Color scheme: High signal intensities were displayed in red, while low signal intensities were depicted in blue, creating a false-color image to visually represent gene expression levels.

Clustering algorithm:

Agglomerative clustering: The process begins with each element (e.g., gene or sample) as an individual cluster. Clusters are then merged iteratively into progressively larger clusters.

Dendrograms: Displayed on the left and/or top of the heatmaps, dendrograms illustrate the clustering process and the hierarchical relationship between clusters.

Distance metrics:

Euclidean distance: Calculated as follows:

$$d(p,q) = \sqrt{\sum_{i=1}^{n}(p_i - q_i)^2}$$

where p and q represent the signal intensities of two RNAs.

Linkage criteria:

Complete linkage (maximum distance): The distance between two clusters X and Y was determined using:

$$D(X,Y) = max_{x \in X \; y \in Y} \, d\,(x,y)$$

where $d(x,y)$ represents the Euclidean distance between elements x and y from clusters X and Y, respectively.

Distance and clustering methods:

Distance methods: Included "euclidean", "maximum", "manhattan", "canberra", "binary", and "minkowski".

Hierarchical clustering methods: Included "ward.D", "ward.D2", "single", "complete", "average", "mcquitty", "median", and "centroid".

Selection criteria:

Method selection: Despite testing various distance and hierarchical clustering methods, results were consistently similar, indicating stable data across methods.

Chosen methods: Euclidean distance and complete linkage were selected due to their clarity in separating endo- and phenotypes, as these methods provided the most distinct and interpretable clusters.

R source code:

```
#Loading packages: gplots, Biobase and tools
library(gplots)
library(Biobase)
library(tools)
#Loading data for heatmap generation
CRSCluster <-
  read.table("C:/CRS-Heatmap-.txt",
  header=TRUE, sep="\t", na.strings="NA", dec=".", strip.white=TRUE)
row.names(CRSCluster) <- CRSCluster$Name
CRSCluster <- CRSCluster[,2:92]
CRSClusterMatrix <- data.matrix(CRSCluster)

#Definition of distance and clustering methods
mydist <- function(x){
 return(dist(x, method="euclidian"))
}
myclust <- function(x){
 return(hclust(x, method="complete"))
}
```

```
#Loading names of diseases
Diseases <-
        read.csv("C:/Disease-Names.txt",
        header=TRUE, sep="\t", strip.white=TRUE)

#Define a color for each phenotype for each patient of the heatmap
color.map <- function(diseases) { if (diseases=="CRSsNP") " slateblue1 " else if
(diseases=="CRSwNP") " lightskyblue3 " else " black "}

patientcolors <- unlist(lapply(Diseases$diseases, color.map))
colors <- seq(0,21, length.out = 101)

#Generation of the heatmap and definition of the appearance
heatmap.2 (CRSClusterMatrix, col = bluered (100), na.color = " grey85 ", main = "Chronische
Rhinosinusitis", xlab = "Patient Samples", ylab = "Regulated Genes",
                na.rm = TRUE, key = TRUE, keysize = 0.7, symkey = FALSE, key.title = NA,
                key.xlab = NA, trace = "none", tracecol = "white", margins = c(5, 6), dist=mydist,
                hclustfun=myclust, ColSideColors = patientcolors, cexRow=0.9, cexCol=0.9,
                breaks = colors)

#Loading data of the legend
Legende <- read.table("C:/Chronische-Sinusitis-Legende.txt",
        header=TRUE, sep="\t", strip.white=TRUE)

#Define a color for each phenotype of the legend
color.map.legende <- function(trans) { if (legend=="CRSsNP") " slateblue1 " else if
(legend=="CRSwNP") " lightskyblue3 " else " black "}
legendcolors <- unlist(lapply(Legende$legend, color.map.legende))

#Show legend next to the heatmap
par (xpd = TRUE)
legend(-0.13, -0.05, legend = Legende$legend, text.col = "black", bty = "o", box.lwd = 0.5, fill
= legendcolors, title ="Diseases", horiz = FALSE, cex = 0.5)
```

4 Results

4.1 Detailed patient cohort description

As detailed in the Methods chapter, a total of 200 patient samples were collected retrospectively and 262 samples were collected prospectively, along with their associated clinical data. The sampling materials include cells obtained from swabs and tissues. Tissue samples consist of mucosal cells extracted during operations at the ENT (ear, nose, and throat) department. All samples, including those from swabs, are stored in a biobank with the patients' consent.

Retrospectively, this doctoral thesis includes all adult patients who provided consent and were treated at the ENT department between January 1, 2010, and October 27, 2022. Prospectively, it includes all adult patients who provided consent and were treated at the ENT department after October 27, 2022. All patient data sets have been pseudonymized (encrypted with numerical codes) to ensure that individuals cannot be identified by third parties.

4.1.1 Filtering of patient samples by origin and corresponding diseases

Figure 4.1.1 provides an overview and detailed counts of the patient samples collected for this thesis, categorized by clinical data. In total, 462 patient samples were collected, comprising 389 swab samples and 73 tissue samples. Among the swab samples, there are 40 from patients with CRSwNP, 11 from patients with CRSsNP, and 338 from patients with other conditions. For the tissue samples, there are 16 from CRSwNP patients, 3 from CRSsNP patients, and 54 from patients with other diseases. The CRS samples are highlighted with bold boxes as they are of primary interest for this thesis.

The overall sample count was categorized by material—swab versus tissue—to assess whether swabs might be sufficient or even preferable for establishing an atraumatic diagnostic method. The number of tissue samples is approximately one-fifth of the swab samples, due to the fact that conservative therapies are typically administered before an operation is considered.

Additionally, **Figure 4.1.1** outlines the most frequently occurring diseases within the patient cohort. Samples categorized under "other diseases" primarily include patients who received sampling for other purposes than CRS. Comorbidities of interest were documented in thes patients like allergies, asthma/COPD, heart disease, hypertension, diabetes, and obstructive sleep apnea syndrome (OSAS). No samples from tumors or acute inflammatory diseases were included.

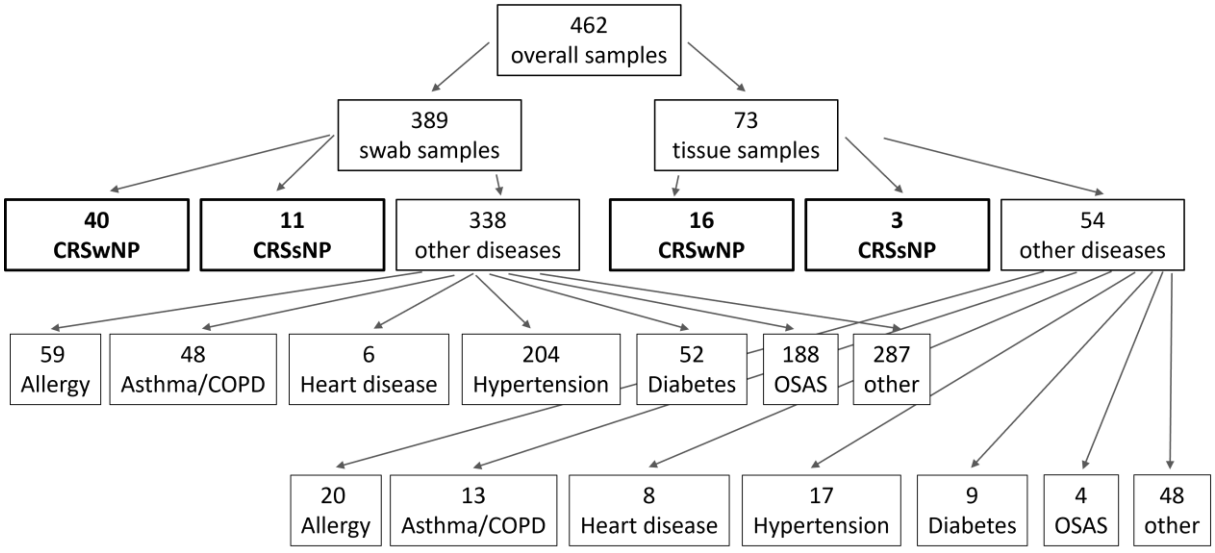

Figure 4.1.1: Overview of collected patient samples and the main diseases. Overall, 462 samples were analysed by origin, chronic rhinosinusitis (CRS) with nasal polyps (wNP), without nasal polyps (sNP) and other diseases and comorbidities including predominantly allergy, asthma/COPD, heart disease, hypertension, diabetes and OSAS (obstructive sleep apnea syndrome).

To gain further insights into the patient samples used for detailed analyses, the next chapter will provide a more in-depth characterization of all collected patient samples, with a particular focus on those from CRS patients.

4.1.2 Characterization of patient samples for further analyses

Table 4.1.2 details the collected samples described in section 4.1.1, categorized by material origin, patient characteristics, and diseases, and compared across CRSwNP, CRSsNP patients, and healthy controls (HC). These three patient groups are the primary focus of the detailed analyses. For each group, the following variables are listed: material origin, age, gender, BMI (body mass index), smoking status, alcohol consumption, disease comorbidities, and medication use, including anticoagulants, steroids, insulin, and Dupilumab. Dupilumab is the only biological agent administered to patients in this cohort.

The CRS patient cohort includes a broad age range from 19 to 70 years. There is a notable predominance of men with CRSwNP, who are nearly three times more frequent than women. The BMI of CRS patients ranges from 20 to over 40 kg/m² and is similar between the CRSwNP and CRSsNP groups. A significant proportion of patients across all samples suffer from hypertension and OSAS. Within the CRS patient groups, there is a higher prevalence of asthma and allergy relative to the number of samples. For the healthy controls, samples were selected from individuals who had no indication for surgery and only minor illnesses or conditions that are not known to influence CRS. Additionally, healthy controls were matched to CRS patients in terms of age and BMI distributions, and the cohort was adjusted to include a higher proportion of males to align with the CRS groups.

Table 4.1.2: Patient cohort in detail. Listed are the numbers of samples for the most important characteristics, diseases and medications of all samples. Separately listed are CRS patient samples and healthy controls used for further analyses.

	All samples	CRSwNP	CRSsNP	HC
Number of swabs	389	40	11	40
Number of tissues	73	16	3	-
Age (years)	19-89	19-70	30-55	23-71
Male/Female	315/147	43/13	8/6	25/15
BMI (kg/cm^2)	14,3-65	20,3-43,5	20,3-41,5	22,9-65
Smoking	65	3	0	4
Alcohol	50	6	1	7
Allergy	79	6	2	6
OSAS	192	1	0	22
Asthma/COPD	61	7	3	0
Hypertension	221	5	2	23
Heart disease	14	1	0	3
Diabetes mellitus	61	2	1	8

Other disease	335	22	10	15
Anticoagulation	84	1	1	6
Steroid	30	0	0	0
Insulin	17	1	0	0
Dupilumab	2	1	0	3

Abbreviations: CRSwNP, chronic rhinosinusitis with nasal polyp; CRSsNP, chronic rhinosinusitis without NP; HC, healthy control; BMI, body mass index; OSAS, obstructive sleep apnea syndrome; COPD, chronic obstructive pulmonary disease

Among the CRS patient samples, there are 16 CRSwNP and 3 CRSsNP patients from whom one swab and one tissue sample were collected for initial analysis (details provided in chapter 4.3.3). All available CRS swab samples were subsequently included in further analyses starting from chapter 4.4. Before conducting these in-depth examinations, it is essential to identify appropriate genes that can serve as endotype-specific biomarkers (Klingler *et al.*, 2021). This identification will be achieved as proof of principle through qRT-PCR, as outlined in chapter 4.2.

4.2 Identification of endotype-specific genes via qRT-PCR

To enhance the characterization of individual endotypes and develop improved therapies for CRS in the future, it is crucial to identify endotype-specific biomarkers. For this purpose, 3 to 5 genes were selected for each endotype, with an additional 2 genes chosen for RAAS-analysis. It is established that *IFN-γ* and *TNF-α* are associated with endotype T1 inflammation, *IL-4, IL-5*, and *IL-13* with endotype T2 inflammation, and *IL-1β* and *IL-6* with endotype T3 inflammation. Furthermore, Klingler *et al.* identified *CXCL9* and *CXCL10* as the most promising biomarkers for T1, *CCL26* and *CLC* for T2, and *CSF3* for T3. Therefore, these 12 genes were selected to determine which can be routinely detected by qRT-PCR within our patient cohort and potentially serve as endotype-specific biomarkers.

Table 4.2 lists all tested genes, including their names and descriptions, categorized by endotype and RAAS. The genes *CXCL9, CXCL10, IFN-γ, CCL26, CLC, CSF3, IL-1β*, and *IL-6* were detected in at least 95% of all CRS patient samples and healthy controls, with a Ct value < 30, and are thus included in further analyses.
Additionally, *ACE* and *ACE2*, which are key components of RAAS, were tested by qRT-PCR. *ACE2*, which also serves as an entry receptor for SARS-CoV-2, was the only gene routinely detected in the majority of CRS patient samples and healthy controls with a Ct value < 30. Consequently, the following 9 potential biomarkers - *CXCL9, CXCL10, IFN-γ, CCL26, CLC*, *CSF3, IL-1β, IL-6,* and *ACE2* - were selected for more detailed analysis.

Table 4.2: Endotype-specific genes. Listed are all tested genes via qRT-PCR and sorted according to their endotypes. Genes detected in at least 95% of all patient samples with a Ct-value < 30 are used for further analyses.

Endotype	Gene name	Gene description	Ct-value	used for analysis
T1	*CXCL10*	C-X-C Motif Chemokine Ligand 10	> 25	yes
	CXCL9	C-X-C Motif Chemokine Ligand 9	> 25	yes
	IFN-γ	Interferon Gamma	> 23	yes
	TNF-α	Tumor Necrosis Factor Alpha	> 35	no
T2	*CCL26*	C-C Motif Chemokine Ligand 26	> 27	yes
	CLC	Charcot-Leyden Crystal Galectin	> 25	yes
	IL-4	Interleukin 4	> 40	no
	IL-5	Interleukin 5	> 34	no
	IL-13	Interleukin 13	> 36	no
T3	*CSF3*	Colony Stimulating Factor 3	> 24	yes
	IL-1β	Interleukin 1 Beta	> 20	yes
	IL-6	Interleukin 6	> 22	yes
RAAS/ COVID-19	*ACE*	Angiotensin I Converting Enzyme	> 35	no
	ACE2	Angiotensin I Converting Enzyme 2	> 25	yes

Abbreviations: T1, T2, T3, (endo-) type 1, 2, 3; RAAS, renin-angiotensin-aldosterone-system

4.3 Data analysis of material origins and CRS diseases

For the initial analysis of CRS phenotypes and endotypes regarding biomarker identification, a dataset was created consisting of 19 swab/tissue pairs. This means that one swab and one tissue sample were collected from each of 19 patients, resulting in a total of 38 samples. Gene expression analyses for all 9 genes (*CXCL9, CXCL10, IFN-γ, CCL26, CLC, CSF3, IL-1β, IL-6,* and *ACE2*) were conducted on these 19 swab/tissue pairs. Both swab and tissue samples from each patient were included in the first dataset and examined concerning material origin, as detailed in chapter 4.3.1.

Figure 4.3.1 illustrates these data through hierarchical clustering, accompanied by a heatmap. Each column in the heatmap represents a patient sample, and each row represents a gene expression profile. The hierarchical clustering is positioned above the heatmap for material origin and on the left side for genes and endotypes. The color code in the upper right corner indicates which colors correspond to swab or tissue material and to which disease (CRSwNP

or CRSsNP). In the upper left corner, the gene expression levels are depicted, showing the distribution of expression values across samples, following a proximate Gaussian curve. Low expression values (0-5) are shown in blue, measured for a few patients; middle expression values (5-15) are represented in light blue, white, and light red, observed in the majority of samples; and high expression values (15-20) are displayed in red, noted for a few patients. Gene names are listed on the right side of the heatmap, along with their associated endotypes (T1, T2, or T3), indicating which genes are potential biomarkers for these endotypes.

4.3.1 Comparison of gene expression profiles concerning material origin

To obtain an overview of the data, an unsupervised hierarchical clustering was performed on the 9 selected genes across the 19 swab/tissue pairs (one swab and one tissue collected from each patient), considering the material origins. This analysis is presented in **Figure 4.3.1**, accompanied by the corresponding heatmap.

The hierarchical clustering shown at the top of the figure reveals that swabs and tissues generally cluster separately from each other. This indicates that the two sample types form distinct groups based on the different expression profiles of the 9 measured genes. For instance, *IL-1β* is highly expressed in 12 swab samples but exhibits middle to low expression in most tissue samples. Conversely, *CXCL9* is highly expressed in more tissue samples compared to swabs. Additionally, *CCL26* and *CLC* (associated with endotype T2) demonstrate lower expression in swab samples relative to tissue samples. The clustering on the left side of the heatmap highlights the presence of two main clusters: one cluster, marked in bold, includes a mixture of endotypes T1 and T3, while the other cluster consists solely of endotype T2, forming a distinct group.

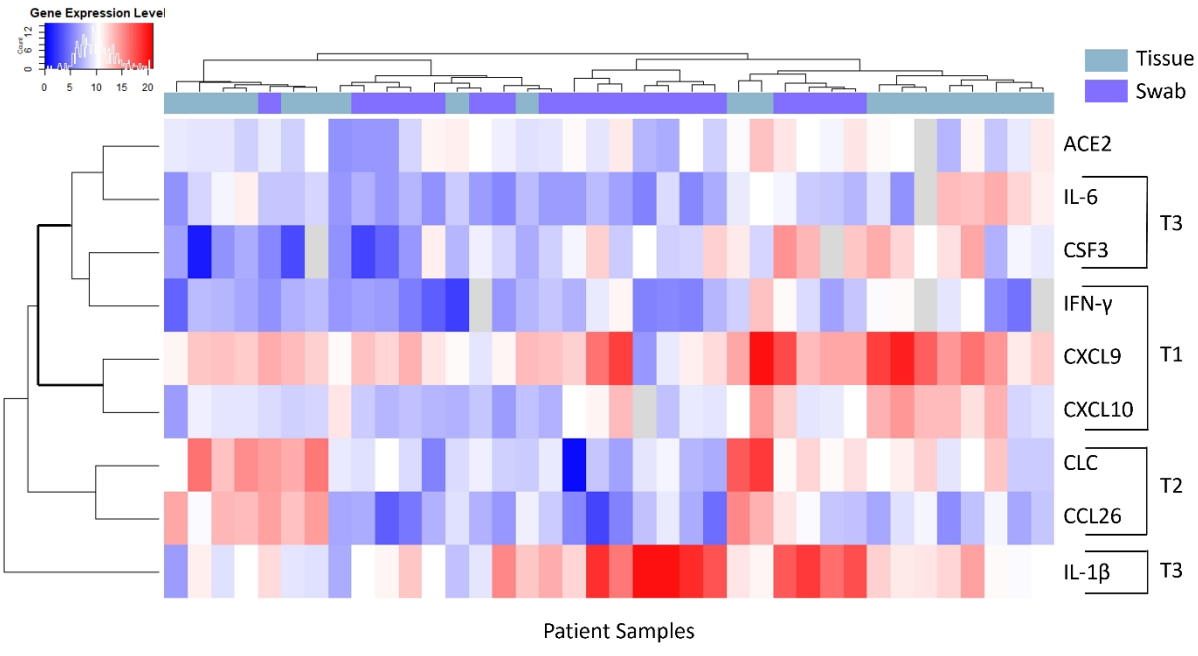

Figure 4.3.1: Gene expression analysis of CRS patient samples concerning material origin using unsupervised hierarchical clustering and heatmap analysis. This analysis includes 9 gene expression profiles for 19 swab/tissue pairs (one swab and one tissue sample collected from each patient), resulting in a total of 38 samples. Gene expression levels were measured using qRT-PCR. The hierarchical clustering displayed at the top and left side of the figure represents the distance or similarity between the gene expression profiles of patient samples and the individual genes, respectively. Below the top clustering, the colored legend bar and the corresponding heatmap are presented. The gene expression spectrum in the upper left corner of the heatmap illustrates high expression levels in red and low expression levels in blue. Undetected genes are shown in light grey. Signal intensities were normalized for each gene using the housekeeping gene *β-Actin*.

The clustering and heatmap presented in **Figure 4.3.1** offer a comprehensive overview by displaying all measured data in a visually comparable format. However, this representation is complex and may make it challenging to discern all details. A simplified depiction of the data concerning material origin is provided in the following chapter.

4.3.2 Correlation calculation between tissue and swab samples

To gain a deeper insight into the data and to validate the results from **Figure 4.3.1**, a correlation analysis was performed between tissue and swab samples across the 38 patient samples for the 9 genes of interest. The calculated correlation coefficient was $r = 0.4002835$ with a t-statistic of $t = 5.2051095$ and a p-value of $p = 0.0000007$.

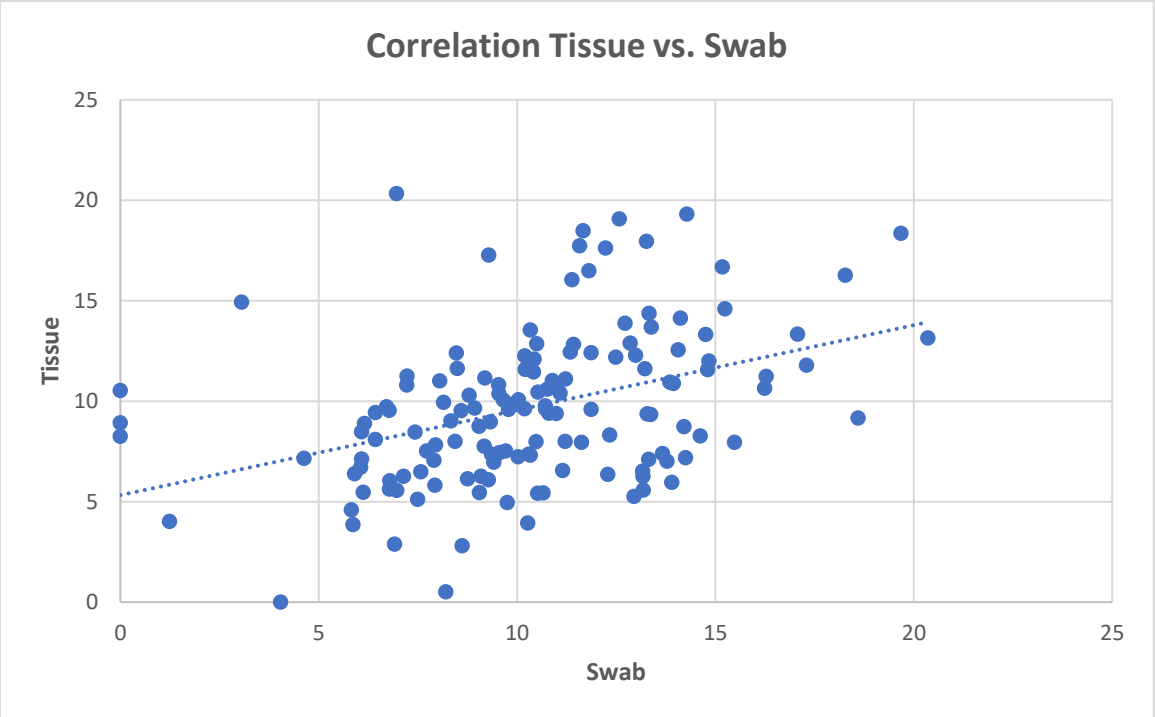

Figure 4.3.2: Correlation calculation between gene expression profiles from tissue and swab samples. The x-coordinate shows the number of swab samples and the y-coordinate the number of tissue samples correlated to each other. Every blue dot indicates one measured expression value for one swab and one tissue sample generated by qRT-PCR. The regression line reinforces the correlation.

The correlation coefficient can range from -1 to +1, indicating either a negative or positive correlation. An r-value closer to zero signifies a weaker linear correlation, and an r-value of 0 implies no linear dependence. The calculated r-value of 0.4 indicates a very weak correlation between gene expression profiles from tissue and swab samples, which aligns with the clustering analysis results showing that tissue and swab samples group separately.

Figure 4.3.2 illustrates that only a small proportion of the expression values (blue dots) lie along the regression line, with most values dispersed throughout the plot. This visual representation supports the finding of a very weak correlation. The result is further validated by the highly significant p-value of 7×10^{-7}.

4.3.3 Comparison of gene expression profiles of CRS diseases

Chapters 4.3.1 and 4.3.2 focused on the gene expression analysis concerning material origin and evaluated the suitability of both materials for further analyses and diagnostics. This chapter, however, shifts the focus to examining the same data with respect to the two CRS diseases, CRSwNP and CRSsNP. The aim is to determine whether these diseases can be distinguished based on their gene expression profiles.

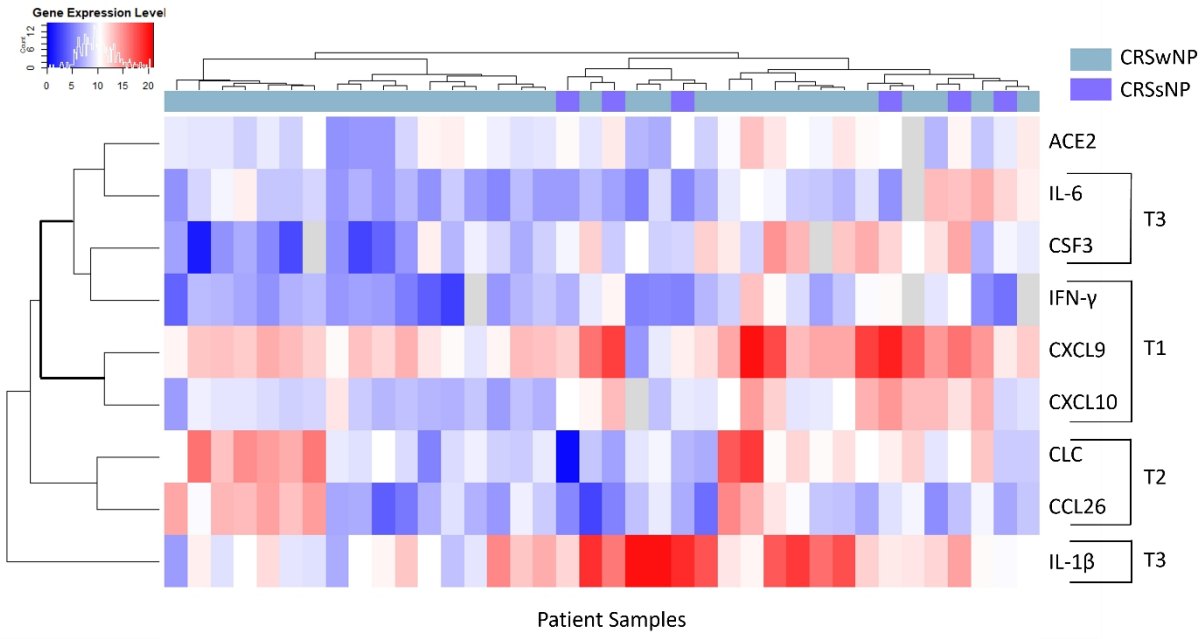

Figure 4.3.3: Gene expression analysis of CRS patient samples concerning disease origin using unsupervised hierarchical clustering and heatmap analysis. This analysis presents 9 gene expression profiles for 19 swab/tissue pairs (one swab and one tissue sample collected from each patient), resulting in a total of 38 samples. Gene expression values were measured using qRT-PCR. The clustering displayed at the top and left sides of the figure represents the distance or similarity between gene expression profiles of the patient samples and between individual genes, respectively. Below the top clustering, the colored legend bar and corresponding heatmap are provided. The gene expression level spectrum in the upper left corner of the heatmap visualizes high expression levels in red and low expression levels in blue. Undetected genes are shown in light grey. Signal intensities were normalized for each gene using the housekeeping gene *β-Actin*.

The same dataset used for the comparison of both diseases is presented here. The figure for clustering and the heatmap appears as shown in chapter 4.3.1, but the legend bar now indicates samples based on their disease classification rather than material origin. Notably, only 3 swab/tissue pairs were available for CRSsNP, compared to 16 swab/tissue pairs for CRSwNP.

Figure 4.3.3 shows that the clustering on the left side of the heatmap indicates that most genes cluster according to their endotypes. Endotype T2 forms a distinct cluster separate from T1 and T3 due to differing gene expression profiles, as previously discussed in chapter 4.3.1. The clustering at the top of the heatmap reveals that the two diseases do not form separate groups; instead, CRSsNP samples are interspersed among CRSwNP samples, reflecting similar underlying expression profiles. Despite this, some distinctions between the diseases are evident. Genes associated with endotype T2, namely *CCL26* and *CLC*, are generally lower expressed or down-regulated in CRSsNP samples, while they are more highly expressed or up-regulated in CRSwNP samples. Conversely, *IL-6* and *CSF3* (endotype T3), along with *IFN-γ* (endotype T1), exhibit lower expression levels in CRSwNP compared to CRSsNP.

To explore these effects in more detail, a larger sample size and an equivalent number of healthy controls were utilized. Since only a limited number of tissue samples were available from CRS patients and none from healthy controls (as they did not require surgical treatment), only swab samples were used for further analysis (see chapter 4.4). Additionally, swabs are preferable for establishing appropriate diagnoses due to their ease of use and non-invasive nature.

4.4 Comparison of CRS patient samples with healthy controls concerning phenotypes

The general explanation of the elements depicted in **Figure 4.4** is provided in chapter 4.3. This chapter will focus on detailing the differences compared to the previous clustering and heatmap figures. The corresponding analysis relied solely on swab samples, as tissue samples from healthy individuals were not available.

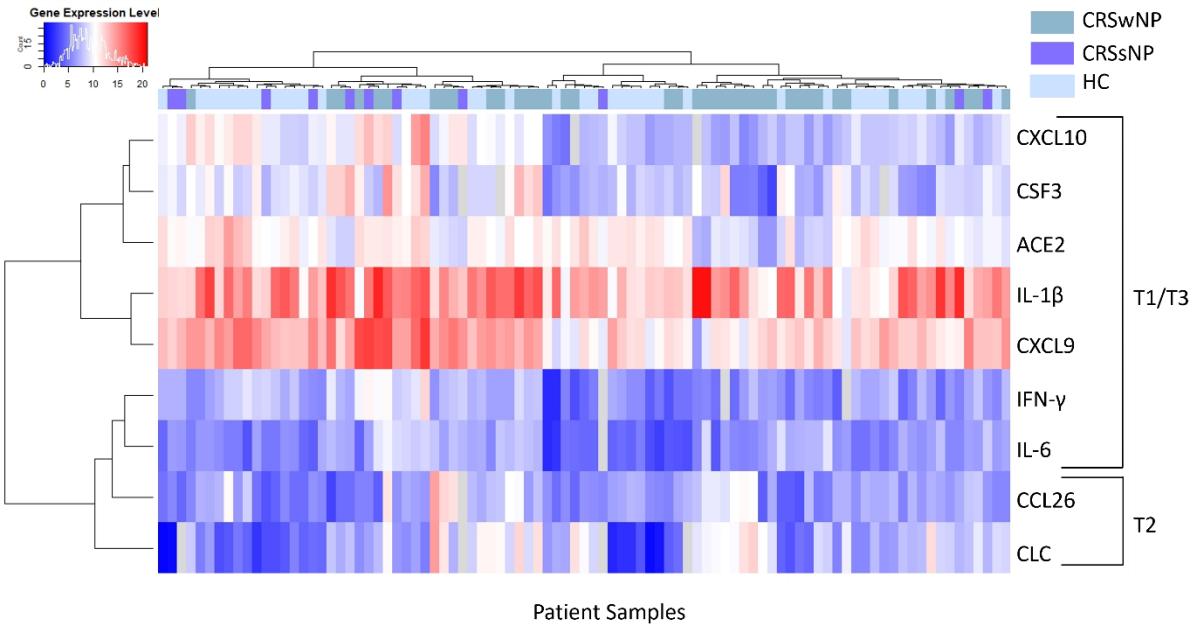

Figure 4.4: Gene expression analysis of CRS patient samples compared with healthy controls. Shown are the 9 gene expression profiles for 40 CRSwNP samples, 11 CRSsNP samples, and 40 healthy controls (HC) using unsupervised hierarchical clustering and a heatmap. Gene expression values were measured with qRT-PCR. The clustering shown at the top and left of the figure represents the distance or similarity between gene expression profiles of patient samples and between individual genes, respectively. Below the top clustering, the colored legend bar and corresponding heatmap are presented. The gene expression level spectrum in the upper left corner of the heatmap visualizes high expression levels in red and low expression levels in blue. Undetected genes are shown in light grey. Signal intensities were normalized for each gene using the housekeeping gene *β-Actin*.

Figure 4.4 presents the hierarchical clustering and corresponding heatmap for the 9 genes of interest across 40 CRSwNP samples, 11 CRSsNP samples, and 40 healthy controls. The heatmap reveals that *CXCL10, CSF3*, and *ACE2* have expression values predominantly in the middle range (5-15), transitioning from light blue through white to light red. In contrast, *IL-1β* and *CXCL9* show high expression values (> 15, in red), while *IFN-γ, IL-6, CCL26*, and *CLC* exhibit low expression values (< 5, in blue).

The clustering on the left side of the heatmap indicates that genes associated with endotype T2 continue to cluster together, as previously shown in **Figures 4.3.1** and **4.3.3**. Most genes associated with endotypes T1 and T3, including *ACE2*, form a distinct cluster due to similar gene expression profiles.

Regarding the clustering at the top of the heatmap, 17 of the 40 CRSwNP samples cluster near to each other, whereas the healthy controls are not clearly separated from the disease samples and are particularly intermixed with both, CRSwNP and CRSsNP samples. Despite the somewhat ambiguous separation of individual phenotypes and endotypes, notable differences between the groups are apparent. These differences will be explored in more detail in chapters 4.5 and 4.6.

4.5 Detailed comparison of CRS patient samples with healthy controls focused on endotypes

To gain a deeper understanding of the data and identify endotypes differentially regulated for each phenotype, the expression values obtained from qRT-PCR were visualized using boxplots, as illustrated in this chapter and chapter 4.6.

A boxplot graphically represents the distribution of the data. It displays key statistical measures, including the median, first and third quartiles, and potential outliers. The box spans the interquartile range (IQR), which is the distance between the first quartile (25th percentile) and the third quartile (75th percentile), covering the middle 50% of the data. The length of the box indicates the spread of this central 50% of the data.

The whiskers extend from the edges of the box to show the range of data outside the IQR. Values beyond these whiskers may be considered outliers or extreme outliers. The median, or the second quartile, is the midpoint of the data distribution, with 50% of the values falling below and 50% above it. It provides a robust measure of central tendency, relatively unaffected by outliers, and its position within the box can indicate skewness in the data distribution. If the median is closer to the bottom of the box, the distribution is right-skewed; if closer to the top, it is left-skewed.

The whiskers often span a broader range than the box itself, capturing the variability outside the central 50% of the data.

4.5.1 Identification of statistically significant endotypes for each phenotype

In this chapter, the focus is on determining whether specific endotypes are significantly upregulated or downregulated in distinct phenotypes (HC, CRSsNP, or CRSwNP). To address this, the expression values of genes associated with each endotype were aggregated and analyzed using boxplots.

For each endotype, the expression values of the relevant genes were combined as follows:

- **Endotype T1**: Combined values of *CXCL9, CXCL10*, and *IFN-γ*
- **Endotype T2**: Combined values of *CCL26* and *CLC*
- **Endotype T3**: Combined values of *CSF3*, *IL-1β*, and *IL-6*

This approach allows for the identification of differentially expressed and regulated endotypes across the different phenotypes, as illustrated in **Figure 4.5.1**. A detailed analysis of individual gene expression (not combined into endotypes) is presented in chapter 4.6.

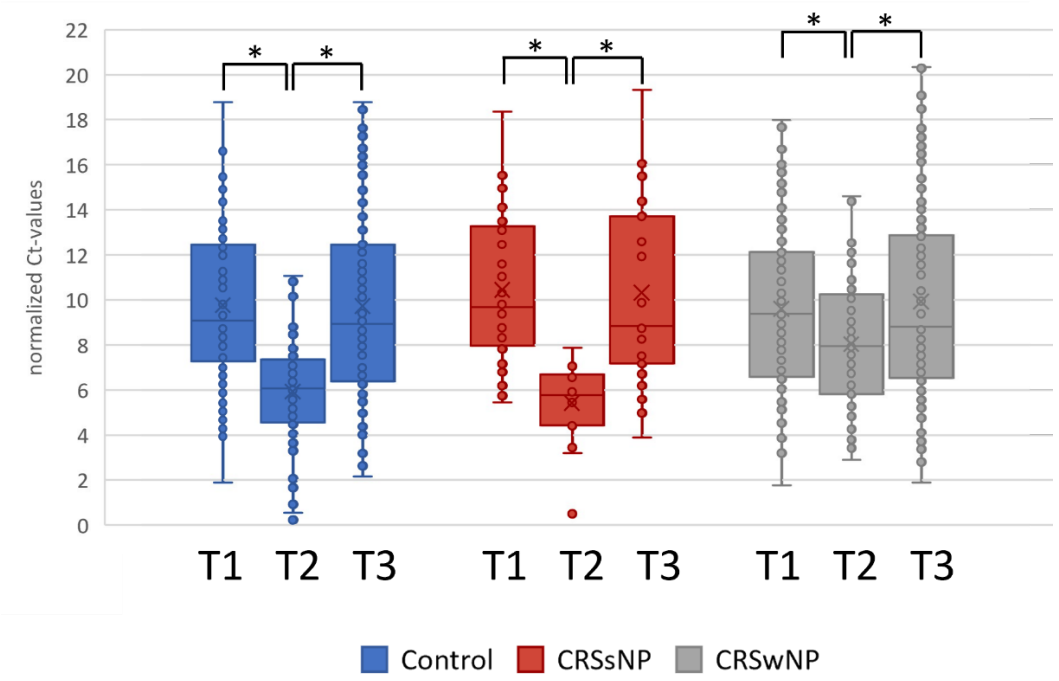

Figure 4.5.1: Boxplots illustrating significantly expressed endotypes for each phenotype. The three endotypes were compared within each phenotype to identify significant differences. Healthy controls are represented in blue, CRSsNP in red, and CRSwNP in grey. Statistically significant differences between endotypes are marked with an asterisk, indicating a significance level of $p < 0.05$. The ordinate of the boxplots represents the expression values, with Ct-values normalized for each gene using *β-Actin* as housekeeping gene.

Figure 4.5.1 displays three boxplots for each endotype across the three phenotypes (HC, CRSsNP, and CRSwNP) to identify differentially expressed endotypes through statistical testing. In all three phenotypes, endotype T2 is significantly lower expressed compared to T1 and T3. However, T1 and T3 do not show significant differences between each other. The significance of T2's lower expression is notably higher in healthy controls and CRSsNP compared to CRSwNP. These findings are consistent with the patterns observed in the clustering and heatmap analyses from the previous chapters.

The calculated fold changes between the three endotypes across the phenotypes - HC, CRSsNP, and CRSwNP - are summarized in **Table 4.5.1.I**. Fold changes indicate whether genes are upregulated or downregulated, with genes associated with the same endotype combined for this analysis. As shown in **Figure 4.5.1**, there are significant differences in fold changes between T1 and T2, as well as between T2 and T3, but not between T1 and T3.

For healthy controls, endotypes T1 and T3 are upregulated by more than 15-fold compared to T2. In CRSsNP, T2 is downregulated by over 20-fold compared to T1 and T3. In CRSwNP, T1 and T3 are upregulated by approximately 2- to 4-fold compared to T2. No significant upregulation or downregulation is observed between T1 and T3.

Table 4.5.1.I: Fold gene expression calculation between the three endotypes. ΔΔCt-values were used to calculate the fold gene expression between the three endotypes analyzed for healthy controls, CRSsNP and CRSwNP. Significant fold changes are marked in bold.

	Fold change	HC	CRSsNP	CRSwNP
T1 vs. T2	**ΔΔCt**	3.9177	5.0679	1.5254
	$2^{-\Delta\Delta Ct}$ / FGE	**15.3486**	**25.6834**	**2.3268**
T1 vs. T3	**ΔΔCt**	0.0170	0.0933	-0.5835
	$2^{-\Delta\Delta Ct}$ / FGE	0.0003	0.0087	-0.3404
T2 vs. T3	**ΔΔCt**	-3.9008	-4.9746	-2.1088
	$2^{-\Delta\Delta Ct}$ / FGE	**15.2159**	**24.7462**	**4.4472**

Abbreviations: FGE, fold gene expression = fold change = $2^{-\Delta\Delta Ct}$; HC, healthy control

Statistical testing results for each endotype compared to the other two endotypes are detailed in **Table 4.5.1.II**. Endotype T2 exhibits extremely significant p-values ranging from $< 5\times10^{-4}$ to 5×10^{-18} when compared to both T1 and T3 across all three phenotypes. In contrast, no significant difference is observed between T1 and T3, which corroborates the findings presented in **Table 4.5.1.I**.

Table 4.5.1.II: Statistic significance calculation for each endotype. All endotypes were compared to each other and tested for significance using the t-statistic and a two-sided t-test for different variances. Significant p-values < 0.05 are written in bold.

	Statistic	HC	CRSsNP	CRSwNP
T1 vs. T2	**df**	197	48	201
	t-statistic	9.56920554	7.130854559	3.56159935
	p-value	**4.6672×10^{-18}**	**4.63436×10^{-9}**	**0.0004602**
T1 vs. T3	**df**	227	58	239
	t-statistic	0.0745177	0.141405891	-0.63962661
	p-value	0.94066409	0.888039312	0.523028
T2 vs. T3	**df**	189	45	207
	t-statistic	-8.2479315	-5.97538092	-3.87285759
	p-value	**2.6798×10^{-14}**	**0.000000339**	**0.00014425**

Abbreviations: df, degree of freedom; p-value, probability value two sided

4.5.2 Identification of statistically significant endotypes between phenotypes

Figure 4.5.2 presents the same boxplots as those shown in chapter 4.5.1, but reordered to focus on the different phenotypes (HC, CRSsNP, and CRSwNP). This reorganization is intended to highlight statistically significant differences between the endotypes across these phenotypes.

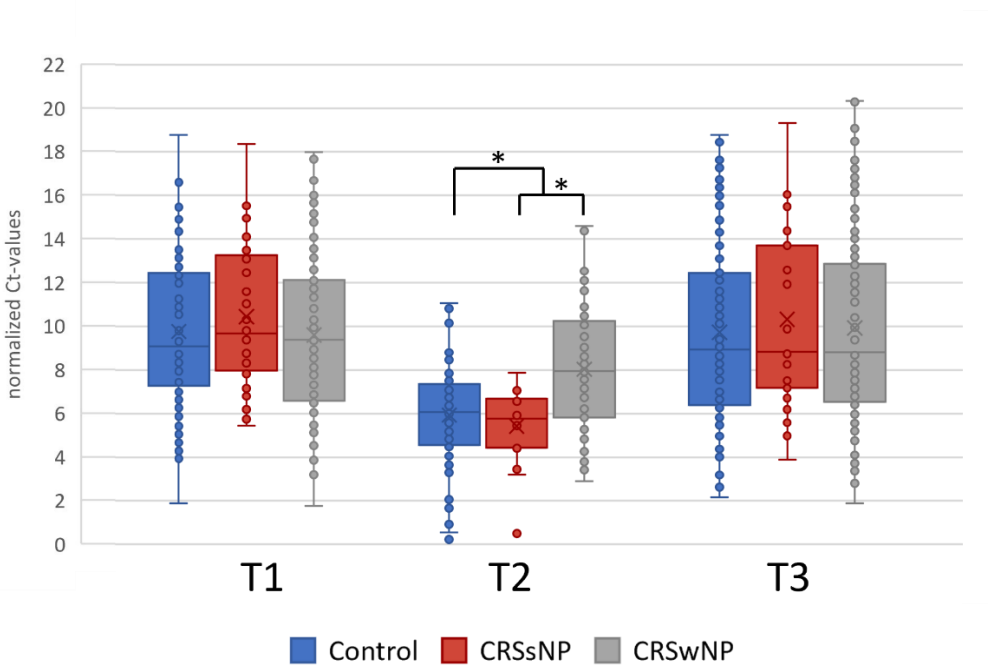

Figure 4.5.2: Boxplots illustrating significantly expressed endotypes across phenotypes. The three phenotypes were compared with respect to the three endotypes to identify significant differences between them. Healthy controls are represented in blue, CRSsNP in red, and CRSwNP in grey. Statistically significant differences between the phenotypes are indicated with an asterisk, signifying a significance level of $p < 0.05$. The ordinate of the boxplots represents the expression values, with Ct-values normalized for each gene using *β-Actin* as housekeeping gene.

As observed in the previous chapter, endotype T2 demonstrates statistically significant differences between healthy controls and both CRS diseases combined, as well as between CRSsNP and CRSwNP (see **Figure 4.5.2**). In contrast, T1 and T3 do not exhibit significant differences in their expression levels across the three phenotypes. Even without statistical analysis, this lack of difference is apparent from the medians of the boxplots for T1 and T3, which are nearly identical.

Table 4.5.2.I: Fold gene expression calculation between the different phenotypes concerning each endotype. ΔΔCt-values were used to calculate the fold gene expression between the different phenotypes concerning the endotypes T1, T2 and T3. Significant fold changes are marked in bold.

	Fold change	T1	T2	T3
HC vs. CRS	**ΔΔCt**	-0.2229	-0.8441	-0.4850
	$2^{-\Delta\Delta Ct}$ / FGE	-0.0497	-0.7124	-0.2352
HC vs. CRSwNP	**ΔΔCt**	0.1367	-2.2557	-0.4638
	$2^{-\Delta\Delta Ct}$ / FGE	0.0187	**5.0882**	-0.2151
HC vs. CRSsNP	**ΔΔCt**	-0.5825	0.5676	-0.5062
	$2^{-\Delta\Delta Ct}$ / FGE	-0.3394	0.3222	-0.2562
CRSwNP vs. CRSsNP	**ΔΔCt**	-0.7192	2.8233	-0.0424
	$2^{-\Delta\Delta Ct}$ / FGE	-0.5172	**7.9711**	-0.0018

Abbreviations: FGE, fold gene expression = fold change = $2^{-\Delta\Delta Ct}$; HC, healthy control

According to **Table 4.5.2.I**, endotype T2 is more than 5-fold downregulated in healthy controls compared to CRSwNP, while CRSwNP is nearly 8-fold upregulated compared to CRSsNP. These findings further support the boxplot representation in **Figure 4.5.2**.

The statistical results for each phenotype comparison based on the endotypes are detailed in **Table 4.5.2.II**. For the statistical analysis, phenotypes were compared across the three endotypes: T1, T2, and T3. This involved comparing the expression values of healthy controls with both CRS diseases combined, as well as comparing CRSwNP with CRSsNP. The analysis used a two-sided t-test for different variances with a significance level of $p < 0.05$. Statistically significant differences were found only for endotype T2, with significant p-values of $< 5 \times 10^{-5}$ between healthy controls and both CRS diseases combined, and between CRSwNP and CRSsNP, as illustrated in **Figure 4.5.2** and reflected in the fold changes in **Table 4.5.2.I**.

Table 4.5.2.II: Statistic significance calculation for each phenotype comparison versus each endotype. All phenotypes were compared to each other and tested for significance using the t-statistic and a two-sided t-test for different variances. Significant p-values < 0.05 are written in bold.

	Statistic	T1	T2	T3
HC vs. CRS	**df**	259	179	255
	t-statistic	-0.039937	-4.354758	-0.54386727
	p-value	0.96817408	**0.0000223**	0.587008
HC vs. CRSwNP	**df**	240	158	242
	t-statistic	0.35411519	-5.31346761	-0.36729982
	p-value	0.72356347	0.00000036	0.71371638
HC vs. CRSsNP	**df**	51	30	50
	t-statistic	-1.0667086	1.028100738	-0.74366629
	p-value	0.29112719	0.312120832	0.46055885
CRSwNP vs. CRSsNP	**df**	53	37	50
	t-statistic	-1.3008313	4.994147282	-0.49330811
	p-value	0.19894367	**0.0000143**	0.62395473

Abbreviations: df, degree of freedom; p-value, probability value two sided

4.6 Identification of statistically significant genes by comparison of the phenotypes

In the previous chapter, the analysis concentrated on the endotypes and phenotypes, examining their statistical significance. This chapter delves deeper into the data, focusing on the identification of statistically significant genes between the phenotypes, independent of endotype classifications.

4.6.1 The special role of *ACE2* concerning phenotypes

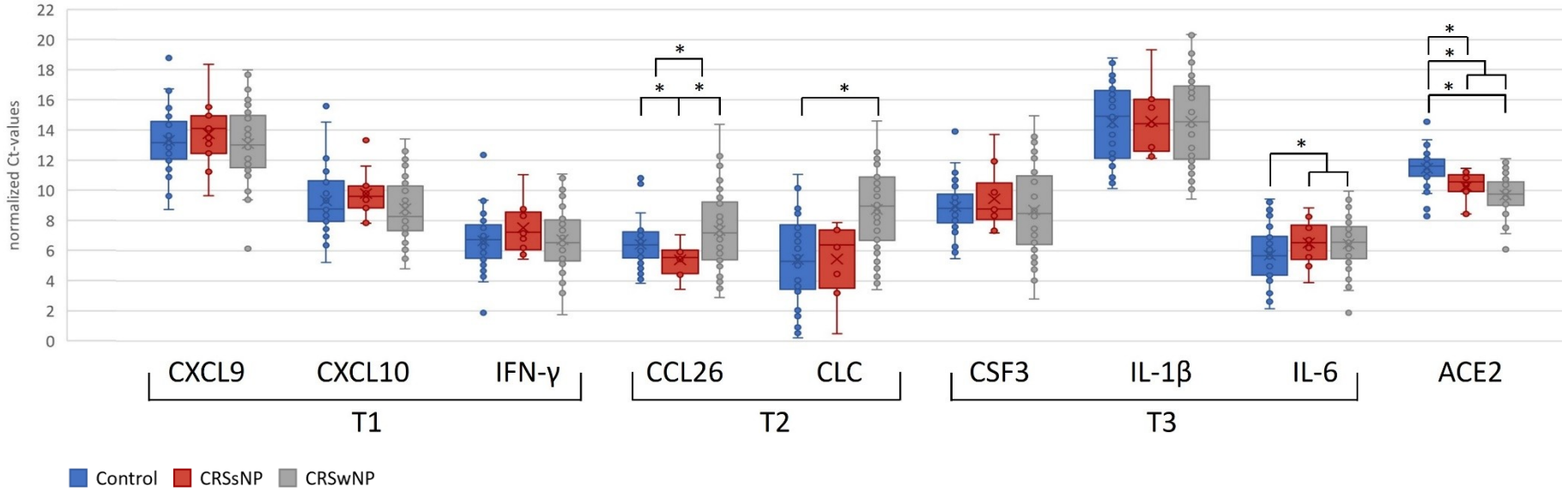

Figure 4.6.1: Boxplots illustrating significantly expressed genes between phenotypes independent from endotypes. These boxplots present gene expression values for the 9 genes of interest across the three phenotypes: healthy controls (blue), CRSsNP (red), and CRSwNP (grey). Statistically significant differences between the phenotypes are indicated by asterisks, with a significance level of $p < 0.05$. The ordinate axis represents the expression values (Ct-values normalized for each gene using *β-Actin* as housekeeping gene).

Figure 4.6.1 displays the gene expression values measured by qRT-PCR for the 9 genes of interest (*CXCL9, CXCL10, IFN-γ, CCL26, CLC, CSF3, IL-1β, IL-6*, and *ACE2*) across the three phenotypes: healthy controls, CRSsNP, and CRSwNP. The boxplots illustrate the comparison of gene expression levels between these phenotypes, with statistical testing performed as outlined in the previous chapter.

Statistically significant differences in expression, with a p-value < 0.05, were observed for *CCL26, CLC, IL-6*, and *ACE2*. As expected, *CCL26* and *CLC*, associated with endotype T2, show significant differential expression between healthy controls and both CRS diseases, reflecting the previously identified differences in cluster and heatmap analyses (chapters 4.3 and 4.4) and boxplot illustrations (chapter 4.5).

IL-6 demonstrates the lowest statistical significance with a p-value of 0.0432, highlighting differences only between healthy controls and both CRS diseases combined. *ACE2* stands out with highly significant p-values $< 5\times10^{-8}$ in comparisons between healthy controls and both CRS diseases, as well as between healthy controls and each CRS subtype (CRSsNP and CRSwNP). Notably, *ACE2* appears to be more highly expressed in healthy controls compared to CRS diseases.

The remaining genes - *CXCL9, CXCL10, CSF3, IFN-γ*, and *IL-1β* - do not exhibit significant differences among the three phenotypes.

Table 4.6.1.I provides a detailed analysis of the fold changes in gene expression for *CCL26*, *CLC*, and *ACE2* across the different phenotypes.

- ***CCL26***, associated with endotype T2, is nearly 5-fold upregulated in CRSwNP compared to CRSsNP. It is slightly downregulated in healthy controls compared to CRSwNP but slightly upregulated in healthy controls compared to CRSsNP.
- ***CLC***, also associated with endotype T2, shows a significant > 11-fold upregulation in CRSwNP compared to both healthy controls and CRSsNP.
- ***ACE2*** exhibits notable differential expression as well. It is > 3-fold upregulated in healthy controls compared to CRSwNP and > 1.5-fold upregulated in healthy controls compared to CRSsNP.

These fold changes highlight significant differences in gene expression between the phenotypes, supporting the observations made in the boxplot analyses and further emphasizing the role of these genes in distinguishing between healthy controls and CRS diseases.

Table 4.6.1.I: Fold gene expression calculation for each phenotype versus each single gene. ΔΔCt-values were used to calculate the fold gene expression between the different phenotypes concerning all nine genes of interest. Significant fold changes are marked in bold.

		T1			T2		T3			RAAS
		CXCL9	**CXCL10**	**IFN-γ**	**CCL26**	**CLC**	**CSF3**	**IL-1β**	**IL-6**	**ACE2**
HC vs. CRS	**ΔΔCt**	-0.2896	0.0936	-0.4729	-0.0312	-1.6569	-0.3117	-0.3928	-0.7505	1.4862
	$2^{-\Delta\Delta Ct}$ / FGE	-0.0839	0.0088	-0.2236	-0.0010	**2.7452**	-0.0971	-0.1543	-0.5633	**2.2087**
HC vs. CRSwNP	**ΔΔCt**	-0.0207	0.5389	-0.1083	-1.1376	-3.3738	-0.0360	-0.6155	-0.7398	1.7452
	$2^{-\Delta\Delta Ct}$ / FGE	-0.0004	0.2904	-0.0117	**1.2942**	**11.3824**	-0.0013	-0.3788	-0.5474	**3.0456**
HC vs. CRSsNP	**ΔΔCt**	-0.5585	-0.3517	-0.8374	1.0752	0.0600	-0.5873	-0.1701	-0.7612	1.2271
	$2^{-\Delta\Delta Ct}$ / FGE	-0.3120	-0.1237	-0.7013	**1.1560**	0.0036	-0.3449	-0.0289	-0.5794	**1.5059**
CRSwNP vs. CRSsNP	**ΔΔCt**	-0.5379	-0.8906	-0.7291	2.2128	3.4338	-0.5513	0.4454	-0.0213	-0.5180
	$2^{-\Delta\Delta Ct}$ / FGE	-0.2893	-0.7931	-0.5316	**4.8965**	**11.7911**	-0.3039	0.1984	-0.0005	-0.2683

Abbreviations: FGE, fold gene expression = fold change = $2^{-\Delta\Delta Ct}$; HC, healthy control

Table 4.6.1.II provides the exact t-statistics and p-values for comparing gene expression values across different phenotypes as depicted in **Figure 4.6.1**. The table includes comparisons of each gene expression between healthy controls, CRSsNP, CRSwNP, and both CRS diseases combined.

The results are summarized as follows:

- **Endotype T2 (*CCL26* and *CLC*)**, ***IL-6***, and ***ACE2*** are significantly differentially expressed between healthy controls and both CRS diseases combined. These differences are corroborated by the significant p-values observed for these genes.
- ***CLC*** and ***ACE2*** show significant differential expression between healthy controls and CRSwNP.
- ***CCL26*** and ***ACE2*** exhibit significant differences between healthy controls and CRSsNP.
- ***CCL26*** and ***CLC*** are significantly different between CRSwNP and CRSsNP.

Table 4.6.1.II: Statistic significance calculation for each phenotype comparison versus each single gene. All phenotypes were compared to each other and tested for significance using the t-statistic and a two-sided t-test for different variances. Statistically significant p-values are written in bold.

		T1			T2		T3			RAAS
	Statistic	**CXCL9**	**CXCL10**	**IFN-γ**	**CCL26**	**CLC**	**CSF3**	**IL-1β**	**IL-6**	**ACE2**
HC vs. CRS	**df**	91	83	87	61	84	85	89	81	71
	t-statistic	0.1530	0.6580	-0.5493	-2.4234	-4.6004	0.1600	-0.1118	-2.0536	6.1255
	p-value	0.8787	0.5124	0.5842	**0.0184**	**0.0000**	0.8733	0.9113	**0.0432**	**0.0000**
HC vs. CRSwNP	**df**	76	78	77	65	78	66	79	79	78
	t-statistic	0.3986	1.0493	-0.1543	-1.9220	-5.4439	0.4169	-0.1053	-1.9039	6.1236
	p-value	0.6913	0.2973	0.8778	0.0590	**0.0000**	0.6781	0.9164	0.0606	**0.0000**
HC vs. CRSsNP	**df**	14	22	15	19	11	12	18	16	18
	t-statistic	-0.5809	-0.8288	-1.4192	2.5403	-0.0221	-0.7381	-0.0701	-1.4612	3.3279
	p-value	0.5706	0.4161	0.1763	**0.0200**	0.9827	0.4747	0.9449	0.1633	**0.0037**
CRSwNP vs. CRSsNP	**df**	18	22	17	39	10	19	21	15	22
	t-statistic	0.8051	1.6916	1.2583	-3.6787	-3.3064	0.9364	-0.0125	0.1042	1.4903
	p-value	0.4313	0.1048	0.2253	**0.0007**	**0.0079**	0.3608	0.9901	0.9184	0.1503

Abbreviations: df, degree of freedom; p-value, probability value two sided

4.6.2 The special role of *ACE2* concerning all three endotypes

Since *ACE2* exhibited significant differences in expression between healthy controls and both CRS disease groups, with higher expression levels in healthy controls (as discussed in chapter 4.6.1), this chapter further investigates *ACE2* expression in relation to the endotypes. It aims to determine whether *ACE2* plays a distinct role in this context.

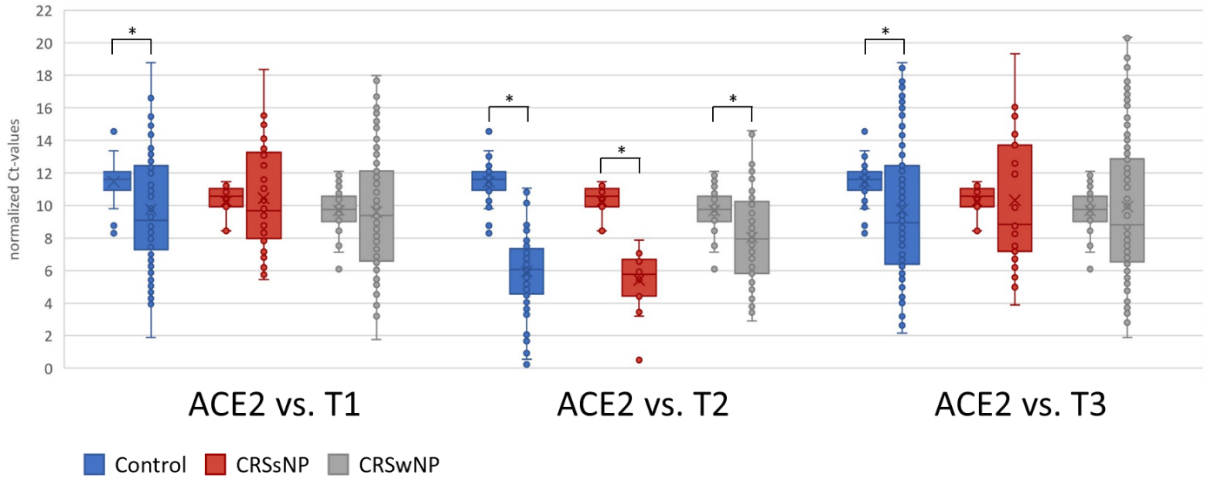

Figure 4.6.2: Boxplots illustrating significant expression of *ACE2* compared to each endotype. Expression values of *ACE2* were compared with those of each endotype across the three phenotypes to identify significant differences. Healthy controls are represented in blue, CRSsNP in red, and CRSwNP in gray. Statistically significant differences between *ACE2* and the compared endotype are marked with an asterisk, indicating a significance level of $p < 0.05$. The ordinate displays the expression values (Ct-values normalized against *β-Actin* as housekeeping gene).

In **Figure 4.6.2**, the expression values measured by qRT-PCR are visualized as boxplots for *ACE2* compared to the three endotypes (T1, T2, and T3) across each phenotype (healthy controls, CRSsNP, and CRSwNP). For each endotype, the expression values of the associated genes are averaged and represented as boxplots. The figure demonstrates that for each endotype, there is a statistically significant difference in expression compared to *ACE2*, though this is observed primarily within the healthy controls, with two exceptions. This detailed analysis reaffirms that there is a significant difference between endotype T2 and *ACE2* across all three phenotypes, highlighting a potential special role of T2 and *ACE2* in chronic rhinosinusitis.

These findings can be summarized as follows:

- ***ACE2* vs. Endotype T1:** Significant difference in expression between *ACE2* and T1 with *ACE2* showing higher expression in healthy controls.
- ***ACE2* vs. Endotype T2:** *ACE2* expression significantly differs from T2 in all three phenotypes with *ACE2* being lower expressed in CRS diseases.
- ***ACE2* vs. Endotype T3:** Significant difference observed between *ACE2* and T3 with *ACE2* showing higher expression in healthy controls like for T1 and T2.

Table 4.6.2.I further underscores the distinctive role of *ACE2* and endotype T2. *ACE2* expression in healthy controls is upregulated in more than half of all comparisons with the endotypes and phenotypes, with the exception of endotypes T1 and T3 in CRS. Additionally, endotype T2 is consistently downregulated compared to *ACE2* across all phenotypes, notably over 36-fold in CRSsNP.

Table 4.6.2.I: Fold gene expression calculation between each endo-/phenotype and *ACE2*. ΔΔCt-values were used to calculate the fold gene expression between the different endo- and phenotypes and *ACE2*. Significant fold changes are marked in bold.

			ACE2		
		Fold change	**HC**	**CRSsNP**	**CRSwNP**
T1	**HC**	**ΔΔCt**	-1.5156	-0.2884	0.2296
		$2^{-\Delta\Delta Ct}$ / FGE	**2.2970**	-0.0832	0.0527
	CRSsNP	**ΔΔCt**	-0.9330	0.2941	0.8121
		$2^{-\Delta\Delta Ct}$ / FGE	-0.8706	0.0865	0.6596
	CRSwNP	**ΔΔCt**	-1.6522	-0.4251	0.0929
		$2^{-\Delta\Delta Ct}$ / FGE	**2.7299**	-0.1807	0.0086
T2	**HC**	**ΔΔCt**	-5.4333	-4.2062	-3.6881
		$2^{-\Delta\Delta Ct}$ / FGE	**29.5209**	**17.6919**	**13.6024**
	CRSsNP	**ΔΔCt**	-6.0009	-4.7738	-4.2557
		$2^{-\Delta\Delta Ct}$ / FGE	**36.0110**	**22.7889**	**18.1114**
	CRSwNP	**ΔΔCt**	-3.1776	-1.9505	-1.4324
		$2^{-\Delta\Delta Ct}$ / FGE	**10.0972**	**3.8043**	**2.0519**
T3	**HC**	**ΔΔCt**	-1.5326	-0.3054	0.2126
		$2^{-\Delta\Delta Ct}$ / FGE	**2.3487**	-0.0933	0.0452
	CRSsNP	**ΔΔCt**	-1.0264	0.2008	0.7188
		$2^{-\Delta\Delta Ct}$ / FGE	**1.0534**	0.0403	0.5167
	CRSwNP	**ΔΔCt**	-1.0688	0.1584	0.6764
		$2^{-\Delta\Delta Ct}$ / FGE	**1.1423**	0.0251	0.4575

Abbreviations: FGE, fold gene expression = fold change = $2^{-\Delta\Delta Ct}$; HC, healthy control

This effect is corroborated by the statistical testing presented in **Table 4.6.2.II**, which compares *ACE2* with endotypes T1, T2, and T3 across all phenotypes. The table indicates that *ACE2* expression in healthy controls shows significant differences compared to all endotypes within the healthy controls. Additionally, *ACE2* in healthy controls is differentially expressed with high significance from all three endotypes in CRSwNP, with p-values ranging from $< 5x10^{-4}$ to $5x10^{-35}$.

Table 4.6.2.II: Statistic significance calculation for each endo-/phenotype compared to *ACE2*. Expression values of the genes associated with the corresponding endotype were combined and compared for each phenotype with *ACE2*. Significance was tested by t-statistic and a two-sided t-test for different variances. Statistically significant p-values are written in bold. Those illustrated in Figure 4.6.2 are written in bold and blue.

			ACE2		
		Statistic	**HC**	**CRSsNP**	**CRSwNP**
T1	**HC**	**df**	158	37	155
		t-statistic	4.7104	1.1455	-0.1708
		p-value	**0.00000538**	0.2594	0.8646
	CRSsNP	**df**	38	41	41
		t-statistic	1.7149	-0.2858	-1.2412
		p-value	0.0945	0.7765	0.2216
	CRSwNP	**df**	160	40	158
		t-statistic	4.9959	1.4765	0.2387
		p-value	**0.00000151**	0.1476	0.8116
T2	**HC**	**df**	117	26	115
		t-statistic	17.6328	10.8403	11.1930
		p-value	**9.75539×10^{-35}**	**3.84974×10^{-11}**	**4.0489×10^{-20}**
	CRSsNP	**df**	24	27	27
		t-statistic	13.0255	9.2104	8.9184
		p-value	**2.24739×10^{-12}**	**8.04314×10^{-10}**	**1.5592×10^{-9}**
	CRSwNP	**df**	121	35	124
		t-statistic	9.6862	5.1689	4.4529
		p-value	**8.97235×10^{-17}**	**9.62339×10^{-6}**	**0.00001866**
T3	**HC**	**df**	154	54	159
		t-statistic	4.0744	1.0917	-0.0638
		p-value	**0.0000736**	0.2798	0.9492
	CRSsNP	**df**	34	38	36
		t-statistic	1.5749	-0.0734	-0.8471
		p-value	0.1246	0.9418	0.4025
	CRSwNP	**df**	161	55	165
		t-statistic	3.5958	0.6850	-0.5134
		p-value	**0.000429657**	0.4962	0.6084

Abbreviations: df, degree of freedom; p-value, probability value two sided

5 Discussion

5.1 Expression profiles reveal distinct differences between nasal swab and tissue samples, yet similarities between CRSwNP and CRSsNP samples

5.1.1 Differential gene expression profiles of swab and tissue samples suggest different underlying pathway activation

In this doctoral thesis, hierarchical cluster and heatmap analyses were conducted using potential inflammatory biomarkers from nasal tissues and swabs collected from healthy controls, CRSwNP (Chronic Rhinosinusitis with Nasal Polyps), and CRSsNP (Chronic Rhinosinusitis without Nasal Polyps). Chapters 4.3.1, 4.3.2, and 4.3.3 present the results from an initial dataset consisting of 19 swab/tissue pairs, resulting in a total of 38 samples, with each pair originating from the same patient. The findings from chapter 4.3.1 reveal that tissue and swab samples from the same patient generally cluster separately due to distinct gene expression profiles. Conversely, CRSwNP and CRSsNP samples do not separate based on the analyzed genes (*CXCL9, CXCL10, CCL26, CSF3, CLC, IFN-γ, IL-1β, IL-6*, and *ACE2*). Additionally, it was observed that swab and tissue samples from the same patient tend to cluster together, suggesting a shared activation of inflammatory genes and pathways within individual patients. However, it was not possible to distinguish individual patients based on the origin of the material, indicating that gene expression patterns are not unique to each patient but rather follow a systemic pattern.

This difference is likely due to the distinct activation of signaling pathways in the mucous membrane and deeper cell layers. Nasal swabs were primarily collected from the middle meatus, a junctional area that shares a common drainage pathway with other paranasal sinuses (Cho *et al*., 2021). Consequently, samples from this region might exhibit increased heterogeneity. Additionally, Ramakrishnan *et al.* collected swab samples from CRS patients at various anatomical sites and compared microbial compositions, finding significant interpersonal variability (Ramakrishnan *et al.*, 2017). „This could be a function of the vulnerability of the nasal surface microbiome to environmental changes such as temperature and humidity“ (Wagner Mackenzie *et al.*, 2019). In contrast, tissue samples from CRSwNP and CRSsNP exhibited less variation between samples (Cho *et al.*, 2021). This suggests that differences in the microbiome between swabs and tissue may lead to the activation of distinct immunological pathways with varying intensities, potentially contributing to the observed separation of tissue and swab samples in hierarchical clustering.

Furthermore, while it is possible that variations in technical procedures might also cause some degree of separation between the two sample types, this factor appears to be secondary. The primary influence is likely the different compartments and localizations from which the samples were obtained, which may play a more significant role in the divergence of gene expression profiles between swabs and tissue samples.

5.1.2 *CXCL9* and *IL-1β* exhibit the greatest difference between swab and tissue samples

The results from chapter 4.3.1 reveal that *CXCL9* and *IL-1β* exhibit the highest gene expression levels compared to other analyzed genes. *CXCL9* shows significantly higher expression in tissue samples compared to swab samples, while *IL-1β* is highly expressed in 12 swab samples but shows only moderate to low expression in most tissue samples. The heatmap presented in chapter 4.4 further illustrates that *CXCL9* and *IL-1β* cluster closely together, displaying high expression levels across most samples.

CXCL9 is a cytokine involved in inflammatory responses, influencing the growth, movement, and activation state of relevant cells. It induces chemotaxis in activated T-cells by binding to CXCR3 (CXC chemokine receptor 3) and is predominantly located in the extracellular region. *CXCL9* has also been shown to induce chemotaxis in many cells such as melanoma cells (Amatschek *et al.*, 2011), T cells (Liu *et al.*, 2012), and HEK293 cells (Vinet *et al.*, 2013).

IL-1β is a pro-inflammatory cytokine which regulates cellular processes by differential gene expression and stabilization of mRNAs as well as activation of the transcription factors NF-κB and AP-1 (The Gene Ontology Resource "The Gene Ontology Resource: 20 years and still

GOing strong," 2019) (Ashburner *et al.*, 2000) (The Universal Protein Resource "UniProt: the universal protein knowledgebase in 2021," 2021).

Some studies have demonstrated that *IL-1β* can induce the upregulation of *CXCR3* in T cells and tumor cells. Additionally, *CXCL9*, a *CXCR3*-specific ligand, can be upregulated by *IL-1β* within an inflammatory microenvironment (Guo *et al.*, 2018). This interaction also occurs on the surface of mesenchymal stem cells, which then migrate toward injured and inflamed tissues via the bloodstream (Guo *et al.,* 2018; Sanmiguel *et al.*, 2009).

Research by Zeng *et al.* indicates that *CXCL9* is similarly induced by *IFN-γ* in the sinonasal mucosa of patients with CRSsNP and CRSwNP. Moreover, the high expression of *CXCL9* and *IL-1β* can be suppressed by treatments such as clarithromycin and dexamethasone (Zeng *et al.*, 2015). Findings from Mohamad *et al*. reveal a strong association between *IL-1β* and both CRSwNP and CRSsNP, particularly when a single nucleotide polymorphism is present within the promoter region of *IL-1β*. This suggests a potential role for *IL-1β* in modulating the pathogenesis of CRS. In contrast, no significant associations were found between *IL-1α*, various polymorphisms, and CRSwNP or CRSsNP (Mohamad *et al.*, 2019).

Given the reported interactions between *CXCL9* and *IL-1β* and their involvement in both CRS phenotypes, it is not surprising that these genes exhibit similar high expression levels. This likely reflects a crucial interactive regulation of inflammatory responses in CRS.

5.1.3 CRSwNP and CRSsNP exhibit similar gene expression profiles

In chapter 4.3.3, the clustering depicted at the top of the heatmap shows that CRSwNP and CRSsNP samples do not separate distinctly. Instead, CRSsNP samples are interspersed among CRSwNP samples due to similar underlying expression profiles. One reason for this lack of separation could be the selection of genes of interest, which were chosen based on endotype-specific criteria rather than being phenotype- or disease-specific. While numerous genes have been identified that are associated with specific phenotypes and endotypes, only a fraction could be examined in this thesis. For instance, Van Zele *et al.* initially found that the T1 cytokine IFN-γ was significantly elevated in CRSsNP, along with the CRSsNP-specific cytokine TGF-β, compared to CRSwNP (Van Zele *et al.*, 2006). On the other hand, T2 cytokines such as IL-4, IL-5, and IL-13 are known to play a role in controlling inflammation in eosinophilic CRSwNP (Fokkens *et al.*, 2020; Kato, 2015) but are less involved in CRSsNP. Despite this, many genes are upregulated in both CRS diseases. For example, various interleukins induce chemokines, which are proteins that recruit inflammatory cells to tissue

sites by binding to chemokine receptors on their target cells, such as CCR3. CCR3 is primarily expressed on eosinophils, along with MCP-4 (CCL13), RANTES (CCL5), eotaxin-1 (CCL11), eotaxin-2 (CCL24), and eotaxin-3 (CCL26) (Kato, 2015). As most of these genes, except *IFN-γ* and *CCL26*, were not included in this thesis, it is not surprising that the clustering of both diseases does not show a clear separation based on a limited number of endotype-specific genes.

Additionally, in T2 CRSsNP, upregulated genes (such as *CCL18, CCL23, CD1c, CD163*, *F13A1, MRC1*) were also significantly elevated in NP tissues from CRSwNP patients. This suggests a similar mechanism of T2 inflammation in T2 CRSsNP and T2 CRSwNP (Klingler *et al.*, 2021), which could also contribute to the mixed clustering observed.

Moreover, CRSsNP is known for its heterogeneity and is diagnosed by the absence of nasal polyps, while CRSwNP is characterized by eosinophilia. The inflammation associated with CRSwNP can vary based on race and regional differences (Kato, 2015). Given these variations, it might be expected that CRSwNP and CRSsNP would cluster separately and form distinct groups. However, this separation was not evident in the presented data.

A primary reason for this lack of separation could be the limited number of CRSsNP patient samples available for analysis, with only 3 swab/tissue pairs and 11 swab samples in total. Although 75-90% of CRS cases do not involve nasal polyps, many CRSsNP patients receive treatment before requiring surgical intervention, which might explain the relatively small size of the CRSsNP cohort in this study.

5.2 Gene expression profiles of healthy controls exhibit subtle yet crucial differences to chronic rhinosinusitis

5.2.1 The endotype T2 differs from T1 and T3 due to different gene expression profiles

According to the clustering results presented in chapters 4.3.1 and 4.3.3, genes associated with endotype T2 tend to cluster together. In contrast, most genes related to endotypes T1 and T3, including *ACE2*, form a distinct cluster due to their more similar gene expression profiles. Chapter 4.4 also reveals two main clusters: one that includes a mixture of endotypes T1 and T3, and another where endotype T2 forms a separate group.

In all three phenotypes (healthy controls, CRSsNP, and CRSwNP), genes associated with endotype T2 (such as *CCL26* and *CLC*) are expressed at significantly lower levels compared to those associated with endotypes T1 and T3. There is no statistically significant difference

between T1 and T3 in terms of gene expression. The significance of T2-related genes is markedly higher in healthy controls and CRSsNP compared to CRSwNP, where *CCL26* and *CLC* are either upregulated or expressed at higher levels. This suggests that, despite the limited number of genes analyzed, *CCL26* and *CLC* are critical inflammatory biomarkers for endotype T2 in CRS and may be useful for distinguishing T2 from T1 and T3.

Endotypes represent different inflammatory patterns of CRS and involve distinct immune cells and inflammatory mediators, which contribute to tissue remodeling in CRS (Lee *et al.*, 2021). Tissue remodeling, a key feature of CRS, is a dynamic and complex process affecting various layers of sinonasal tissues, including the epithelium, subepithelium, and underlying bone (Lee *et al.*, 2021). Each endotype plays specific roles within this process. T2 inflammation-mediated immunity is known for its role in defending against helminth infections and is also involved in allergic diseases. Key cytokines associated with T2 inflammation include IL-4, IL-5, and IL-13, which could not be detected at sufficient levels by qRT-PCR in this thesis. Additionally, biomarkers for T2 inflammation, such as *CCL26* and *CLC*, as well as markers of T2 cytokine-producing cells (Th2 cells, mast cells, basophils, and ILC2s), were all significantly upregulated in T2 CRSsNP (Klingler *et al.*, 2021; Scheckenbach & Wagenmann, 2016). In this thesis, it was observed that *CCL26* and *CLC* are highly expressed or upregulated in most CRSwNP samples. However, contrary to Klingler *et al*.'s findings, these genes are lower expressed or even downregulated in nearly all CRSsNP samples. Additionally, *CCL26* and *CLC* (endotype T2) show lower expression levels in swab samples compared to tissue samples. These discrepancies may be attributed to Klingler *et al*.'s focus on CRSsNP samples with fewer CRSwNP samples analyzed, as well as the limited number of CRSsNP patient samples (only 11 swabs and 3 tissue samples) available in this thesis.

5.2.2 Comparison of chronic rhinosinusitis with healthy controls indicates higher similarity of endotypes T1 and T3

In chapters 4.3.1, 4.3.3, and 4.4, two main clusters emerge: one consisting of a mixture of endotypes T1 and T3, and another where endotype T2 forms a separate group across all three phenotypes (healthy controls, CRSsNP, and CRSwNP). Notably, T1 and T3 do not show significant statistical differences between each other, primarily due to the similarly high expression levels of *CXCL9* (T1) and *IL-1β* (T3). This suggests an interaction and potential overlap between these endotypes in the inflammatory processes of CRS, indicating that T1 and T3 may share more similarities than previously understood.

For instance, complement factor B levels are elevated in both T1 and T3 CRSsNP, suggesting a possible collaboration between these endotypes through the activation of the alternative

complement pathway (Klingler *et al.*, 2021). While further investigation is needed to explore these similarities in more detail, it is already established that chronic inflammatory responses can involve T1 and T3 pathways either independently or in combination (Fokkens *et al.*, 2020).

Classically, T1-mediated immunity provides defense against intracellular bacteria and viruses. IFN-γ, a key immune effector cytokine, is produced by activated CD4+ Th1 cells, as well as CD8+ cytotoxic T cells, NK cells, and group 1 innate lymphoid cells (ILC1s) (Klingler *et al*., 2021; Scheckenbach & Wagenmann, 2016). Many genes induced by IFN-γ, such as MHC molecules and CXCR3 ligands like CXCL9 and CXCL10, as well as T cell markers, were upregulated in T1 CRSsNP. This suggests that virus-mediated inflammation in T1 CRSsNP is likely regulated primarily by adaptive T cell-mediated responses (Klingler *et al.*, 2021; Scheckenbach & Wagenmann, 2016).

In contrast, T3-mediated immunity provides defense against extracellular microbes such as bacteria and fungi. The T3 endotype is strongly associated with acute inflammatory and host defense responses. Key effector cytokines for T3 include IL-17A and IL-17F, which are produced mainly by Th17 cells and group 3 ILCs (ILC3s), along with CSF3, a biomarker for T3. Gene ontology (GO) and pathway analyses indicate that the T3 endotype is closely linked to neutrophilic inflammation. Despite these differences in gene activation, it is suggested that more specific biomarkers for T1 and T3 may exist, which could lead to a clearer separation of T1 and T3 clusters. However, identifying these biomarkers falls beyond the scope of this thesis (Klingler *et al.*, 2021).

5.3 *ACE2* represents the main difference between chronic rhinosinusitis and healthy controls

In chapter 4.6 of the results section, *ACE2* was identified as differentially expressed between healthy controls (HC) and both combined CRS diseases, as well as between HC and each individual CRS phenotype (CRSsNP and CRSwNP), with highly significant p-values. The analysis demonstrated that *ACE2* exhibits a significant difference in expression between HC and all endotypes, particularly between HC and CRSwNP, but not between CRSsNP and CRSwNP. This indicates that *ACE2* is generally expressed at higher levels or is upregulated in healthy controls compared to CRS diseases, suggesting that *ACE2* may play a distinct role in chronic rhinosinusitis.

5.3.1 Correlation between SARS-CoV-2 entry receptor, ACE2, and CRS

SARS-CoV-2 utilizes ACE2 as a cellular receptor to enter host cells, and increased *ACE2* expression facilitates viral replication in the sinonasal epithelium, potentially elevating the risk of infection (Hoffmann *et al.*, 2020; Liu *et al.*, 2020). While it is well-established that CRS patients can be infected by various viruses, it is not yet confirmed whether CRS itself serves as a comorbidity or risk factor for COVID-19. Conversely, some evidence suggests a possible protective effect against COVID-19 infection (Akhlaghi *et al.,* 2021; Workman & Bhattacharyya, 2022). Studies have indicated that T1 and T2 inflammation modulates *ACE2* expression in the airway epithelium. Notably, there appears to be a lower risk of COVID-19 infection among CRS patients, which may be attributed to the differential expression of *ACE2* (Sajuthi *et al.,* 2020). In CRSwNP, including respiratory airway epithelial cells and nasal polyps, *ACE2* expression at both mRNA and protein levels is significantly lower compared to non-eosinophilic CRS and control subjects (Marin *et al.*, 2021; Ziegler *et al.,* 2020). Similar results have been observed in asthmatic patients (Bradding *et al.*, 2020; Wakabayashi *et al.*, 2021). The data presented in chapter 4.6 align with these findings, showing that *ACE2* expression is significantly lower in both CRS diseases compared to healthy controls. This suggests a potential protective effect of CRS against COVID-19 due to reduced opportunities for viral binding. All patients included in this thesis tested negative for COVID-19, but further investigation is required to validate these findings (**Figure 4.6.1**).

5.3.2 Interactions between *ACE2* and endotypes T2 and T1

A negative correlation between *ACE2* expression and the levels of cytokines IL-4, IL-5, and IL-13, which are associated with T2 inflammation, has been identified in epithelial cells of the respiratory airway in CRS patients (Kimura *et al.*, 2020). This suggests a potential mechanism where reduced *ACE2* expression in airway epithelial cells, driven by endotype T2 inflammation, may confer a protective effect, leading to less severe outcomes of COVID-19 infection.

Although this thesis was unable to detect *IL-4, IL-5,* and *IL-13* at evaluable levels via qRT-PCR, *CCL26* and *CLC* were analyzed as representative markers for endotype T2. These genes also exhibit a negative correlation with *ACE2* expression, as illustrated in **Figure 4.6.2**. The figure clearly demonstrates that higher *ACE2* expression is associated with lower expression of T2 markers, with the greatest difference observed in healthy controls, followed by CRSsNP, and the smallest difference in CRSwNP. This indicates a regulatory interaction in the inflammatory processes of CRS, suggesting that the presence of *ACE2* may influence the expression of T2 inflammatory markers.

Furthermore, previous studies have demonstrated a correlation between increased *ACE2* expression and higher levels of endotype T1 markers, particularly *IFN-γ*, in CRSwNP patients and in primary human upper airway basal cells (Ziegler *et al.*, 2020). According to **Figure 4.6.1**, *IFN-γ* is also expressed at lower levels compared to *ACE2*; however, the extent of its influence on *ACE2* expression requires further investigation. Similarly, *CXCL9* and *CXCL10*, which are associated with endotype T1 and are expressed at higher levels than *IFN-γ*, may have a more substantial impact on *ACE2* expression. However, this potential relationship could not be fully elucidated with the data available in this thesis.

5.3.3 Influence of *ACE2* on RAAS and cytokines involved in CRS

Aside from its role as a receptor for SARS-CoV-2 entry, ACE2 is a crucial component of the Renin-Angiotensin-Aldosterone System (RAAS). RAAS is integral to various physiological and pathological processes. It is activated by the secretion of renin from the kidneys, which hydrolyzes angiotensinogen released from the liver into angiotensin I. Angiotensin I is then converted into angiotensin II by ACE (Hackenthal *et al.*, 1990; Rodrigues Prestes *et al.*, 2017). Angiotensin II is involved in vasoconstriction, fluid retention, aldosterone secretion, cell proliferation, cell hypertrophy, and the stimulation of inflammatory and fibrotic processes (Gray *et al.,* 1998). ACE2, a homologous enzyme to ACE, converts angiotensin I into angiotensin-(1-9) and angiotensin II into angiotensin-(1-7) (Vickers *et al.*, 2002). Currently, RAAS is understood to consist of two main, opposing arms: the classical arm, which includes ACE, angiotensin II, and the AT1 receptor, and the counter-regulatory arm, which involves ACE2, angiotensin-(1-7), and the Mas receptor (Iwai & Horiuchi, 2009). The protective effects of angiotensin-(1-7) extend beyond its well-known cardiovascular and renal benefits. It plays a crucial role in anti-inflammatory processes, including the reduction of cytokine release, leukocyte attraction, tissue damage, and fibrosis (Simões e Silva *et al.,* 2013).

Cytokines are the principal regulators of inflammation, orchestrating interactions between cells during inflammatory responses. Pro-inflammatory cytokines such as CXCL9, CXCL10, IL-1β, and IL-6 have diverse effects, including the activation of immune cells, recruitment, and proliferation of leukocytes (Kelso, 1998). IL-6, in particular, is a key cytokine in numerous pathological processes. It activates the acute-phase inflammatory response, upregulates adhesion molecules on endothelial cells, and directs the differentiation of B and T cells (Rincon, 2012). Treatment with angiotensin-(1-7) has been shown to significantly reduce IL-6 levels in atherosclerotic plaques (Thomas *et al.*, 2010). Numerous studies have indicated that ACE2 can reduce *IL-6* expression in various inflammation models (Simões e Silva *et al.,* 2013). This is supported by the results of this thesis, as depicted in **Figure 4.6.1**. A negative correlation between *ACE2* and *IL-6* is observed across the three phenotypes studied. Despite the low

expression of *ACE2* in CRS, its effect on *IL-6* is evident, with this cytokine being expressed at notably lower levels. This effect is particularly pronounced in healthy controls, where upregulation of *ACE2* may lead to a more substantial downregulation of *IL-6*.

The IL-1 family of cytokines, which includes IL-1α and IL-1β, plays a significant role in the development of immune responses and inflammation (Garlanda *et al.*, 2013). It has been demonstrated that activation of *ACE2* leads to a reduction in *IL-1* levels (Garlanda *et al.*, 2013). The data presented in this thesis indicate that *ACE2* expression is lower and possibly downregulated in CRS compared to healthy controls. Consequently, the reduced expression of *ACE2* in CRS may be insufficient to decrease *IL-1β* levels, which are notably elevated across all phenotypes.

The anti-inflammatory effects of ACE2, including the reduction of cytokine levels in various diseases, may explain why *ACE2* expression is significantly higher in healthy controls. In healthy individuals, ACE2 effectively modulates cytokine expression. In contrast, in CRSwNP and CRSsNP, cytokine levels remain elevated, suggesting that ACE2's regulatory effects are less effective or overwhelmed, necessitating further activation of cytokines to manage the immune response appropriately.

5.4 Conclusions

In conclusion, this doctoral thesis has demonstrated that the inflammatory endotypes T1, T2, and T3 in CRSwNP and CRSsNP are governed by distinct gene signatures and expression profiles, each employing different mechanisms and signaling pathways. The identified mechanisms specific to each endotype may facilitate the discovery of new, endotype-specific therapeutic targets and contribute to the development of more precise and personalized treatment strategies for patients with chronic rhinosinusitis.

In this thesis, qRT-PCR assays were developed to validate key biomarkers identified by Klingler *et al.*, including *CXCL9, CXCL10, CCL26, CLC*, and *CSF3*, which distinguish between the three endotypes. Additionally, the assays were used to examine *ACE2*, a key player in the renin-angiotensin-aldosterone system (RAAS), as well as important cytokines such as IFN-γ, IL-1β, and IL-6.

Furthermore, this thesis demonstrates that the type of sample—tissue versus swab—affects biomarker identification. It was observed that swab and tissue samples from the same patient tend to cluster together, likely due to individual variations in the activation of inflammatory

genes and corresponding pathways. However, patients cannot be distinctly separated based on the material origin alone, suggesting that gene expression patterns are not individualized but rather follow systemic trends. Overall, tissue and swab samples cluster separately due to differing gene expression profiles and biomarker activation. In contrast, CRSwNP and CRSsNP cannot be differentiated based on the analyzed and expressed genes.

Additionally, the selected biomarkers do not effectively differentiate between the CRS phenotypes or healthy controls, as indicated by the clustering results in chapter 4.3.3. More than 50% of CRSwNP patient samples separate into two distinct clusters, while healthy controls cannot be clearly separated from disease samples and are often mixed with CRSsNP samples. This may be due to the fact that the chosen biomarkers are endotype-specific rather than phenotype-specific. The results show that genes associated with endotype T2 (*CCL26* and *CLC*) cluster together with significantly lower expression, especially in swab samples. In contrast, most genes related to endotypes T1 and T3, including *ACE2*, form a separate cluster due to their similar gene expression profiles. T1 and T3 do not show significant statistical differences between them. Further investigation into these similarities is needed, although it is already known that chronic inflammatory responses often involve both T1 and T3 pathways simultaneously.

Furthermore, a distinct role of *ACE2* in CRS compared to healthy controls has been identified in relation to COVID-19 infection, endotype T2, and *IL-6*. The results of this thesis indicate a significantly lower expression of *ACE2* in both CRSwNP and CRSsNP compared to healthy controls, which may suggest a protective effect of CRS by reducing the potential for viral binding of SARS-CoV-2 to its receptor, ACE2. Additionally, a negative correlation between *ACE2* and endotype T2 was observed: higher *ACE2* expression is associated with lower expression of T2 biomarkers. For healthy controls, a high *ACE2* / low T2 expression pattern was evident, whereas CRSsNP and CRSwNP samples exhibited the smallest difference between *ACE2* and T2 expression. This suggests a regulatory interaction in the inflammatory processes of CRS. Moreover, the results indicate that *ACE2* may reduce *IL-6* expression in inflammatory diseases, as evidenced by a negative correlation between *ACE2* and *IL-6* across all three phenotypes.

The complex and detailed analyses, including clustering, heatmap, boxplot, and statistical evaluations presented in this thesis, underscore the challenges in identifying biomarkers specific to CRS phenotypes and endotypes. Leveraging prior knowledge of inflammatory responses in CRS and the foundational work by Klingler *et al*., this study was able to confirm *CCL26* and *CLC* as potential and suitable biomarkers for distinguishing endotype T2 from T1

and T3. Additionally, the study has illuminated the intricate interactions between ACE2 and key cytokines involved in CRS development. According to a review by Lee *et al*., CRS can be classified into T2 and non-T2 endotypes (Lee *et al.,* 2021). While it is established that endotype T2 differs from T1 and T3, suitable biomarkers for these distinctions are still lacking. **Table 5.4** provides a concise overview of the differences between these two endotypes.

Table 5.4: Differences between type 2 (T2) and non-type 2 (T1 and T3) CRS (Lee *et al.,* 2021)

	Type 2	**Non-Type 2**
External stimuli	Allergen, *Staphylococcus aureus* biofilm/enterotoxin, and Fungi	Pollution and bacteria
Effector cells	Eosinophils, Th2 cells, ILC2s, B cells, basophils, and mast cells	Neutrophils, NK cells, Type 1: CD8+ T cells, Th1 cells, and ILC1s Type 3: Th17 cells and ILC3s
Primary cytokines	IL-4, IL-5, and IL-13	Type 1: IFN-γ and IL-12 Type 3: IL-17 and IL-22
Other mediators	IL-25, IL-33, TSLP, and IgE	IL-1β, IL-36, IL-6, IL-8, TGF-β, CXCL1, and CXCL10
Clinical features	Bilateral disease Ethmoid sinus > Maxillary sinus Headache/migraine, anosmia, nasal polyposis, asthma, aspirin-induced respiratory disease	Maxillary sinus > Ethmoid sinus Purulent nasal discharge
Tissue remodeling features	Barrier disruption, basal membrane thickening, and stromal edema	Basal membrane thickening, goblet cell hyperplasia, fibrosis, and collagen deposition

Based on the results of this work, the main findings provide a foundation for developing a new diagnostic strategy that utilizes a T2-based qRT-PCR approach, focusing on biomarkers such as *CCL26* and *CLC*, alongside *ACE2*, from swab samples to differentiate between CRSwNP and CRSsNP. Additionally, the identification of these promising biomarkers offers potential candidates for the development of biologics. These biomarkers may play a crucial role in the future design of more precise and personalized medicine strategies, aiming to more effectively prevent or treat CRS diseases.

5.5 Outlook

5.5.1 More personalized therapies are needed for treatment of CRS patients

The findings of this doctoral thesis underscore the pressing need for personalized medicine approaches for patients with CRSwNP and CRSsNP. While numerous scientific approaches aim to address this need, most current treatment strategies focus primarily on managing the CRS phenotype rather than targeting the underlying endotype activated in CRS. In recent

years, it has become evident that CRS is a complex and multifactorial disease with a variety of pathomechanisms at play. Factors such as genetics, prenatal conditions, anatomical abnormalities, allergic diseases, infections with bacteria or fungi, immune deficiencies, gastroesophageal reflux, cigarette smoking, and air pollution all significantly influence the development and progression of CRS (Hamilos, 2011).

For CRS patients, the primary goal is to alleviate symptoms and enhance quality of life through personalized treatment strategies. This often includes the use of intranasal corticosteroid sprays and, if medical management is insufficient, endoscopic sinus surgery. However, there is a pressing need for new, personalized therapies that can better control or even potentially cure this chronic condition. Emerging biologics such as Omalizumab (anti-IgE antibody), Mepolizumab and Reslizumab (anti-IL-5), and Dupilumab (anti-IL-4Rα) represent promising options in this regard (Klimek *et al.*, 2019). To identify more targeted treatments and develop novel therapeutic strategies, including biomarkers for endotype stratification, it is essential to gain deep insights into the cellular and molecular processes underlying specific molecular mediators of rhinosinusitis inflammation (Scheckenbach & Wagenmann, 2016).

5.5.2 More biomarkers have to be identified for personalized medicine

In this thesis, at least two new candidates associated with endotype T2, *CCL26* and *CLC*, were identified as potential biomarkers and future targets for personalized medicine. These markers demonstrated significant differential expression between T2 and T1/T3 endotypes, although their expression levels were lower compared to those of genes associated with T1/T3. For a biomarker or therapeutic target to be practical in clinical settings, it is ideal if it is highly expressed and detectable with routine diagnostic techniques such as qRT-PCR. Consequently, *CXCL9* (associated with T1) and *IL-1β* (associated with T3), which showed the highest expression levels in this study, could also be promising candidates for personalized medicine.

To identify additional potential biomarkers, extensive high-throughput methods, such as microarray or whole genome sequencing analyses at the mRNA, gene, and protein levels, should be employed. Furthermore, to validate the findings of this thesis and explore these targets' roles and interactions in CRS inflammation, large-scale clinical studies with a greater number of patient samples from various CRS phenotypes are required. Functional experiments will also be essential to confirm the relevance and efficacy of these targets.

5.5.3 Deeper insights into the interactions between *ACE2* and CRS are needed

Moreover, the relationship between cytokine-triggered inflammation and the influence of the SARS-CoV-2 entry receptor, ACE2, in CRS remains poorly understood (Chhiba *et al.,* 2020). While the inflammatory mechanisms of RAAS are well-documented (Chen & Hao, 2020; Patel *et al.*, 2017), the specific role of RAAS, particularly ACE2, in CRS is less clear. The COVID-19 pandemic has brought ACE2 into the scientific spotlight, yet its function in the context of CRS is not well-explored.

Based on the results of this thesis, *ACE2* appears to interact with various genes across all CRS endotypes, leading to differential gene expression. However, the precise mechanisms underlying these interactions warrant further investigation. Future research should include a larger cohort of COVID-19 patients for comparison with CRS patients. Additionally, to gain a more comprehensive understanding of the interactions between *ACE2*, CRS, COVID-19, RAAS, and endotype T2 regulation, more samples from diverse sources - such as tumors, healthy controls treated with ACE inhibitors, and other relevant populations - are needed.

5.5.4 Knowledge about molecular functions and biological processes of endotypes are needed

„The gene ontology (GO) project has developed three structured controlled vocabularies (ontologies) that describe gene products in terms of their associated biological processes, cellular components and molecular functions in a species-independent manner“ ("The Gene Ontology Resource: 20 years and still GOing strong," 2019). The genes of interest - *CXCL9, CXCL10, CCL26, CSF3, CLC, ACE2, IFN-γ, IL-1β*, and *IL-6* - can be classified into Gene Ontology (GO) terms to elucidate their primary molecular functions and biological processes. For instance, GO term analyses reveal that the pro-inflammatory cytokines CXCL9 and CXCL10 are crucial for the activation and differentiation of immune cells involved in inflammatory responses and chemotaxis. When airway epithelial cells are infected, they release various pro-inflammatory mediators, including interleukins (IL-1, IL-6, IL-8), CXCL10, granulocyte-macrophage colony-stimulating factor (CSF3), and eotaxin (CCL26) (Spurrell *et al.*, 2005). These cytokines and chemokines are pivotal for recruiting immune cells such as lymphocytes, neutrophils, and eosinophils to sites of inflammation, thereby exacerbating both acute and chronic inflammatory responses (Saji *et al.*, 2000).

Additionally, GO term and KEGG pathway analyses (Ashburner *et al.,* 2000; Kanehisa & Goto, 2000) highlight that natural killer cells and T cells, especially T helper cells (Th1), are activated by CXCL10, which targets the CXC chemokine receptor 3 (CXCR3). This interaction plays a

critical role in several Th1-dominant conditions, including CRS, bacterial and viral infections, autoimmune diseases, and transplant rejection (Yoshikawa *et al.,* 2013).

However, further studies and functional experiments are necessary to provide direct evidence of the specific GO terms and pathways involved in each endotype, which extends beyond the scope of this medical doctoral thesis.

6 References

Akhlaghi, A., Darabi, A., Mahmoodi, M., Movahed, A., Kaboodkhani, R., Mohammadi, Z., Goreh, A., & Farrokhi, S. (2021). The Frequency and Clinical Assessment of COVID-19 in Patients With Chronic Rhinosinusitis. *Ear Nose Throat J*, 1455613211038070. https://doi.org/10.1177/01455613211038070

Albu, S. (2020). Chronic Rhinosinusitis-An Update on Epidemiology, Pathogenesis and Management. *J Clin Med*, *9*(7). https://doi.org/10.3390/jcm9072285

Amatschek, S., Lucas, R., Eger, A., Pflueger, M., Hundsberger, H., Knoll, C., Grosse-Kracht, S., Schuett, W., Koszik, F., Maurer, D., & Wiesner, C. (2011). CXCL9 induces chemotaxis, chemorepulsion and endothelial barrier disruption through CXCR3-mediated activation of melanoma cells. *Br J Cancer*, *104*(3), 469-479. https://doi.org/10.1038/sj.bjc.6606056

Annunziato, F., & Romagnani, S. (2009). Heterogeneity of human effector CD4+ T cells. *Arthritis Res Ther*, *11*(6), 257. https://doi.org/10.1186/ar2843

Ashburner, M., Ball, C. A., Blake, J. A., Botstein, D., Butler, H., Cherry, J. M., Davis, A. P., Dolinski, K., Dwight, S. S., Eppig, J. T., Harris, M. A., Hill, D. P., Issel-Tarver, L., Kasarskis, A., Lewis, S., Matese, J. C., Richardson, J. E., Ringwald, M., Rubin, G. M., & Sherlock, G. (2000). Gene ontology: tool for the unification of biology. The Gene Ontology Consortium. *Nat Genet*, *25*(1), 25-29. https://doi.org/10.1038/75556

Bachert, C., Zhang, N., Cavaliere, C., Weiping, W., Gevaert, E., & Krysko, O. (2020). Biologics for chronic rhinosinusitis with nasal polyps. *J Allergy Clin Immunol*, *145*(3), 725-739. https://doi.org/10.1016/j.jaci.2020.01.020

Bachert, C. and G. Holtappels (2015). "Pathophysiology of chronic rhinosinusitis, pharmaceutical therapy options." GMS Curr Top Otorhinolaryngol Head Neck Surg 14: Doc09.

Batra, P. S., Setzen, M., Li, Y., Han, J. K., & Setzen, G. (2015). Computed tomography imaging practice patterns in adult chronic rhinosinusitis: survey of the American Academy of Otolaryngology-Head and Neck Surgery and American Rhinologic Society membership. *Int Forum Allergy Rhinol*, *5*(6), 506-512. https://doi.org/10.1002/alr.21483

Beule, A. G. (2015). [Epidemiology of chronic rhinosinusitis, selected risk factors, comorbidities and economic burden]. *Laryngorhinootologie*, *94 Suppl 1*, S1-s23. https://doi.org/10.1055/s-0034-1396869 (Epidemiologie der chronischen Rhinosinusitis, ausgewählter Risikofaktoren und Komorbiditäten, und ihre ökonomischen Folgen.)

Bousquet, J., Burney, P. G., Zuberbier, T., Cauwenberge, P. V., Akdis, C. A., Bindslev-Jensen, C., Bonini, S., Fokkens, W. J., Kauffmann, F., Kowalski, M. L., Lodrup-Carlsen, K., Mullol, J., Nizankowska-Mogilnicka, E., Papadopoulos, N., Toskala, E., Wickman, M., Anto, J., Auvergne, N., Bachert, C., . . . Zock, J. P. (2009). GA2LEN (Global Allergy and Asthma European Network) addresses the allergy and asthma 'epidemic'. *Allergy*, *64*(7), 969-977. https://doi.org/10.1111/j.1398-9995.2009.02059.x

Bradding, P., Richardson, M., Hinks, T. S. C., Howarth, P. H., Choy, D. F., Arron, J. R., Wenzel, S. E., & Siddiqui, S. (2020). ACE2, TMPRSS2, and furin gene expression in the airways of people with asthma-implications for COVID-19. *J Allergy Clin Immunol*, *146*(1), 208-211. https://doi.org/10.1016/j.jaci.2020.05.013

Bresciani, M., Paradis, L., Des Roches, A., Vernhet, H., Vachier, I., Godard, P., Bousquet, J., & Chanez, P. (2001). Rhinosinusitis in severe asthma. *J Allergy Clin Immunol*, *107*(1), 73-80. https://doi.org/10.1067/mai.2001.111593

Carr, T. F. (2016). Complications of sinusitis. *Am J Rhinol Allergy*, *30*(4), 241-245. https://doi.org/10.2500/ajra.2016.30.4322

Carroll, K. N., Wu, P., Gebretsadik, T., Griffin, M. R., Dupont, W. D., Mitchel, E. F., & Hartert, T. V. (2009). The severity-dependent relationship of infant bronchiolitis on the risk and morbidity of early childhood asthma. *J Allergy Clin Immunol*, *123*(5), 1055-1061, 1061.e1051. https://doi.org/10.1016/j.jaci.2009.02.021

Chen, L., & Hao, G. (2020). The role of angiotensin-converting enzyme 2 in coronaviruses/influenza viruses and cardiovascular disease. *Cardiovasc Res*, *116*(12), 1932-1936. https://doi.org/10.1093/cvr/cvaa093

Chhiba, K. D., Patel, G. B., Vu, T. H. T., Chen, M. M., Guo, A., Kudlaty, E., Mai, Q., Yeh, C., Muhammad, L. N., Harris, K. E., Bochner, B. S., Grammer, L. C., Greenberger, P. A., Kalhan, R., Kuang, F. L., Saltoun, C. A., Schleimer, R. P., Stevens, W. W., & Peters, A. T. (2020). Prevalence and characterization of asthma in hospitalized and nonhospitalized patients with COVID-19. *J Allergy Clin Immunol*, *146*(2), 307-314.e304. https://doi.org/10.1016/j.jaci.2020.06.010

Cho, S. H., Hamilos, D. L., Han, D. H., & Laidlaw, T. M. (2020). Phenotypes of Chronic Rhinosinusitis. *J Allergy Clin Immunol Pract*, *8*(5), 1505-1511. https://doi.org/10.1016/j.jaip.2019.12.021

Cho, S. W., Kim, D. Y., Choi, S., Won, S., Kang, H. R., & Yi, H. (2021). Microbiome profiling of uncinate tissue and nasal polyps in patients with chronic rhinosinusitis using swab and tissue biopsy. *PLoS One*, *16*(4), e0249688. https://doi.org/10.1371/journal.pone.0249688

Chung, S. D., Chen, P. Y., Lin, H. C., & Hung, S. H. (2014). Comorbidity profile of chronic rhinosinusitis: a population-based study. *Laryngoscope*, *124*(7), 1536-1541. https://doi.org/10.1002/lary.24581

Cuevas, M., & Zahnert, T. (2021). [Biologics: A New Option in Treatment of Severe Chronic Rhinosinusits with Nasal Polyps]. *Laryngorhinootologie*, *100*(2), 134-145. https://doi.org/10.1055/a-1309-6631 (Biologika: Neue Therapieoption bei schwerer chronisch polypöser Rhinosinusitis.)

Dammann, F. (2007). [Imaging of paranasal sinuses today]. *Radiologe*, *47*(7), 576, 578-583. https://doi.org/10.1007/s00117-007-1502-z (Bildgebung der Nasennebenhöhlen (NNH) in der heutigen Zeit.)

De Boeck, K., Wilschanski, M., Castellani, C., Taylor, C., Cuppens, H., Dodge, J., & Sinaasappel, M. (2006). Cystic fibrosis: terminology and diagnostic algorithms. *Thorax*, *61*(7), 627-635. https://doi.org/10.1136/thx.2005.043539

Dhamija R, Das N, Ding P. Complication Rates Following Endoscopic Sinus Surgery for Chronic Sinusitis. Am J Rhinol Allergy. 2025 May;39(3):197-204. doi: 10.1177/19458924251315434. Epub 2025 Jan 29. PMID: 39881591.

Donoghue, M., Hsieh, F., Baronas, E., Godbout, K., Gosselin, M., Stagliano, N., Donovan, M., Woolf, B., Robison, K., Jeyaseelan, R., Breitbart, R. E., & Acton, S. (2000). A novel angiotensin-converting enzyme-related carboxypeptidase (ACE2) converts angiotensin I to angiotensin 1-9. *Circ Res*, *87*(5), E1-9. https://doi.org/10.1161/01.res.87.5.e1

Farrell, P. M., Rosenstein, B. J., White, T. B., Accurso, F. J., Castellani, C., Cutting, G. R., Durie, P. R., Legrys, V. A., Massie, J., Parad, R. B., Rock, M. J., & Campbell, P. W., 3rd. (2008). Guidelines for diagnosis of cystic fibrosis in newborns through older adults: Cystic Fibrosis Foundation consensus report. *J Pediatr*, *153*(2), S4-s14. https://doi.org/10.1016/j.jpeds.2008.05.005

Fokkens, W. J., Lund, V. J., Hopkins, C., Hellings, P. W., Kern, R., Reitsma, S., Toppila-Salmi, S., Bernal-Sprekelsen, M., Mullol, J., Alobid, I., Terezinha Anselmo-Lima, W., Bachert, C., Baroody, F., von Buchwald, C., Cervin, A., Cohen, N., Constantinidis, J., De Gabory, L., Desrosiers, M., . . . Zwetsloot, C. P. (2020). European Position Paper on Rhinosinusitis and Nasal Polyps 2020. *Rhinology*, *58*(Suppl S29), 1-464. https://doi.org/10.4193/Rhin20.600

Garlanda, C., Dinarello, C. A., & Mantovani, A. (2013). The interleukin-1 family: back to the future. *Immunity*, *39*(6), 1003-1018. https://doi.org/10.1016/j.immuni.2013.11.010

The Gene Ontology Resource: 20 years and still GOing strong. (2019). *Nucleic Acids Res*, *47*(D1), D330-d338. https://doi.org/10.1093/nar/gky1055

Gevaert, P., Lang-Loidolt, D., Lackner, A., Stammberger, H., Staudinger, H., Van Zele, T., Holtappels, G., Tavernier, J., van Cauwenberge, P., & Bachert, C. (2006). Nasal IL-5 levels determine the response to anti-IL-5 treatment in patients with nasal polyps. *J Allergy Clin Immunol*, *118*(5), 1133-1141. https://doi.org/10.1016/j.jaci.2006.05.031

Gevaert P, Van Bruaene N, Cattaert T, et al. Mepolizumab, a humanized anti-IL-5 mAb, as a treatment option for severe nasal polyposis. *J Allergy Clin Immunol* 2011; 128: 989–95.

Gevaert, P., …, Bachert C., (2020) Efficacy and safety of omalizumab in nasal polyposis: 2 randomized phase 3 trials. J Allergy Clin Immunol. 146(3):595-605. https://doi: 10.1016/j.jaci.2020.05.032.

Gray, M. O., Long, C. S., Kalinyak, J. E., Li, H. T., & Karliner, J. S. (1998). Angiotensin II stimulates cardiac myocyte hypertrophy via paracrine release of TGF-beta 1 and endothelin-1 from fibroblasts. *Cardiovasc Res*, *40*(2), 352-363. https://doi.org/10.1016/s0008-6363(98)00121-7

Guglielmo, M., Gulotta, C., Mancini, F., Sacchi, M., & Tarantini, F. (2009). Recalcitrant nasal polyposis: achievement of total remission following treatment with omalizumab. *J Investig Allergol Clin Immunol*, *19*(2), 158-159.

Guo, Y. C., Chiu, Y. H., Chen, C. P., & Wang, H. S. (2018). Interleukin-1β induces CXCR3-mediated chemotaxis to promote umbilical cord mesenchymal stem cell transendothelial migration. *Stem Cell Res Ther*, *9*(1), 281. https://doi.org/10.1186/s13287-018-1032-9

Gwaltney, J. M. (2002). Clinical significance and pathogenesis of viral respiratory infections. *Am J Med*, *112 Suppl 6A*, 13s-18s. https://doi.org/10.1016/s0002-9343(01)01059-2

Hackenthal, E., Paul, M., Ganten, D., & Taugner, R. (1990). Morphology, physiology, and molecular biology of renin secretion. *Physiol Rev*, *70*(4), 1067-1116. https://doi.org/10.1152/physrev.1990.70.4.1067

Hamilos, D. L. (2011). Chronic rhinosinusitis: epidemiology and medical management. *J Allergy Clin Immunol*, *128*(4), 693-707; quiz 708-699. https://doi.org/10.1016/j.jaci.2011.08.004

Hamilos, D. L. (2016). Chronic Rhinosinusitis in Patients with Cystic Fibrosis. *J Allergy Clin Immunol Pract*, *4*(4), 605-612. https://doi.org/10.1016/j.jaip.2016.04.013

Han, J. K. (2021). Mepolizumab for chronic rhinosinusitis with nasal polyps (SYNAPSE): a randomised, double-blind, placebo-controlled, phase 3 trial. Lancet Respir Med, (10):1141-1153. https://doi: 10.1016/S2213-2600(21)00097-7

Hoffmann, M., Kleine-Weber, H., Schroeder, S., Krüger, N., Herrler, T., Erichsen, S., Schiergens, T. S., Herrler, G., Wu, N. H., Nitsche, A., Müller, M. A., Drosten, C., & Pöhlmann, S. (2020). SARS-CoV-2 Cell Entry Depends on ACE2 and TMPRSS2 and Is Blocked by a Clinically Proven Protease Inhibitor. *Cell*, *181*(2), 271-280.e278. https://doi.org/10.1016/j.cell.2020.02.052

Ihaka, R., & Gentleman, R. (1996). R: A Language for Data Analysis and Graphics. *Journal of Computational and Graphical Statistics*, *5*(3), 299-314. http://www.jstor.org/stable/1390807

Iwai, M., & Horiuchi, M. (2009). Devil and angel in the renin-angiotensin system: ACE-angiotensin II-AT1 receptor axis vs. ACE2-angiotensin-(1-7)-Mas receptor axis. *Hypertens Res*, *32*(7), 533-536. https://doi.org/10.1038/hr.2009.74

Jackson, D. J., Busse, W. W., Bacharier, L. B., Kattan, M., O'Connor, G. T., Wood, R. A., Visness, C. M., Durham, S. R., Larson, D., Esnault, S., Ober, C., Gergen, P. J., Becker, P., Togias, A., Gern, J. E., & Altman, M. C. (2020). Association of respiratory allergy, asthma, and expression of the SARS-CoV-2 receptor ACE2. *J Allergy Clin Immunol*, *146*(1), 203-206.e203. https://doi.org/10.1016/j.jaci.2020.04.009

Jaksha, A. F., Weitzel, E. K., & Laury, A. M. (2016). Recent advances in the surgical management of rhinosinusitis. *F1000Res*, *5*. https://doi.org/10.12688/f1000research.9163.1

James, K. M., Peebles, R. S., Jr., & Hartert, T. V. (2012). Response to infections in patients with asthma and atopic disease: an epiphenomenon or reflection of host susceptibility? *J Allergy Clin Immunol*, *130*(2), 343-351. https://doi.org/10.1016/j.jaci.2012.05.056

Kanehisa, M., & Goto, S. (2000). KEGG: kyoto encyclopedia of genes and genomes. *Nucleic Acids Res*, *28*(1), 27-30. https://doi.org/10.1093/nar/28.1.27

Kato, A. (2015). Immunopathology of chronic rhinosinusitis. *Allergol Int*, *64*(2), 121-130. https://doi.org/10.1016/j.alit.2014.12.006

Kato, A., Peters, A. T., Stevens, W. W., Schleimer, R. P., Tan, B. K., & Kern, R. C. (2022). Endotypes of chronic rhinosinusitis: Relationships to disease phenotypes, pathogenesis, clinical findings, and treatment approaches. *Allergy*, *77*(3), 812-826. https://doi.org/10.1111/all.15074

Kelso, A. (1998). Cytokines: principles and prospects. *Immunol Cell Biol*, *76*(4), 300-317. https://doi.org/10.1046/j.1440-1711.1998.00757.x

Kimura, H., Francisco, D., Conway, M., Martinez, F. D., Vercelli, D., Polverino, F., Billheimer, D., & Kraft, M. (2020). Type 2 inflammation modulates ACE2 and TMPRSS2 in airway epithelial cells. *J Allergy Clin Immunol*, *146*(1), 80-88.e88. https://doi.org/10.1016/j.jaci.2020.05.004

Klimek et al., U. F.-R., H Olze 2 , A G Beule 3 4 , A M Chaker 5 6 , J Hagemann 7 , T Huppertz 7 , T K Hoffmann 8 , S Dazert 9 , T Deitmer 10 , S Strieth 11 , H Wrede 12 , W Schlenter 13 , H J Welkoborsky 14 , B Wollenberg 5 , S Becker 15 , F Klimek 1 , A Sperl 1 , I Casper 1 , J Zuberbier 2 , C Rudack 3 , M Cuevas 16 , C A Hintschich 17 , O Guntinas-Lichius 18 , T Stöver 19 , C Bergmann 20 , O Pfaar 21 , J Gosepath 22 , M Gröger 23 , C Beutner 24 , M Laudien 25 , R K Weber 26 , T Hildenbrand 27 , A S Hoffmann 28 , C Bachert 29. (2022). Empfehlungen zur Überprüfung der Wirksamkeit und Verlaufsdokumentation von Dupilumab bei chronischer Rhinosinusitis mit Nasenpolypen (CRSwNP) im deutschen Gesundheitssystem. *Laryngorhinootologie*. https://doi.org/10.1055/a-1908-3074

Klimek, L., Koennecke, M., Hagemann, J., Wollenberg, B., & Becker, S. (2019). [Immunology of chronic rhinosinusitis with nasal polyps as a basis for treatment with biologicals]. *Hno*, *67*(1), 15-26. https://doi.org/10.1007/s00106-018-0557-7 (Immunologie der Polyposis nasi als Grundlage für eine Therapie mit Biologicals.)

Klingler, A. I., Stevens, W. W., Tan, B. K., Peters, A. T., Poposki, J. A., Grammer, L. C., Welch, K. C., Smith, S. S., Conley, D. B., Kern, R. C., Schleimer, R. P., & Kato, A. (2021). Mechanisms and biomarkers of inflammatory endotypes in chronic rhinosinusitis without nasal polyps. *J Allergy Clin Immunol*, *147*(4), 1306-1317. https://doi.org/10.1016/j.jaci.2020.11.037

Koennecke, M., Klimek, L., Mullol, J., Gevaert, P., & Wollenberg, B. (2018). Subtyping of polyposis nasi: phenotypes, endotypes and comorbidities. *Allergo J Int*, *27*(2), 56-65. https://doi.org/10.1007/s40629-017-0048-5

Lang, S., Jäger, L., & Grevers, G. (2002). [Value of secondary coronal reconstructions in computed tomography of the paranasal sinuses]. *Laryngorhinootologie*, *81*(6), 418-421. https://doi.org/10.1055/s-2002-32212 (Zur Aussagefähigkeit koronarer Sekundärrekonstruktionen computertomographischer Sequenzen der Nasennebenhöhlen.)

Larsen, P. L., Tingsgaard, P. K., Harcourt, J., Sofsrud, G., & Tos, M. (1998). Nasal polyps and their relation to polyps/hypertrophic polypoid mucosa in the paranasal sinuses: a macro-, endo-, and microscopic study of autopsy materials. *Am J Rhinol*, *12*(1), 45-51. https://doi.org/10.2500/105065898782103052

Lee, K., Tai, J., Lee, S. H., & Kim, T. H. (2021). Advances in the Knowledge of the Underlying Airway Remodeling Mechanisms in Chronic Rhinosinusitis Based on the Endotypes: A Review. *Int J Mol Sci*, *22*(2). https://doi.org/10.3390/ijms22020910

Leung, R. M., Kern, R. C., Conley, D. B., Tan, B. K., & Chandra, R. K. (2011). Osteomeatal complex obstruction is not associated with adjacent sinus disease in chronic rhinosinusitis with polyps. *Am J Rhinol Allergy*, *25*(6), 401-403. https://doi.org/10.2500/ajra.2011.25.3672

Lin, D. C., Chandra, R. K., Tan, B. K., Zirkle, W., Conley, D. B., Grammer, L. C., Kern, R. C., Schleimer, R. P., & Peters, A. T. (2011). Association between severity of asthma and degree of chronic rhinosinusitis. *Am J Rhinol Allergy*, *25*(4), 205-208. https://doi.org/10.2500/ajra.2011.25.3613

Liu, W., Ren, H. Y., Dong, Y. J., Wang, L. H., Yin, Y., Li, Y., Qiu, Z. X., Cen, X. N., & Shi, Y. J. (2012). Bortezomib regulates the chemotactic characteristics of T cells through downregulation of CXCR3/CXCL9 expression and induction of apoptosis. *Int J Hematol*, *96*(6), 764-772. https://doi.org/10.1007/s12185-012-1195-6

Liu, Z., Xiao, X., Wei, X., Li, J., Yang, J., Tan, H., Zhu, J., Zhang, Q., Wu, J., & Liu, L. (2020). Composition and divergence of coronavirus spike proteins and host ACE2 receptors predict potential intermediate hosts of SARS-CoV-2. *J Med Virol*, *92*(6), 595-601. https://doi.org/10.1002/jmv.25726

Lourijsen, E. S., Fokkens, W. J., & Reitsma, S. (2020). Direct and indirect costs of adult patients with chronic rhinosinusitis with nasal polyps. *Rhinology*, *58*(3), 213-217. https://doi.org/10.4193/Rhin19.468

Mafee, M. F., Tran, B. H., & Chapa, A. R. (2006). Imaging of rhinosinusitis and its complications: plain film, CT, and MRI. *Clin Rev Allergy Immunol*, *30*(3), 165-186. https://doi.org/10.1385/criai:30:3:165

Marin, C., Tubita, V., Langdon, C., Fuentes, M., Rojas-Lechuga, M. J., Valero, A., Alobid, I., & Mullol, J. (2021). ACE2 downregulation in olfactory mucosa: Eosinophilic rhinosinusitis as COVID-19 protective factor? *Allergy*, *76*(9), 2904-2907. https://doi.org/10.1111/all.14904

Marple, B. F., Stankiewicz, J. A., Baroody, F. M., Chow, J. M., Conley, D. B., Corey, J. P., Ferguson, B. J., Kern, R. C., Lusk, R. P., Naclerio, R. M., Orlandi, R. R., & Parker, M. J. (2009). Diagnosis and management of chronic rhinosinusitis in adults. *Postgrad Med*, *121*(6), 121-139. https://doi.org/10.3810/pgm.2009.11.2081

Min, J. Y., & Tan, B. K. (2015). Risk factors for chronic rhinosinusitis. *Curr Opin Allergy Clin Immunol*, *15*(1), 1-13. https://doi.org/10.1097/aci.0000000000000128

Mohamad, S., Hamid, S. S. A., Azlina, A., & Md Shukri, N. (2019). Association of IL-1 gene polymorphisms with chronic rhinosinusitis with and without nasal polyp. *Asia Pac Allergy*, *9*(3), e22. https://doi.org/10.5415/apallergy.2019.9.e22

Nayak, C., Singh, V., Singh, V. P., Oberai, P., Roja, V., Shitanshu, S. S., Sinha, M. N., Deewan, D., Lakhera, B. C., Ramteke, S., Kaushik, S., Sarkar, S., Mandal, N. R., Mohanan, P. G., Singh, J. R., Biswas, S., & Mathew, G. (2012). Homeopathy in chronic sinusitis: a prospective multi-centric observational study. *Homeopathy*, *101*(2), 84-91. https://doi.org/10.1016/j.homp.2012.02.002

Nayan, S., Alizadehfar, R., & Desrosiers, M. (2015). Humoral Primary Immunodeficiencies in Chronic Rhinosinusitis. *Curr Allergy Asthma Rep 15*(8). https://doi.org/10.1007/s11882-015-0547-8

Patel, S., Rauf, A., Khan, H., & Abu-Izneid, T. (2017). Renin-angiotensin-aldosterone (RAAS): The ubiquitous system for homeostasis and pathologies. *Biomed Pharmacother*, *94*, 317-325. https://doi.org/10.1016/j.biopha.2017.07.091

Pfaar, O., Beule, A. G., Laudien, M., & Stuck, B. A. (2023). [Treatment of chronic rhinosinusitis with nasal polyps (CRSwNP) with monoclonal antibodies (biologics): S2k guideline of the German Society of Oto-Rhino-Laryngology, Head and Neck Surgery (DGHNO-KHC), and the German College of General Practitioners and Family Physicians (DEGAM)]. *Hno*. https://doi.org/10.1007/s00106-023-01273-2 (Therapie der chronischen Rhinosinusitis mit Polyposis nasi (CRScNP) mit monoklonalen Antikörpern (Biologika): S2k-Leitlinie der Deutschen Gesellschaft für Hals-Nasen-Ohren-Heilkunde, Kopf- und Hals-Chirurgie (DGHNO-KHC) und der Deutschen Gesellschaft für Allgemeinmedizin und Familienmedizin (DEGAM).)

Ramakrishnan, V. R., Gitomer, S., Kofonow, J. M., Robertson, C. E., & Frank, D. N. (2017). Investigation of sinonasal microbiome spatial organization in chronic rhinosinusitis. *Int Forum Allergy Rhinol*, *7*(1), 16-23. https://doi.org/10.1002/alr.21854

Rimmer, J., Fokkens, W., Chong, L. Y., & Hopkins, C. (2014). Surgical versus medical interventions for chronic rhinosinusitis with nasal polyps. *Cochrane Database Syst Rev*(12), Cd006991. https://doi.org/10.1002/14651858.CD006991.pub2

Rincon, M. (2012). Interleukin-6: from an inflammatory marker to a target for inflammatory diseases. *Trends Immunol*, *33*(11), 571-577. https://doi.org/10.1016/j.it.2012.07.003

Rodrigues Prestes, T. R., Rocha, N. P., Miranda, A. S., Teixeira, A. L., & Simoes, E. S. A. C. (2017). The Anti-Inflammatory Potential of ACE2/Angiotensin-(1-7)/Mas Receptor Axis: Evidence from Basic and Clinical Research. *Curr Drug Targets*, *18*(11), 1301-1313. https://doi.org/10.2174/1389450117666160727142401

Romano A, Barone S, Borriello G, De Fazio GR, Paesano S, Grassia G, Bonavolontà P, Dell'Aversana Orabona G, Sivero S. Impact of FESS on symptomatology and quality of life of patients with CRSsNP. Eur Arch Otorhinolaryngol. 2025 Apr;282(4):1891-1900. doi: 10.1007/s00405-024-09139-1. Epub 2024 Dec 19. PMID: 39702803.

Rudmik, L., & Soler, Z. M. (2015). Medical Therapies for Adult Chronic Sinusitis: A Systematic Review. *Jama*, *314*(9), 926-939. https://doi.org/10.1001/jama.2015.7544

Saji, F., Nonaka, M., & Pawankar, R. (2000). Expression of RANTES by IL-1 beta and TNF-alpha stimulated nasal polyp fibroblasts. *Auris Nasus Larynx*, *27*(3), 247-252. https://doi.org/10.1016/s0385-8146(00)00052-3

Sajuthi, S. P., DeFord, P., Li, Y., Jackson, N. D., Montgomery, M. T., Everman, J. L., Rios, C. L., Pruesse, E., Nolin, J. D., Plender, E. G., Wechsler, M. E., Mak, A. C. Y., Eng, C., Salazar, S., Medina, V., Wohlford, E. M., Huntsman, S., Nickerson, D. A., Germer, S., . . . Seibold, M. A. (2020). Type 2 and interferon inflammation regulate SARS-CoV-2 entry factor expression in the airway epithelium. *Nat Commun*, *11*(1), 5139. https://doi.org/10.1038/s41467-020-18781-2

Sanmiguel, J. C., Olaru, F., Li, J., Mohr, E., & Jensen, L. E. (2009). Interleukin-1 regulates keratinocyte expression of T cell targeting chemokines through interleukin-1 receptor associated kinase-1 (IRAK1) dependent and independent pathways. *Cell Signal*, *21*(5), 685-694. https://doi.org/10.1016/j.cellsig.2009.01.005

Scheckenbach, K., & Wagenmann, M. (2016). Cytokine Patterns and Endotypes in Acute and Chronic Rhinosinusitis. *Curr Allergy Asthma Rep*, *16*(1), 3. https://doi.org/10.1007/s11882-015-0583-4

Schwitzguébel, A. J., Jandus, P., Lacroix, J. S., Seebach, J. D., & Harr, T. (2015). Immunoglobulin deficiency in patients with chronic rhinosinusitis: Systematic review of the literature and meta-analysis. *J Allergy Clin Immunol*, *136*(6), 1523-1531. https://doi.org/10.1016/j.jaci.2015.07.016

Settipane, R. A., Borish, L., & Peters, A. T. (2013). Chapter 16: Determining the role of allergy in sinonasal disease. *Am J Rhinol Allergy*, *27 Suppl 1*(3 Suppl), S56-58. https://doi.org/10.2500/ajra.2013.27.3929

Simões e Silva, A. C., Silveira, K. D., Ferreira, A. J., & Teixeira, M. M. (2013). ACE2, angiotensin-(1-7) and Mas receptor axis in inflammation and fibrosis. *Br J Pharmacol*, *169*(3), 477-492. https://doi.org/10.1111/bph.12159

Spurrell, J. C., Wiehler, S., Zaheer, R. S., Sanders, S. P., & Proud, D. (2005). Human airway epithelial cells produce IP-10 (CXCL10) in vitro and in vivo upon rhinovirus infection. *Am J Physiol Lung Cell Mol Physiol*, *289*(1), L85-95. https://doi.org/10.1152/ajplung.00397.2004

Starry, A., Hardtstock, F., Wilke, T., Weihing, J., Ultsch, B., Wernitz, M., Renninger, M., Maywald, U., & Pfaar, O. (2022). Epidemiology and treatment of patients with Chronic rhinosinusitis with nasal polyps in Germany-A claims data study. *Allergy*, *77*(9), 2725-2736. https://doi.org/10.1111/all.15301

Stevens, W. W., Peters, A. T., Tan, B. K., Klingler, A. I., Poposki, J. A., Hulse, K. E., Grammer, L. C., Welch, K. C., Smith, S. S., Conley, D. B., Kern, R. C., Schleimer, R. P., & Kato, A. (2019). Associations Between Inflammatory Endotypes and Clinical Presentations in Chronic Rhinosinusitis. *J Allergy Clin Immunol Pract*, *7*(8), 2812-2820.e2813. https://doi.org/10.1016/j.jaip.2019.05.009

Stevens, W. W., Schleimer, R. P., & Kern, R. C. (2016). Chronic Rhinosinusitis with Nasal Polyps. *J Allergy Clin Immunol Pract*, *4*(4), 565-572. https://doi.org/10.1016/j.jaip.2016.04.012

Stuck, B. A., Bachert, C., Federspil, P., Hosemann, W., Klimek, L., Mösges, R., Pfaar, O., Rudack, C., Sitter, H., Wagenmann, M., Weber, R., & Hörmann, K. (2012). [Rhinosinusitis guidelines--unabridged version: S2 guidelines from the German Society of Otorhinolaryngology, Head and Neck Surgery]. *Hno*, *60*(2), 141-162. https://doi.org/10.1007/s00106-011-2396-7 (Leitlinie "Rhinosinusitis"--Langfassung: S2-Leitlinie der Deutschen Gesellschaft für Hals-Nasen-Ohren-Heilkunde, Kopf- und Hals-Chirurgie.)

Stuck, B. A., Beule, A., Jobst, D., Klimek, L., Laudien, M., Lell, M., Vogl, T. J., & Popert, U. (2018). [Guideline for "rhinosinusitis"-long version : S2k guideline of the German College of General Practitioners and Family Physicians and the German Society for Oto-Rhino-Laryngology, Head and Neck Surgery]. *Hno*, *66*(1), 38-74. https://doi.org/10.1007/s00106-017-0401-5 (Leitlinie „Rhinosinusitis“ – Langfassung : S2k-Leitlinie der Deutschen Gesellschaft für Allgemeinmedizin und Familienmedizin und der Deutschen Gesellschaft für Hals-Nasen-Ohren-Heilkunde, Kopf- und Hals-Chirurgie e. V.)

Sylvester, D. C., Carr, S., & Nix, P. (2013). Maximal medical therapy for chronic rhinosinusitis: a survey of otolaryngology consultants in the United Kingdom. *Int Forum Allergy Rhinol*, *3*(2), 129-132. https://doi.org/10.1002/alr.21084

Tan, B. K., Chandra, R. K., Pollak, J., Kato, A., Conley, D. B., Peters, A. T., Grammer, L. C., Avila, P. C., Kern, R. C., Stewart, W. F., Schleimer, R. P., & Schwartz, B. S. (2013). Incidence and associated premorbid diagnoses of patients with chronic rhinosinusitis. *J Allergy Clin Immunol*, *131*(5), 1350-1360. https://doi.org/10.1016/j.jaci.2013.02.002

Tan, B. K., Schleimer, R. P., & Kern, R. C. (2010). Perspectives on the etiology of chronic rhinosinusitis. *Curr Opin Otolaryngol Head Neck Surg*, *18*(1), 21-26. https://doi.org/10.1097/MOO.0b013e3283350053

Thomas, M. C., Pickering, R. J., Tsorotes, D., Koitka, A., Sheehy, K., Bernardi, S., Toffoli, B., Nguyen-Huu, T. P., Head, G. A., Fu, Y., Chin-Dusting, J., Cooper, M. E., & Tikellis, C. (2010). Genetic Ace2 deficiency accentuates vascular inflammation and atherosclerosis in the ApoE knockout mouse. *Circ Res*, *107*(7), 888-897. https://doi.org/10.1161/circresaha.110.219279

Tint, D., Kubala, S., & Toskala, E. (2016). Risk Factors and Comorbidities in Chronic Rhinosinusitis. *Curr Allergy Asthma Rep*, *16*(2), 16. https://doi.org/10.1007/s11882-015-0589-y

Tipnis, S. R., Hooper, N. M., Hyde, R., Karran, E., Christie, G., & Turner, A. J. (2000). A human homolog of angiotensin-converting enzyme. Cloning and functional expression as a captopril-insensitive carboxypeptidase. *J Biol Chem*, *275*(43), 33238-33243. https://doi.org/10.1074/jbc.M002615200

Tomassen, P., Vandeplas, G., Van Zele, T., Cardell, L. O., Arebro, J., Olze, H., Förster-Ruhrmann, U., Kowalski, M. L., Olszewska-Ziąber, A., Holtappels, G., De Ruyck, N., Wang, X., Van Drunen, C., Mullol, J., Hellings, P., Hox, V., Toskala, E., Scadding, G., Lund, V., . . . Bachert, C. (2016). Inflammatory endotypes of chronic rhinosinusitis based on cluster analysis of biomarkers. *J Allergy Clin Immunol*, *137*(5), 1449-1456.e1444. https://doi.org/10.1016/j.jaci.2015.12.1324

UniProt: the universal protein knowledgebase in 2021. (2021). *Nucleic Acids Res*, *49*(D1), D480-d489. https://doi.org/10.1093/nar/gkaa1100

Van Zele, T., Claeys, S., Gevaert, P., Van Maele, G., Holtappels, G., Van Cauwenberge, P., & Bachert, C. (2006). Differentiation of chronic sinus diseases by measurement of inflammatory mediators. *Allergy*, *61*(11), 1280-1289. https://doi.org/10.1111/j.1398-9995.2006.01225.x

Vickers, C., Hales, P., Kaushik, V., Dick, L., Gavin, J., Tang, J., Godbout, K., Parsons, T., Baronas, E., Hsieh, F., Acton, S., Patane, M., Nichols, A., & Tummino, P. (2002). Hydrolysis of biological peptides by human angiotensin-converting enzyme-related carboxypeptidase. *J Biol Chem*, *277*(17), 14838-14843. https://doi.org/10.1074/jbc.M200581200

Vinet, J., van Zwam, M., Dijkstra, I. M., Brouwer, N., van Weering, H. R., Watts, A., Meijer, M., Fokkens, M. R., Kannan, V., Verzijl, D., Vischer, H. F., Smit, M. J., Leurs, R., Biber, K., & Boddeke, H. W. (2013). Inhibition of CXCR3-mediated chemotaxis by the human chemokine receptor-like protein CCX-CKR. *Br J Pharmacol*, *168*(6), 1375-1387. https://doi.org/10.1111/bph.12042

Wagner Mackenzie, B., Chang, K., Zoing, M., Jain, R., Hoggard, M., Biswas, K., Douglas, R. G., & Taylor, M. W. (2019). Longitudinal study of the bacterial and fungal microbiota in the human sinuses reveals seasonal and annual changes in diversity. *Sci Rep*, *9*(1), 17416. https://doi.org/10.1038/s41598-019-53975-9

Wahid NWB, Shermetaro C. Rhinitis Medicamentosa. [Updated 2023 Sep 4]. In: StatPearls [Internet]. Treasure Island (FL): StatPearls Publishing; 2025 Jan-. Available from: https://www.ncbi.nlm.nih.gov/books/NBK538318/

Wakabayashi, M., Pawankar, R., Narazaki, H., Ueda, T., & Itabashi, T. (2021). Coronavirus disease 2019 and asthma, allergic rhinitis: molecular mechanisms and host-environmental interactions. *Curr Opin Allergy Clin Immunol*, *21*(1), 1-7. https://doi.org/10.1097/aci.0000000000000699

Walls, A. C., Park, Y. J., Tortorici, M. A., Wall, A., McGuire, A. T., & Veesler, D. (2020). Structure, Function, and Antigenicity of the SARS-CoV-2 Spike Glycoprotein. *Cell*, *181*(2), 281-292.e286. https://doi.org/10.1016/j.cell.2020.02.058

Wang, H., Song, J., Pan, L., Deng, Y. K., Yao, Y., Wang, Z. C., Liao, B., Ma, J., Zeng, M., & Liu, Z. (2021). Regional differences in ACE2 expression in the sinonasal mucosa of adult Chinese patients with chronic rhinosinusitis. *Allergy*, *76*(5), 1565-1568. https://doi.org/10.1111/all.14623

Wang, H., Song, J., Pan, L., Yao, Y., Deng, Y. K., Wang, Z. C., Liao, B., Ma, J., He, C., Zeng, M., & Liu, Z. (2020). The characterization of chronic rhinosinusitis in hospitalized patients with COVID-19. *J*

Allergy Clin Immunol Pract, *8*(10), 3597-3599.e3592. https://doi.org/10.1016/j.jaip.2020.09.013

Wang, H., Song, J., Yao, Y., Deng, Y. K., Wang, Z. C., Liao, B., Ma, J., He, C., Pan, L., Liu, Y., Xie, J. G., Zeng, M., & Liu, Z. (2021). Angiotensin-converting enzyme II expression and its implication in the association between COVID-19 and allergic rhinitis. *Allergy*, *76*(3), 906-910. https://doi.org/10.1111/all.14569

Wang, M., Bu, X., Fang, G., Luan, G., Huang, Y., Akdis, C. A., Wang, C., & Zhang, L. (2021). Distinct expression of SARS-CoV-2 receptor ACE2 correlates with endotypes of chronic rhinosinusitis with nasal polyps. *Allergy*, *76*(3), 789-803. https://doi.org/10.1111/all.14665

Weber, R. K., & Hosemann, W. (2015). Comprehensive review on endonasal endoscopic sinus surgery. *GMS Curr Top Otorhinolaryngol Head Neck Surg*, *14*, Doc08. https://doi.org/10.3205/cto000123

Wenzel, S., Castro, M., Corren, J., Maspero, J., Wang, L., Zhang, B., Pirozzi, G., Sutherland, E. R., Evans, R. R., Joish, V. N., Eckert, L., Graham, N. M., Stahl, N., Yancopoulos, G. D., Louis-Tisserand, M., & Teper, A. (2016). Dupilumab efficacy and safety in adults with uncontrolled persistent asthma despite use of medium-to-high-dose inhaled corticosteroids plus a long-acting β2 agonist: a randomised double-blind placebo-controlled pivotal phase 2b dose-ranging trial. *Lancet*, *388*(10039), 31-44. https://doi.org/10.1016/s0140-6736(16)30307-5

Workman, A. D., & Bhattacharyya, N. (2022). Do Patients With Chronic Rhinosinusitis Exhibit Elevated Rates of Covid-19 Infection? *Laryngoscope*, *132*(2), 257-258. https://doi.org/10.1002/lary.29961

Wuister, A. M., Goto, N. A., Oostveen, E. J., de Jong, W. U., van der Valk, E. S., Kaper, N. M., Aarts, M. C., Grolman, W., & van der Heijden, G. J. (2014). Nasal endoscopy is recommended for diagnosing adults with chronic rhinosinusitis. *Otolaryngol Head Neck Surg*, *150*(3), 359-364. https://doi.org/10.1177/0194599813514510

Xu, X., Reitsma, S., Wang, Y., & Fokkens, W. J. (2021). Highlights in the advances of chronic rhinosinusitis. *Allergy*, *76*(11), 3349-3358. https://doi.org/10.1111/all.14892

Yao, Y., Wang, H., & Liu, Z. (2020). Expression of ACE2 in airways: Implication for COVID-19 risk and disease management in patients with chronic inflammatory respiratory diseases. *Clin Exp Allergy*, *50*(12), 1313-1324. https://doi.org/10.1111/cea.13746

Yoshikawa, M., Wada, K., Yoshimura, T., Asaka, D., Okada, N., Matsumoto, K., & Moriyama, H. (2013). Increased CXCL10 expression in nasal fibroblasts from patients with refractory chronic rhinosinusitis and asthma. *Allergol Int*, *62*(4), 495-502. https://doi.org/10.2332/allergolint.13-OA-0572

Younis, R. T., Anand, V. K., & Davidson, B. (2002). The role of computed tomography and magnetic resonance imaging in patients with sinusitis with complications. *Laryngoscope*, *112*(2), 224-229. https://doi.org/10.1097/00005537-200202000-00005

Zeng, M., Li, Z. Y., Ma, J., Cao, P. P., Wang, H., Cui, Y. H., & Liu, Z. (2015). Clarithromycin and dexamethasone show similar anti-inflammatory effects on distinct phenotypic chronic rhinosinusitis: an explant model study. *BMC Immunol*, *16*, 37. https://doi.org/10.1186/s12865-015-0096-x

Ziegler, C. G. K., Allon, S. J., Nyquist, S. K., Mbano, I. M., Miao, V. N., Tzouanas, C. N., Cao, Y., Yousif, A. S., Bals, J., Hauser, B. M., Feldman, J., Muus, C., Wadsworth, M. H., 2nd, Kazer, S. W., Hughes, T. K., Doran, B., Gatter, G. J., Vukovic, M., Taliaferro, F., . . . Ordovas-Montanes, J. (2020). SARS-CoV-2 Receptor ACE2 Is an Interferon-Stimulated Gene in Human Airway Epithelial Cells and Is Detected in Specific Cell Subsets across Tissues. *Cell*, *181*(5), 1016-1035.e1019. https://doi.org/10.1016/j.cell.2020.04.035

Zinreich, S. J., Kennedy, D. W., Rosenbaum, A. E., Gayler, B. W., Kumar, A. J., & Stammberger, H. (1987). Paranasal sinuses: CT imaging requirements for endoscopic surgery. *Radiology*, *163*(3), 769-775. https://doi.org/10.1148/radiology.163.3.3575731

Zygmunt, B., & Veldhoen, M. (2011). T helper cell differentiation more than just cytokines. *Adv Immunol*, *109*, 159-196. https://doi.org/10.1016/b978-0-12-387664-5.00005-4

Acknowledgements

On this place, I wish to thank all persons involved in this project for the great support during my medical doctoral thesis. A special thanks goes to Prof. Dr. med. Kathrin Scheckenbach und Prof. Dr. med. Martin Wagenmann for giving me the opportunity to successfully complete my MD thesis in the Department of HNO and for excellent supervision during my project. I would also like to thank Prof. Dr. med. Johannes Stegbauer for the evaluation of my thesis as secondary referee and the great thought-provoking impulses.

Furthermore, I would like to thank Dr. Katja Geipel and Dr. Constanze Wiek who gave me the possibility to investigate such an interesting and fascinating topic and for the great mentoring and the many scientific discussions and for reading my MD thesis and for giving me a lot of scientific advices.

Finally, I wish to thank my family for personal encouragement and reinforcement for invaluable personal support, endurance and several discussions.